Dissertation
submitted to
the Combined Faculties for Natural Sciences and Mathematics
of the Ruperto-Carola University
of Heidelberg, Germany
for the degree of Doctor of Natural Sciences

Presented by
Diplom-Biologin Sheena Dominique Pinto
Mumbai, India
Date of Oral Examination: 10th May 2010

Promiscuous Gene Expression in Thymic Medullary Epithelial Cells: Scope, Phylogenetic Conservation and Regulation at the Single Cell Level

Referees: Prof. Dr. Günter Hämmerling
Prof. Dr. Bruno Kyewski

This thesis was completed in the Department of Developmental Immunology,
headed by Prof. Dr. Bruno Kyewski, at the German Cancer Research Center, Heidelberg.

I hereby confirm that the research and analysis performed on this thesis is entirely my own without contributions from any third party. Wherever my research on this thesis entailed reference to established theories and publications, appropriate mention has been made.

Sheena Pinto

Heidelberg, 25th March 2010

Table of Contents

Summary

In the thymus a specific subset of thymic stromal cells - medullary thymic epithelial cells (mTECs) - express a highly diverse set of tissue-restricted antigens (TRAs) representing essentially all tissues of the body, which is known as promiscuous gene expression (pGE). This allows self-antigens, which otherwise are expressed in a spatially or temporally restricted manner to become continuously accessible to developing T-cells thus, rendering them tolerant to most self-antigens. The scope of central tolerance is to a large extent dictated by this pool of promiscuously expressed genes. Lack of a single TRA can result in spontaneous organ-specific autoimmunity. Therefore, it is important to define the scope of pGE and parameters/mechanisms that regulate this gene pool.

Promiscuously expressed genes display two prominent features: they are highly clustered in the genome and show a preference for TRAs. To link these features we focused on studying genes which are up-regulated in mature mTECs. The analysis was performed in mouse, rat and human in order to assess evolutionary conservation of pGE. Our analysis proceeded from the bioinformatic definition of TRA clusters, gene clustering and homology mapping via gene expression analysis using whole genome arrays to the in depth analysis of selected TRA clusters by RT-PCR at the population level. The mTEC compartment represents a mosaic of clonally derived mTEC clusters undergoing continuous renewal, whereby the sets of genes expressed in single mTECs ultimately add up to a complete representation of the promiscuous gene pool at the population level. Hence, we wanted to elucidate what dictates pGE at the single cell level, i.e. whether it was random or subject to rules of co-expression.

We observed that TRAs *per se* are clustered in the genome in all three species irrespective of structural relatedness or antigenic properties. Most of the clusters are localized in syntenic regions. In the thymus, the promiscuously expressed genes are enriched in TRAs that are partitioned into clusters, again conserved between species. These clusters harbor both TRAs and non-TRAs that are interspersed among each other. TRAs are preferentially regulated over non-TRAs during mTEC differentiation. Moreover, genes within a particular gene cluster are subject to partial co-regulation. Based on these data, we propose these clusters to be the "operational genomic unit" of pGE in the thymus.

Single cell studies of a mTEC subpopulation expressing a particular antigen revealed a deterministic component in the regulation of pGE. Co-expression groups in single cells not only defined intra-chromosomal but also inter-chromosomal (e.g. chromosome 1 and 19) gene co-regulation. Strikingly, these co-expression patterns correlated with *in situ* co-localization of the respective chromosomal domains upon mTEC maturation as analyzed by fluorescence *in situ* hybridization. Taken together, our data show that pGE is highly conserved between species, maps to gene clusters and is governed by certain co-expression rules at the single cell level.

Zusammenfassung

Medulläre Thymusepithelzellen (mTEZ), ein spezieller Zelltyp des Thymus, exprimieren ein höchst diverses Repertoire an gewebespezifischen Antigenen (*tissue restricted antigens,* TRAs), welche (vermutlich) jedes Gewebe des Körpers repräsentieren. Dieses Phänomen ist als promiske Genexpression (pGE) bekannt. PGE ermöglicht es, Selbst-Antigene, welche sonst nur in peripheren Geweben örtlich und zeitlich begrenzt exprimiert werden, den T-Zellen während ihrer Entwicklung im Thymus permanent zugänglich zu machen und dadurch Toleranzinduktion gegenüber diesen TRAs zu gewährleisten. Selbst das Fehlen eines einzigen Selbstantigens im Thymus kann zu einer spontanen organspezifischen Auto-immunantwort führen. Daher ist es wichtig, den Umfang des im Thymus exprimierten Genpools im Detail zu bestimmen und die Regulation dieser Genexpression zu verstehen.

Promisk exprimierte Gene zeigen zwei Charakteristika: Zum einen liegen sie im Genom größtenteils in Clustern vor, zum anderen sind die meisten von ihnen TRAs. Um eine mögliche Verbindung zwischen diesen Eigenschaften herzustellen, wurden Gene untersucht, deren Expression in reifen mTEZ im Vergleich zu unreifen mTEZ hochreguliert ist. Die Expression dieser Gene wurde in Maus, Ratte und Mensch vergleichend analysiert, um das Ausmaß der evolutionären Konservierung von pGE zu bestimmen. Die Analyse umfasste die bioinformatische Definition von TRA- und Gen-Clustern, das Erfassen von Homologien mittels genomweiter Genexpressionsanalysen und die detaillierte Untersuchung ausgewählter TRA-Cluster mittels RT-PCR auf der Ebene von Zellpopulationen. Diese Analysen ergaben, dass TRAs in allen untersuchten Spezies im Genom als Cluster organisiert sind unabhängig von ihren Funktionen und Struktur. Die meisten Cluster, die sowohl TRAs als auch Nicht-TRA beinhalten, liegen in syntenischen Regionen. Gene eines einzelnen Clusters war teilweise co-reguliert. TRAs in Clustern waren im Thymus häufiger exprimiert als Nicht-TRAs. Wir postulieren daher, dass diese Cluster die operationelle genomische Einheit darstellen, die der pGE im Thymus zugrunde liegt.

Das mTEZ-Kompartiment setzt sich aus einem Mosaik von mTEZ-Klonen zusammen, die sich ständig erneuern. Da die Gesamtheit promisk exprimierter Gene in der mTEZ-Population sich aus der Summe der pGE der einzelnen mTEZ-Klone zusammensetzt, ist es notwendig, die Regulation von pGE auf Einzelzellebene zu verstehen: Ist pGE auf Einzelzellebene ein völlig zufälliger Prozess oder werden Gene co-reguliert? Dazu wurden zusätzlich Analysen in Einzelzellen durchgeführt. Diese zeigten, dass Gengruppen in einzelnen Zellen entweder auf demselben oder auch auf unterschiedlichen Chromosomen co-reguliert werden. Dabei co-lokalisierten die Genloci von gemeinsam regulierten Gene *in situ,* wie mittels FISH Analyse gezeigt werden konnte. Wir schließen aus diesen Ergebnissen, dass pGE neben einer stochastischen auch eine deterministische Komponente beinhaltet.

Abbreviations

APS-1	autoimmune polyglandular syndrome type 1
APC	antigen presenting cell
aRNA	antisense RNA
ATP	adenosine tri-phosphate
BAC	bacterial artificial chromosome
BSA	bovine serum albumin
CD	cluster of differentiation
cDNA	complementary DNA
CLSM	confocal laser scanning microscopy
cRNA	complementary RNA
cTEC	cortical thymic epithelial cell
Cy	cyanine
DC	dendritic cell
DEPC	diethylpyrocarbonate
DN	double negative
DNA	deoxyribonucleic acid
DNase	deoxyribonuclease
DNMT	DNA-methyltransferase
dNTP	deoxyribonucleoside triphosphate
DP	double positive
DTT	dithiothreitol
dTTP	deoxythymidine-triphosphate
dUTP	deoxyuridine-triphosphate
EDTA	ethylene diamine tetra acetic acid
eGE	ectopic gene expression
FACS	fluorescence activated cell sorting
FISH	fluorescence *in situ* hybridization
FITC	fluorescein isothiocyanate
FCS	fetal calf serum
HEPES	4-(2-hydroxyethyl)-1-piperazineethanesulfonic acid
HPSF	high pure salt free
KO	knock-out
LPA	linear polyacrylamide
Lti	lymphoid tissue inducer cell
MACS	magnetic cell separation
MHC	major histocompatibility complex
mTEC	medullary thymic epithelial cell
$mTEC^{hi}$	mTEC expressing high levels of co-stimulatory molecules
$mTEC^{lo}$	mTEC expressing low levels of co-stimulatory molecules
PBS	phosphate buffered saline
PCR	polymerase chain reaction
PE	phycoerythrin
PerCP	peridinin chlorophyll protein
PFA	paraformaldehyde
pGE	promiscuous gene expression
PI	propidium iodide
psi	pound per square inch
qPCR	quantitative PCR
rpm	revolutions per minute
RAG	recombinase activating genes
RANKL	receptor activator for nuclear factor $\varkappa$ B ligand
RNA	ribonucleic acid
RPMI-1640	medium developed at Roswell Park Memorial institute
RT	reverse transcription
Sav	streptavidin
SC	single cell
SD rats	Sprague Dawley rats
SP	single positive
SSC	sodium saline citrate
TAE	tris-acetate EDTA
TCR	T-cell receptor
TRA	tissue-restricted antigen
Treg	regulatory T-cell
WT	wild type

1. Introduction

The immune system is a remarkably versatile defense system that has evolved to protect multi-cellular organisms from invading pathogens. The hallmark of all metazoan species is innate immunity, which primarily depends on the recognition of highly conserved pathogen associated molecular patterns (PAMPs) by germ line-encoded pattern recognition receptors. However, microorganisms continually develop new ways to evade host defense tactics that have been termed the "host-versus-pathogen arms race". This selective pressure presumably led to the evolution of a new, more sophisticated defense mechanism, called adaptive immune system (Cannon *et al.*, 2004; Flajnik and Du Pasquier, 2004). The adaptive immune system is capable of specifically recognizing an apparently limitless variety of foreign invaders owing to its ability to generate an enormous variety of cells and molecules that act together in a dynamic network whose complexity rivals that of the nervous system.

It was approximately 500 million years ago in jawed vertebrates that the adaptive immune system evolved the remarkable ability to mount specific immune responses to a virtually unlimited variety of antigens. The two arms of recombinatorial adaptive effector system are developmentally separated, but functionally intertwined lineages of clonally diverse lymphocytes. These are named T- and B-cells because they are generated in the thymus or in the avian bursa of Fabricius respectively (Cooper *et al.*, 1965; Cooper and Alder, 2006). For antigen recognition, both T- and B-cells use the same type of immunoglobulin domain (Ig)-based receptors. The T-cell receptors (TCR) and B cell receptors (BCR) are assembled during lymphocyte differentiation by somatic recombination of different variable (V), diversity (D) and joining (J) immunoglobulin (Ig) gene segments, imprecise V(D)J splicing, and insertion of non-template nucleotides at the junctions (Tonegawa, 1983; Yanagi *et al.*, 1984). As a consequence of this random rearrangement process potentially harmful receptors that recognize self constituents are also generated. Thus, to eliminate these auto-reactive lymphocytes, self-tolerance mechanisms are invoked to distinguish foreign from self, which is a fundamental feature of the adaptive immune system.

The T-cells which are one of the main players in adaptive immunity carry a highly diverse repertoire of TCRs which they use to recognize foreign- or self-antigens in combination with self major histocompatibility complex (MHC) (self-restriction of the T-cell repertoire). The generation, maturation and selection of this highly diverse T-cell repertoire occur in the thymus. In the thymus immature T-cells (designated thymocytes) undergo a strict quality control ensuring a repertoire of T-cells that under normal, i.e. healthy conditions does not attack and destroy host tissue (i.e. self-tolerant), but holds the competence to react to a vast range of foreign antigens. Thus, the function of the thymus which was only discovered in the early 1960s by Jacques Miller confers this fundamental self-tolerance (Miller, 1961).

1.1. The thymus

1.1.1. Evolution of the thymus

The appearance of the thymus in evolution is linked to the appearance of lymphocytes expressing highly diverse antigen-recognition receptors. T-cell development is strictly restricted to well-organized three-dimensional microenvironments of a specialized organ-the thymus, while B-cell development proved rather flexible with regards to its site, occurring in the bursa of Fabricius in birds, Ileal Peyer's patches in sheep, appendix in rabbits and bone marrow in mammals (Alitheen *et al.*, 2010). The thymus evolved as the primary lymphoid organ to allow the generation of a large MHC-restricted T-cell repertoire. Only T-cells required an autonomous, physically separated organ, and not merely a niche to develop and confine the destructive potential of T-cells (Rodewald, 2008).

Invertebrates and the most primitive vertebrates are not known to posses a thymus. Among vertebrates, the lowest showing key features of an adaptive immune system, such as re-arranging T- and B-cell receptor, *RAG* genes, MHC genes and a thymus, are the cartilaginous fish (jawed vertebrates, gnathostomes) like rays and sharks. The jawless (agnatha such as lamprey and hagfish), vertebrates have no thymus. They have been found to assemble diverse lymphocyte antigen receptor (VLRs) through gene conversion of leucine-rich repeat (LRR)-encoding modular units that are expressed on the surface of two distinct lymphocyte lineages (Cooper and Alder, 2006; Guo *et al.*, 2009). Thus, recombinatorial mechanisms for the generation of anticipatory receptors have evolved independently in both jawless and jawed vertebrates (Cooper and Alder, 2006).

The origin of the thymus in the inner layer of an embryonic gut ancestor is reminiscent of GALT (gut-associated lymphoid tissue), which is a key lymphoid structure in species prior to the appearance of a thymus. Thus, the thymus may have evolved as a GALT derivative (Du Pasquier, 1993). In the most primitive thymus-bearing species i.e. cartilaginous fish (rays and sharks), the thymus anlagen are located in the second to sixth pouch, whereas they are found in the second pouch in frogs, in the second and third in reptiles, and in the third and/or fourth in bony fish, birds and mammals. Thus, species are flexible in positioning of the thymus anlage somewhere along the pharyngeal foregut endoderm. Numbers and positions of the final thymus or thymi may also vary. Chickens have seven, sharks five, and urodele amphibians (e.g. salamander) three thymus pairs, while many teleost fish species, anuran amphibians (e.g. frogs), and many mammals have only one thymus composed of two bilateral lobes (Rodewald, 2008). In the end, irrespective of the number and positioning, the function of the thymus is T-cell development and the

selective elimination of potentially auto-reactive T-cells that is likely to be universal throughout all jawed vertebrates (Hansen and Zapata, 1998).

1.1.2. Cellular composition of the thymus

The thymus is the primary site for T lymphopoiesis, providing the essential niches and signals for maturing T-cells not only during the fetal stages of development but throughout postnatal life. The thymic structure and cellular composition is conserved throughout evolution (Anderson and Jenkinson, 2001) into anatomical separate compartments which include the sub-capsular area, the cortex, the cortical-medullary junction and the medulla (Figure 1). Thymic epithelial cells (TECs) constitute the major component of the stromal compartment and can be subdivided according to their function, morphology and specific antigen profile into different subpopulations- the cortical (c) and medullary (m) TECs. The different TECs together with other stromal cells of hematopoietic (dendritic cells, macrophages) and non-hematopoietic origin (fibroblasts and endothelial cells) form a three dimensional meshwork (Boyd *et al.*, 1993). The thymic stroma plays a key role at multiple stages of thymocyte development: on the one hand it ensures T-cell lineage specification of common lymphoid precursors and on the other hand it is essential for self-MHC restriction via positive selection and the elimination of auto-reactive T-cells via negative selection (Petrie, 2003; Starr *et al.*, 2003). "Thymic-cross-talk" between the thymic stromal cells and developing thymocytes is essential to provide appropriate signals for promoting and regulating thymocyte development and in turn thymocyte-derived signals are essential for the development of the stromal cell compartment (van Ewijk *et al.*, 1995; van Ewijk *et al.*, 2000).

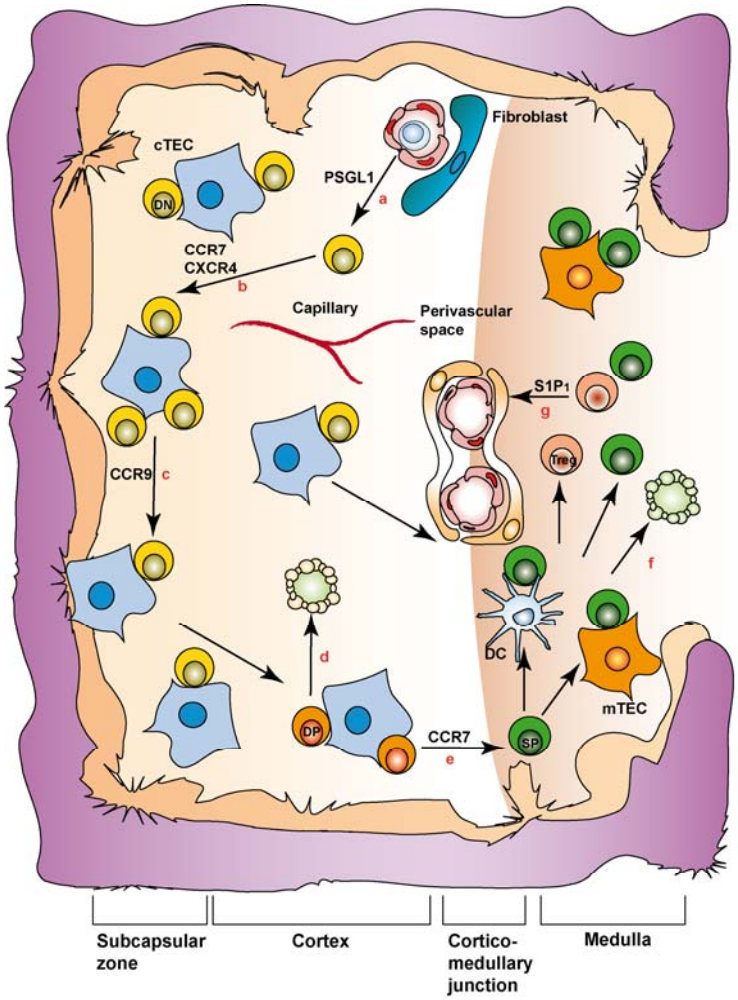

Figure 1

Cellular composition of and traffic of thymocytes within the thymus

In the post-natal thymus, **a)** circulating multi-potent lymphoid progenitors enter the thymus through the vasculature that is enriched around the cortico-medullary junction. This entry is regulated by (P)-selectin glycoprotein ligand 1 (PSGL1). **b)** They migrate towards the capsule as $CD4^-$ $CD8^-$ double-negative (DN) thymocytes, which is regulated by chemokine signals through CXC-chemokine receptor 4 (CXCR4) and CC-chemokine receptor 7 (CCR7). **c)** Further migration to the subcapsular region is mediated by CCR9 signals. **d)** These DN thymocytes go through a transition from DN to DP which is marked by the up-regulation of the CD4 and CD8 co-receptors. The double positive (DP) $CD4^+$ $CD8^+$ thymocytes expressing appropriate TCR$\alpha\beta$s, undergo positive selection. High-affinity interactions or lack of interactions result in deletion of thymocytes via apoptosis. **e)** Those that survive this selection differentiate into either CD4 or CD8 single-positive (SP) thymocytes. They show an increase in surface expression of CCR7, are attracted to the medulla by a gradient, where mTECs express CCR7 ligands. **f)** In the medulla, further selection (negative) of SP thymocytes includes the deletion of tissue-specific-antigen-reactive T-cells, survival of non-self reactive T-cells and the generation of regulatory T-cells. **g)** Mature SP T-cells express sphingosine-1-phosphate receptor 1 ($S1P_1$) through which the cells are attracted back to the circulation that contains a high concentration of sphingosine-1-phosphate. cTEC, cortical thymic epithelial cell; DC, dendritic cell; mTEC, medullary thymic epithelial cell. (Adapted from Takahama, 2006)

1.2. Thymocyte differentiation and selection

Most of the hematopoietic cell lineages undergo differentiation in the bone marrow, whereas T-cells develop within the thymus. This process consists of multiple steps that require a relocation of developing lymphocytes into the thymus (Figure 1). During their journey through the thymus, developing thymocytes pass several checkpoints at which they either die or survive until they are released to join the peripheral T-cell pool as mature T-cells.

1.2.1. Early T-cell development within the thymic cortex

The seeding of the thymus with lymphoid progenitor cells occurs in the area close to the cortico-medullary junction, where the vasculature is well developed (Lind *et al.*, 2001). This mechanism is not completely understood, however it has been reported that the seeding into the adult thymus is regulated by the adhesive interaction between platelet (P)-selectin glycoprotein ligand 1 (PSGL1), which is expressed by circulating lymphoid progenitor cells, and P-selectin, which is expressed by the thymic endothelium (Rossi *et al.*, 2005). Interestingly, the entry of lymphoid progenitor cells into the thymus is not a continuous event but an intermittent and gated event that occurs in waves during embryogenesis and in adulthood (Le Douarin and Jotereau, 1975; Havran and Allison, 1988; Fossa *et al.*, 2001).

Upon entry into the thymus, T-lymphoid progenitor cells begin to differentiate, proceeding through the double-negative (DN) stages of T-cell development (Benz *et al.*, 2008). These cells lack the expression of CD4 and CD8 and are named CD4/CD8 double-negative thymocytes (Scollay *et al.*, 1988). The DN T-lymphoid progenitor cells are commonly identified by the expression profiles of CD25 and CD44 (Pearse *et al.*, 1989; Shinkai *et al.*, 1992) and sequentially go through the DN1 ($CD44^+CD25^-$), DN2 ($CD44^+CD25^+$), DN3 ($CD44^-CD25^+$) and DN4/pre-DP ($CD44^-CD25^-$) stages. The survival and development of DN thymocytes are supported by Notch ligands (delta-like 4) and cytokines such as interleukin-7, both of which are produced by cTECs (Zuniga-Pflucker, 2004).

Along this developmental process, DN thymocytes migrate outward from the cortico-medullary junction to the sub-capsular region of the cortex (Lind *et al.*, 2001; Petrie, 2003). Chemokine receptors, especially CXCR4, CCR9 and CCR7, are important in this outward migration of DN thymocytes (Plotkin *et al.*, 2003; Benz *et al.*, 2004; Misslitz *et al.*, 2004). A prerequisite for directional cell migration is not only a gradient of an attractant, but also a substrate for cell adhesion. Adhesion molecules, such as integrins a4b1 and a4b7 expressed by DN thymocytes and

vascular cell adhesion molecule-1 (VCAM-1) expressed by cTECs mediate this adhesion. In addition, chemokines are critical for the "crawl" and are involved in the movement of DN thymocytes to the sub-capsular region (Prockop *et al.*, 2002).

DN1 cells have by far the longest single period of intra-thymic residence lasting for up to two weeks until they progress to the DN2 stage, during which they expand by about 1000-fold (Egerton *et al.*, 1990; Porritt *et al.*, 2003). In the thymic cortex, on their way to the sub-capsular region, DN thymocytes begin to rearrange their *Tcrβ* locus. The cells that succeed in generating an in-frame *Tcrβ* rearrangement begin assembling TCRβ and along with the invariant pre-TCRα chain form the cell-surface pre-TCR complex (von Boehmer and Fehling, 1997). This first checkpoint of thymocyte development known as β-selection allows cells to progress beyond the DN3 stage. This is marked by an up-regulation of the CD4 and CD8 co-receptors (Petrie and Zuniga-Pflucker, 2007). The transition from CD4/CD8 double negative to double positive immature T-cells is referred to as DN4 or pre-DP stage. They show a low expression of CD25 and CD44 and are immediate precursors to CD4/CD8 double-positive (DP) thymocytes (Petrie and Zuniga-Pflucker, 2007). The rearrangement of the TCRα gene locus is initiated only after a massive expansion of cells carrying a functional pre-TCR. During this expansion phase, the Rag genes are turned off to prevent any premature rearrangements of the TCRα locus. The expression of the pre-TCR complex on the cell surface along with Delta-Notch interactions, initiate the signals for further development to DP thymocytes that express αβTCR antigen receptors (Zuniga-Pflucker, 2004). The DP thymocytes expressing a αβTCR in the cortex constitute the unselected repertoire of T-cells (Jameson *et al.*, 1995).

1.2.2. Positive selection

Highly motile DP thymocytes pause to interact through their TCR with peptide-MHC complexes that are expressed on cTECs (Bousso *et al.*, 2002; Ehrlich *et al.*, 2009). Following TCR recognition of peptide-MHC ligands with low-affinity, DP thymocytes receive signals for survival and further differentiation into single-positive (SP) thymocytes. This second checkpoint, referred to as positive selection, enriches for 'useful' T-cells that recognize self-MHC molecules. High-affinity interactions result in deletion of thymocytes via apoptosis, this process contributes to the deletion of self-reactive T-cells. DP thymocytes which fail to receive TCR signals are also destined to die at this stage. Only 3-5 % of developing thymocytes survive this checkpoint of T-cell development at the cortical DP-thymocyte stage (Egerton *et al.*, 1990; Goldrath and Bevan, 1999).

1.2.3. CD4/CD8 lineage commitment

Concomitantly with positive selection occurs the so-called CD4/CD8 lineage choice in which thymocytes either differentiate into MHCII-restricted CD4 or MHCI-restricted CD8 single positive (SP) T-cells. This decision-making process is not yet fully understood. Two models have been proposed based on a stochastic or instructive mechanism of lineage choice.

Both models are based on the assumption that the selective termination of one or the other co-receptor irreversibly defines the lineage fate. The stochastic selection model suggests that the termination of CD4 or CD8 co-receptor gene expression during positive selection of DP thymocytes occurs randomly and thymocytes receive a second TCR rescue signal in case the expression of the right co-receptor was maintained, otherwise they die. The instructional model suggested that MHCI- and MHCII-restricted TCR signals are distinct from one another with respect to signal strength. A modification of the instructive model is the kinetic model which poses that the duration of the TCR signal and not the signal strength determines the lineage choice. TCR signals of long duration result in CD4 expression, short TCR signals result in CD8 expression. The kinetic model is the most compatible with experimental data (Singer *et al.*, 2008).

The positively selected thymocytes then begin relocating from the cortex to the medulla (Witt *et al.*, 2005). The CCR7 ligands (CCL19 and CCL21), predominantly produced by mTECs, were shown to be involved in the chemotactic attraction of these cells into the medulla (Ueno *et al.*, 2004). It was recently shown that CCR7-mediates chemotaxis of CD4 SP cells towards the medulla can be separated from migration into the medulla which is under the control of distinct G protein-coupled receptors (GPCR). Both CCR7 and GPCR act in concert to properly target CD4 SP cells to the medulla (Ehrlich *et al.*, 2009).

1.3. Central tolerance

It was more than 100 years ago that the clonal selection theory by Paul Ehrlich first conceptualized the problem of self-reactivity ('horror autotoxicus') as inherent to the adaptive immune system and postulated the existence of mechanisms (contrivances) that could prevent deleterious self-reactivity. It took eighty years of work and great advance in immunology until the paradigm of "developmental tolerance" was demonstrated in the chicken/quail model by Le Douarin and associates. They found that embryonic tissues from quail engrafted into age-matched chickens were rejected soon after birth and more importantly, this graft rejection could be prevented by solely transplanting thymic rudiments from the graft donor (Ohki *et al.*, 1987). Subsequent studies in mice demonstrated that transplantation of the thymus anlage, i.e., pure thymic epithelium, confers tolerance to transplanted tissues such as limb buds or skin

(Salaun *et al.*, 1990; Le Douarin *et al.*, 1996; Salaun *et al.*, 2005). In addition, neonatal thymectomy up to day 3 was shown to lead to a multiorgan autoimmune syndrome including gastritis, sialadenitis, hepatitis, and diabetes (Asano *et al.*, 1996). At that time, the mechanism how thymic epithelium can induce tolerance to a wide spectrum of peripheral antigens was not understood. In 1989 Linsk *et al.* proposed on pure theoretical grounds that the thymus represents a patch quilt of ectopically expressed genes (Linsk *et al.*, 1989).

It was long believed that the pool of self-epitopes available for T-repertoire selection comprises ubiquitous antigens and antigens specific to the various types of thymic antigen-presenting cells (APCs). Moreover, self-antigens were known to gain access to the thymus either via the circulation or by association with immigrating cells (Kyewski *et al.*, 1984; Klein and Kyewski, 2000b; Klein *et al.*, 2009). The first impactful evidence for ectopic expression of insulin in wild type mice was reported by Hanahan and colleagues (Jolicoeur *et al.*, 1994) in a study of tolerance toward antigens implicated in diabetes. This seminal study was supported over the years by several reports showing the existence of specialized peripheral antigen expressing cells in the thymus (Pribyl *et al.*, 1996; Wakkach *et al.*, 1996; Egwuagu *et al.*, 1997; Kojima *et al.*, 1997; Pugliese *et al.*, 1997; Hanahan, 1998; Heath *et al.*, 1998; Klein *et al.*, 1998; Sospedra *et al.*, 1998; Mallet *et al.*, 1999; Klein *et al.*, 2000; Diez *et al.*, 2001; Bruno *et al.*, 2002). Direct proof of the expression of a highly diverse set of TRA (tissue-restricted antigens) representing essentially all tissues of the body by medullary thymic epithelial cells (mTECs) within the thymus was shown by two groups (Derbinski *et al.*, 2001; Anderson *et al.*, 2002). This phenomenon of "promiscuous gene expression" (pGE) allows self-antigens, which are expressed in a spatially or temporally restricted manner (such as pregnancy- or puberty-associated self-antigens) to become continuously accessible to developing T-cells (Derbinski *et al.*, 2005), thus rendering the T-cell repertoire self-tolerant (pGE, is described in more detail in later chapters).

Two modes of how auto-reactive T-cells are directly rendered harmless were shown; first T-cells are clonally deleted from the repertoire, a hallmark of T-cells central tolerance (negative selection) and second potentially harmful T-cells are silenced by undergoing anergy. "Clonal anergy" involves the functional inactivation of self-reactive T-cells. There are several mouse models supporting this model (Ramsdell *et al.*, 1989). It should be added that the molecular definition of anergy lags behind its functional characterization (Mueller, 2010).

1.3.1. Negative selection

Negative selection is the third and last checkpoint, which is crucial for the induction of tolerance to self-antigens (central T-cell tolerance). In this process, autoreactive SP thymocytes are removed from the repertoire. In 1987, Marrack *et al.* showed that T-cells carrying the Vβ17a TCR chain were deleted in animals expressing super-antigens derived from the mouse mammary tumor virus and presented in the context of I-E MHC molecules, while the same T-cells normally matured and migrated to the periphery in the absence of super-antigens. Thus, for the first time clonal deletion of T-cells that recognized antigen in the thymus was reported (Kappler *et al.*, 1987). The clonal deletion model was further validated in various TCR transgenic mouse models expressing a receptor for a self-antigen along with the corresponding self-antigen (e.g. Hemagglutinin, HA) or a naturally expressed antigen (e.g. H-Y) (Starr *et al.*, 2003).

SP thymocytes migrating from the cortex to the medulla are negatively selected through high-affinity interactions with peptide-MHC presenting APCs, which lead to apoptosis. This clonal deletion of self-reactive thymocyte occurring mainly in the medulla is induced by mTECs and DCs. MTECs do so by promiscuous gene expression while DCs can cross-present mTEC derived self-peptides (Lo and Sprent, 1986; Marrack *et al.*, 1988; Matzinger and Guerder, 1989; Gallegos and Bevan, 2004; Kyewski and Derbinski, 2004; Koble and Kyewski, 2009). Gallegos *et al.* showed that presentation of Ova peptide exclusively by mTECs allowed deletion of cognate $CD8^+$ T-cells. It was only for the deletion of Ova specific $CD4^+$ T-cells, that cross-presentation of Ova on DCs was indispensable (Gallegos and Bevan, 2004). Thus, clonal deletion can be induced autonomously by mTECs and DCs, but different thresholds for deletion may exist.

Several co-stimulatory cell surface molecules like CD28, CD5, CD43, CD40 and Fas have been described to play a role in the induction of negative selection (Punt *et al.*, 1994; Kishimoto and Sprent, 1999; Williams *et al.*, 2002). It has also been reported that CCR4 ligands, TSLP, CCL17 and CCL22 expressed in the medulla by Hassall's corpuscles, DCs and mTECs play a role in establishing central tolerance, though the precise function still remains obscure (Takahama, 2006).

The SP thymocytes spend approximately 4 days in the medulla where they presumably scan a sufficient number of APCs to cover the entire self-antigen repertoire presented by these APCs before being exported from the thymus (McCaughtry *et al.*, 2007). Negative selection is believed to occur mainly in the medulla or at the cortical-medullary junction (Sprent, 2005). This process involves several synergistic events including the activation of the JNK/p38 pathways which leads to the induction of the pro-apoptotic factors- BIM, Bax and Bak, ultimately resulting in induced cell death which is the basis of negative selection (Bouillet *et al.*, 2002; Rathmell *et al.*, 2002).

1.3.2. Dominant tolerance - regulatory T-cells

The mechanisms of T-cell tolerance described above act by elimination or inactivation of a given T-cell specificity and thus can be defined as "recessive" (cell-intrinsic) mechanisms. Yet self-reactive T-cells exist in the normal periphery despite the existence of deletion operative in the thymus (Sakaguchi *et al.*, 2007). Obviously, central tolerance mechanisms do not cripple all self-reactive T-cells, thus raising the question of the existence of additional mechanisms of tolerance to keep these cells in check. Efforts in the 1980s propounded another mechanism of self-tolerance, namely "dominant tolerance" (trans-acting), in which regulatory T-cells actively and dominantly suppress lymphocytes, in particular the self-reactive T-cells that exist in the normal periphery. Three main cell types have been considered as potential regulatory T-cell subsets: $CD4^+CD25^+$ regulatory T-cells (Treg), $CD8\alpha\alpha^+$ intestinal epithelial lymphocytes and natural killer T (NKT) cells. All are thought to be induced by cognate recognition of self-peptide-MHC in the thymus (Baldwin *et al.*, 2004; Hogquist *et al.*, 2005).

It was in the early 1970s that Gershon demonstrated that T-cells not only enhance but also suppress immune responses to exogenous antigens (Gershon and Kondo, 1970). Treg cells were first recognized as natural controllers of self-reactive T-cells and characterized by $CD25^+CD4^+$ and were later shown to specifically express the transcription factor FoxP3. The deficiency of Tregs produces autoimmune disease and also other aberrant or excessive immune responses to non-self antigens (Sakaguchi, 2005).

$Foxp3^+$ Treg cells make up 5-10 % of the peripheral $CD4^+$ T-cell repertoire and are generated in the thymus (natural Tregs) but also in the periphery from naive T-cells (induced Tregs). In the thymus, $Foxp3^+$ cells are detected as early as late $CD4^+CD8^+$ double-positive to $CD4^+CD8^-$ single-positive stages (Fontenot *et al.*, 2005). The interaction of developing thymocytes with thymic stromal cells activates a transcriptional program in parallel with or upstream of Foxp3. Once the Foxp3 gene is switched on, Foxp3 may stabilize and sustain the Treg cell phenotype and confer suppressive activity (Gavin *et al.*, 2007). It has been suggested that Treg fate is instructed by high-affinity/avidity self-reactive TCRs for self-antigens, which is just below the threshold for negative selection (Maloy and Powrie, 2001; Hogquist and Moran, 2009), as discussed in the next chapter (Figure 2). Recent studies show that TCR repertoires of Treg cell and conventional T-cell overlap, although according to different studies the extent of overlap varies (Pacholczyk *et al.*, 2006; Pacholczyk *et al.*, 2007). Thus, it appears that additional signals and molecules seem to play a role in the branching of Treg lineage from the conventional developing thymocyte.

MTECs were hypothesized to be the major Treg-inducing cells but other APCs such as cTECs or DCs were also considered (Bensinger *et al.*, 2001; Watanabe *et al.*, 2005). The absence of mature mTECs due to deficiency of NF-κB kinase or TRAF6, which transduce CD40 signals from the TNF receptor family, hampers Treg cell development (Kajiura *et al.*, 2004; Akiyama *et al.*, 2005). Aschenbrenner *et al.* directly showed mTECs to be able to generate Tregs (Aschenbrenner *et al.*, 2007). Presently it is known that thymic epithelial cells as well as different thymic DC-subtypes can efficiently induce Treg development of immature thymocytes, albeit strikingly different optimal doses of cognate antigen were needed in *in vitro* studies (Wirnsberger *et al.*, 2009). A combination of factors, TCR affinity/avidity and the time point of Treg induction by different APCs seem to matter.

Notably, Treg cell deficiency and Aire deficiency produce a similar spectrum of autoimmune diseases (Anderson *et al.*, 2002; Kuroda *et al.*, 2005). It is supposed, however not formally shown, whether Aire deficiency affects the generation of tissue-restricted antigen-specific Foxp3$^+$ Treg cells in addition to its established effect on negative selection of tissue-restricted antigen-specific self-reactive T-cells. The significance of central tolerance processes has been highlighted in two inherited autoimmune syndromes. In both cases, the affected molecules are transcriptional regulators that are crucial for these two distinct central-tolerance mechanisms (recessive and dominant): mutations in the autoimmune regulator-*AIRE* gene lead to defective pGE and as a result a defective clonal deletion of auto-reactive T-cells resulting in a multi-organ syndrome known as autoimmune polyendocrinopathy-candidiasis-ectodermal-dystrophy (APECED) (Villasenor *et al.*, 2005), whereas mutations in the forkhead box P3 (*FOXP3*) gene impairs the development of Treg cells causing immune deficiency-polyendocrinopathy-X-linked syndrome (IPEX) (Sakaguchi, 2005). Although, there are various peripheral mechanisms (not described in this thesis) that control self-reactive lymphocyte, central-tolerance mechanisms, are essential for the maintenance of self-tolerance. Foxp3$^+$ Treg cells bridge central and peripheral tolerance. The two tolerance mechanisms are complementary as Aire$^{-/-}$Foxp3$^{-/-}$ mice show a faster and more extensive disease than either Aire$^{-/-}$Foxp3$^{+/+}$ or Aire$^{+/+}$Foxp3$^{-/-}$ mice (Chen *et al.*, 2005; Mathis and Benoist, 2010).

1.4. Models of selection of the T-cell repertoire which is self-MHC restricted and self-tolerant

At present there are two hypotheses based on the avidity or the affinity of the TCR-peptide-MHC interaction. The avidity model predicts that the quantity of peptide-MHC complexes expressed by cTECs dictates whether a thymocyte expressing an interacting TCR will be positively selected or deleted, whereas the affinity model instead postulates a crucial role of the quality of the individual TCR-peptide-MHC interaction. Fetal thymic organ culture (FTOC) with

very low concentrations of antigenic peptide could mediate positive selection, while high avidity interactions promoted cell death, thus, supporting the avidity model (Sebzda *et al.*, 1994). Other studies clearly speak in favor of the affinity hypothesis. Irrespective of whether the selecting peptide was related or not, *in vitro* studies supported the idea that the TCR affinity for ligands mediating positive selection was much lower than for negative selection (Hogquist *et al.*, 1994). More recent refinements of the affinity model suggest a very small window of affinity defining whether a thymocyte is positively or negatively selected (Daniels *et al.*, 2006). Additionally, thymocytes having a TCR with an affinity too low to interact sufficiently with any self-protein/MHC complex undergo apoptosis, an event also termed as 'death by neglect'. Thymocytes having a high affinity (higher than those positively selected but lower than those negatively selected) may become natural Tregs (Figure 2). Nevertheless, Tregs require additional signals to commit to the Treg lineage.

A recent study by Hinterberger, M. provided evidence for the avidity model of Treg induction. She showed that high antigen dose presented by mTECs lead to deletion of specific T-cells, whereas lower antigen doses on mTECs favored Treg development at the expense of negative selection. The optimal antigen dose might vary between different TCR affinities as well as between different APC, i.e. DC and mTECs. Thus, there is a window of avidity for the development of Tregs that might partially overlap with positive selection or negative selection. This could explain why negative selection and Treg induction of T-cells with the very same TCR occurs in parallel *in vivo* (Hinterberger, 2009). There appears to be a balance between Treg induction and negative selection, which is shifted to the one or the other direction depending on the availability of the given antigen and the overall avidity.

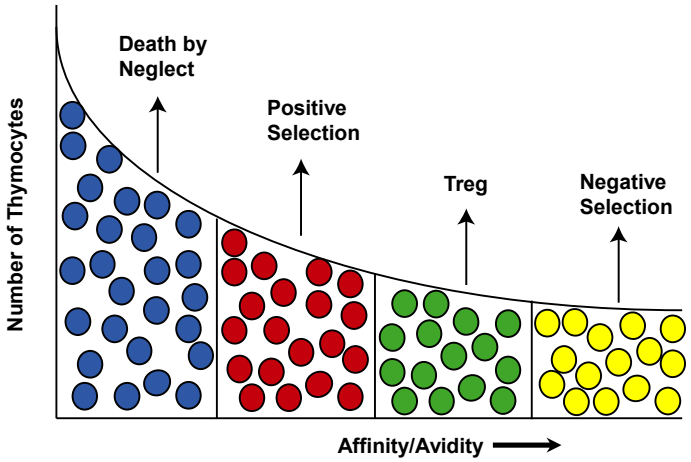

Figure 2

The affinity/avidity model of thymocyte selection

The affinity/avidity of the T-cell receptor for self-peptide-MHC ligands is a crucial parameter that drives the developmental outcome of T-cell selection. Progenitors having no affinity or very low affinity will die by neglect. This is the fate of most thymocytes. If the TCR has a low affinity/avidity for self-peptide-MHC, the progenitor survives and is positively selected. If the progenitor has a higher affinity/avidity for self-peptide-MHC, it may lead to clonal deletion or differentiate into a 'regulatory'-cell phenotype-Treg. It is not exactly known what determines whether an individual T-cell is tolerized by negative selection or is selected to become a regulatory T-cell. (Adapted from Hogquist *et al.*, 2005)

Another controversial issue of T-cell selection is the nature of the peptides presented in the cortex that are required for positive selection. The so-called "altered peptide hypothesis" suggested that the ligands presented by cTECs differ from those presented in the medulla and in the periphery. Previous findings did not support an altered peptide hypothesis, though several recent studies changed this view. They indicate that cTECs generate MHC-bound peptides through pathways distinct from other APCs (i.e. peripheral and thymic medullary, also mTECs) (Klein *et al.*, 2009). First evidence for a distinct proteolytic pathway was the detection of a cTEC-specific endoprotease, Cathepsin L that was critical for $CD4^+$ T-cell development, presumably generating peptides for MHCII suitable for positive selection (Nakagawa *et al.*, 1998). Similarly, a cTEC-specific serine protease TSSP was identified, whose inactivation lead to the decreased positive selection of some transgenic TCRs (Gommeaux *et al.*, 2009). Recently, a cTEC-specific thymoproteosome was identified which is essential for normal CD8 T-cell development (Murata *et al.*, 2007; Nitta *et al.*, 2010). Furthermore, another study by the Klein group showed the

importance of macroautophagy in the generation of certain but not all peptide-MHCII complexes for positive selection (Nedjic *et al.*, 2008). It is argued that the generation of a unique set of self-peptides for positive selection would prevent a disproportionately large fraction of SP cells to be subject to clonal deletion due to the re-encounter of the same/shared peptides on mTECs or DCs that promoted their positive selection. Such an "excessive" loss of T-cells could have resulted in an evolutionary pressure on cTECs to evolve mechanisms for an altered peptide generation (Klein *et al.*, 2009).

1.5. MTEC differentiation and promiscuous gene expression (pGE)

In order to render T-cells tolerant to most self-antigens, developing T-cells are presented with a comprehensive repertoire of antigens by thymic APCs including spatially and temporally restricted antigens. It was in 1989 that Linsk *et al.* proposed that the thymus represents a patch quilt of ectopically expressed genes (Linsk *et al.*, 1989). Efforts since then put forth the present scenario in which a specific subset of thymic stromal cells - mTECs - express a highly diverse set of tissue-restricted antigens (TRAs) representing essentially all tissues of the body, a phenomenon which is known as "promiscuous gene expression" (pGE) (Derbinski *et al.*, 2001; Anderson *et al.*, 2002). This allows self-antigens to become continuously accessible to developing T-cells.

PGE is a characteristic feature of mTECs, though a less pronounced expression of tissues specific transcripts could be detected in other thymic APCs; mTECs show the highest expression of promiscuous genes, followed by cTECs, thymic DCs and macrophages (Gotter *et al.*, 2004; Derbinski *et al.*, 2005). MTECs are highly heterogeneous with regard to ectopic gene expression as only 1-3 % of all mTECs express a given antigen at the protein or mRNA level (Smith *et al.*, 1997; Hanahan, 1998; Derbinski *et al.*, 2001; Klein *et al.*, 2001; Avichezer *et al.*, 2003; Chentoufi *et al.*, 2004; Cloosen *et al.*, 2007; Taubert *et al.*, 2007; Derbinski *et al.*, 2008).

1.5.1. MTEC development

During mouse development, the thymic anlage arises from the third pharyngeal pouch around E10, with the potential to generate both cortical and medullary structures (Bennett *et al.*, 2002). Recent studies indicate that a common TEC progenitor can give rise to both lineages during embryonic thymogenesis and during adulthood (Bleul *et al.*, 2006; Rossi *et al.*, 2006). The early thymus development occurs independently of thymocytes, showing that TEC differentiation is either cell autonomous or involves input from additional non-hematopoietic and/or non-T-lineage hematopoietic cells (Klug *et al.*, 2002; Jenkinson *et al.*, 2005). In addition, it was found that the neural crest-derived mesenchyme and its product, fibroblast growth factor (FGF) is crucial

for early thymus organogenesis and thymus function (Jenkinson *et al.*, 2003). A member of the forkhead family of transcription factors, Foxn1 is necessary to direct differentiation of bipotential progenitor cells into fully functional TECs and to date is the only marker that identifies early thymic epithelial cell commitment (Nehls *et al.*, 1996; Bleul *et al.*, 2006). Reversion of a conditional allele of Foxn1 to wild-type function in single cells *in vivo* leads to the formation of either delineated mTEC clusters ("clones"), cTEC clusters or both suggesting the existence of bi- and uni-potent precursors in the postnatal thymus. Hence, from these data one can envisage two scenarios, the first being a self-renewing bipotent precursor that gives rise to two lineage-committed and transient precursors without self-renewing capacity (Figure 3). Alternatively, a committed precursor may have limited self-renewing capacity thus replenishing a finite precursor pool throughout adult-hood without resorting to bipotent TEC stem cells (Anderson *et al.*, 2007).

MTECs can be subdivided into three populations based on their expression of the co-stimulatory molecules CD80, MHCII and the transcriptional regulator Aire with the sequential order of differentiation: $CD80^{lo}MHCII^{lo}Aire^{-}$ mTECs, $CD80^{hi}MHCII^{hi}Aire^{-}$ mTECs and $CD80^{hi}MHCII^{hi}Aire^{+}$ mTECs. PGE increases in this order (i.e. the ability to express a larger and more diverse array of TRAs), being highest in $Aire^{+}$ mTECs (Figure 3). PGE is largely governed by the transcriptional regulator Aire and is crucial for central tolerance (Anderson *et al.*, 2002; Derbinski *et al.*, 2005; Johnnidis *et al.*, 2005; Gray *et al.*, 2007).

There have been debates as to whether $MHCII^{hi}$ expressing mTECs represent the most mature terminally differentiated cell or immature cell subset. Two models have been proposed: the "developmental or progressive restriction model" contends that immature mTECs transcribe the greatest number and diversity of promiscuous genes, and can be thought of as "multi-potential." As a consequence of Aire expression, the cells would be provoked to differentiate according to peripheral epithelial cell type specific programs, during which each mTEC would follow one particular pathway and pGE would be progressively restricted to adhere to that program (Gillard and Farr, 2005). An alternative explanation, the "terminal differentiation model", proposes a hierarchy in pGE based on the mTEC differentiation stage: as these cells mature from an $Aire^{-}CD80^{lo}MHCII^{lo}$ (immature) stage to the end-stage $Aire^{+}CD80^{hi}MHCII^{hi}$ (mature), they would transcribe and display the highest degree and diversity of pGE. According to this model, single mTECs would express TRAs of mixed tissue origin rather than emulating cell lineage-affiliated patterns (Derbinski *et al.*, 2005). In recent years there has been accumulating evidence that strongly supports the "terminal differentiation model". For example Gray and colleagues showed that $MHCII^{lo}$ mTECs contain actively dividing cells while $Aire^{+}$ $MHCII^{hi}$ mTEC cells are post-mitotic and undergo apoptosis within a few days (Gray *et al.*, 2007). The turnover of $MHCII^{hi}$ mTECs was recently shown to be around 3 weeks (Gabler *et al.*, 2007). This post-mitotic cell population had a longer half-life in the absence of Aire (in $Aire^{-/-}$ mice). Thus, Aire has been implicated in mediating apoptosis in post-mitotic mTECs (Gray *et al.*, 2007; Dooley *et*

al., 2008). It remains an unresolved issue why Aire^{+} mTECs are driven into apoptosis. One possible explanation would be that the overload of the transcription and translation machinery (due to pGE) may lead to apoptosis of Aire^{+} mTECs and the other would be that Aire promotes DNA double-stranded breaks, that would incite the DNA-damage response, thus providing an explanation for induction of mTEC death (Kyewski and Derbinski, 2004; Ferguson *et al.*, 2008; Abramson *et al.*, 2010).

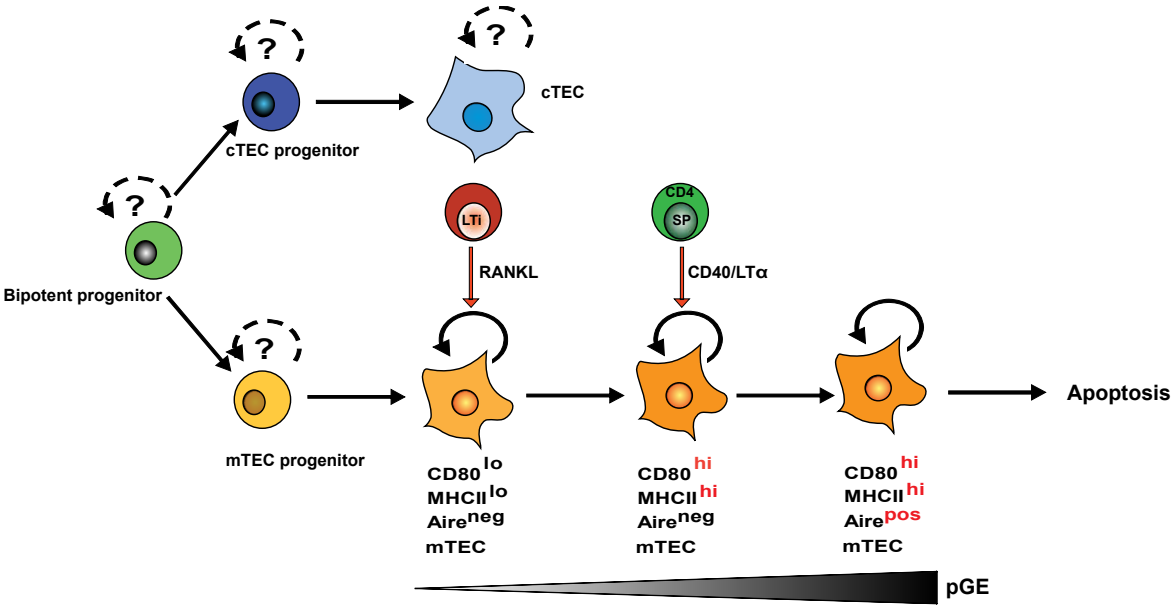

Figure 3

Development and differentiation of TEC subpopulations

CTECs and mTECs are derived from a common self-renewing bipotent progenitor that gives rise to two lineage-committed, transient precursors with/without self-renewing capacity. Further, the progenitor differentiates from immature MHCII^{lo} mTECs to Aire^{-} MHCII^{hi} mTECs to finally form the mature Aire^{+} MHCII^{hi} mTECs. During embryogenesis mTECs receive critical RANKL signals from lymphoid tissue inducer cells. Postnatally the CD4 SP thymocytes provide RANKL, CD40 and lymphotoxin signals. As the mTECs mature, the level of pGE increases and finally terminally differentiated Aire^{+} MHCII^{hi} mTECs are driven into apoptosis (Adapted from Tykocinski *et al.*, 2008).

The identification of precursor-progeny relationships and different stages of mTECs that are developmentally connected is important in elucidating the checkpoints that regulate formation of thymic microenvironments and provides an opportunity to identify the molecular mediators. Early TEC development is independent of thymocytes, proper cTEC and mTEC development however requires "cross-talk" with T-cells. Several molecules and pathways have been implicated in mTEC development. The NF-κB pathway plays an important role in mTEC development.

Inactivation of the TNF receptor-associated factor TRAF6 or the NF-κB complex component RelB and NF-κB inducing kinase (NIK) severely disrupted mTEC development and medulla formation (Burkly *et al.*, 1995; Boehm *et al.*, 2003; Kajiura *et al.*, 2004; Akiyama *et al.*, 2005; Tykocinski *et al.*, 2008). Also, the receptor activator of NF-κB (RANK) expression by mTECs, is directly responsible for differentiation of $Aire^+$ mTECs (Rossi *et al.*, 2007). During fetal thymus development, lymphoid tissue inducer cells were identified as a key population of RANK ligand (RANKL)-expressing cells. Subsequent studies have shown a role for RANK and CD40 in postnatal thymic maintenance and development of adult mTECs (Akiyama *et al.*, 2008; Hikosaka *et al.*, 2008; Irla *et al.*, 2008). Interestingly in the adult thymus both RANKL and CD40L are provided by $CD4^+CD8^-$ thymocytes (Hikosaka *et al.*, 2008; White *et al.*, 2008). The lymphotoxin-β receptor (LTβ-R) was also initially thought to induce development of $Aire^+$ mTECs (Chin *et al.*, 2003), though others showed that this was not the case although LTβ-R signalling clearly influences some aspects of mTEC development (Boehm *et al.*, 2003; Martins *et al.*, 2008; Seach *et al.*, 2008). Collectively these data imply the persistence of a common TEC progenitor throughout life that can finally differentiate into mature cTEC and mTEC lineages through signalling pathways that are non-redundant but complementary and share common second messengers.

1.5.2. The role of Aire in pGE

The importance of the transcriptional regulator Aire in tolerance was revealed in the genetic analysis of a rare autosomal recessive disorder, autoimmune polyendocrinopathy-candidiasis ectodermal dystrophy (APECED). Over 60 mutations have by now been localized in the *AIRE* gene of different APECED patients (Mathis and Benoist, 2009). Affected patients develop a spontaneous autoimmune disease targeted primarily at endocrine organs including the parathyroids, adrenals, thyroid, ovaries and pancreatic islets (Vogel *et al.*, 2002). After the generation of Aire-deficient mice, it became clear that Aire is directly linked to central tolerance and loss of Aire resulted in the development of multi-organ immune infiltrates and autoantibodies (Anderson *et al.*, 2002; Ramsey *et al.*, 2002; Kuroda *et al.*, 2005). Within the thymus, several studies have consistently demonstrated that Aire is restricted to mTECs and DCs (Derbinski *et al.*, 2001; Anderson *et al.*, 2002). It was these initial observation that lead to the speculation that Aire might control TRA expression in the thymus (Klein and Kyewski, 2000a). This was confirmed by detailed analysis using microarrays. Aire controls the expression of a large set (hundreds or thousand) of TRAs in mTECs (Anderson *et al.*, 2002; Derbinski *et al.*, 2005; Johnnidis *et al.*, 2005). It was however observed that even lack of a single TRA can result in organ-specific autoimmunity as shown in the case of an eye-specific antigen (IRBP), stomach-specific antigen (Mucin 6) and insulin (DeVoss *et al.*, 2006; Gavanescu *et al.*, 2007; Fan *et al.*, 2009).

Aire targets an unusually diverse set of genes that are highly enriched in tissue-specific genes and preferentially clustered in the genome. The precise molecular mechanism of Aire's action is still unclear. It was observed that Aire is necessary but not sufficient for transcription of its target genes in single-mTECs and their expression appears to be stochastic (Derbinski *et al.*, 2008). Moreover, a number of Aire-dependent genes have been identified which are expressed independently of their tissue-specific transcription factors in mTECs. Regulation of these genes thus differs between the peripheral tissue and their ectopic expression in mTECs. It is therefore perhaps not surprising that different transcriptional start sites are used in the thymus and periphery (Villasenor *et al.*, 2008).

Previous studies from several groups show Aire to have multiple potentials (Peterson *et al.*, 2008; Tykocinski *et al.*, 2008; Kyewski and Peterson, 2010). Recently, the Mathis group screened for Aire interaction partners and identified a large set of proteins that associate with Aire. They fell into four major functional classes involving nuclear transport, chromatin binding/structure, transcription and pre-mRNA processing. They speculate that after translocation in the nucleus through the nucleopore complex, Aire preferentially localizes to transcriptionally inert chromatin regions via binding to unmethylated H3/4 tails, thus conferring targeting of specific genes. Within these regions, it interacts with TOP2a to promote DNA double-stranded breaks, activates DNA-PK and other partners and in turn attracts chromatin remodeling complexes. Several of these Aire-interactors might also participate in the so-called "eviction complex" that removes H2A-H2B dimer in front of RNAPII as it proceeds along nucleosome-packaged DNA, and reassembles the octamer behind, thereby enhancing elongation efficiency. Additionally, Aire-containing complex would promote the accumulation of fully mature mRNA by re-activating RNAPII stalled at the 5' end, by suppressing improperly initiated transcripts, and/or by stabilizing short-lived pre-mRNAs through proper splicing (Abramson *et al.*, 2010).

Two recent papers showed the expression of Aire in peripheral lymphoid stromal cells. Lee *et al.* described a population of lymph node stromal cells expressing a repertoire of TRA transcripts that overlaps quite a bit, with that of thymic mTECs (Lee *et al.*, 2007). Gardner *et al.* also found TRA transcripts in stromal cells residing in both the lymph nodes and spleen (Gardner *et al.*, 2008). The repertoire of TRA transcripts in these stromal cells appeared to be of limited diversity and seemed rather distinct from that of thymic mTECs. Till date the physiological relevance of this phenomenon is unknown, though there are speculations that Aire participates in peripheral tolerance.

1.6. Objective of this study

In view of the essential role of pGE by mTECs in negatively selecting T-cells, this project aimed at studying certain aspects of the regulation of pGE. The scope of central tolerance is to a large extent dictated by the pool of promiscuously expressed genes. Promiscuous genes expressed at sufficient levels will induce self-tolerance. More so, lack of a single TRA can result in spontaneous organ-specific autoimmunity. Therefore, it is important to precisely define the scope of pGE and parameters/mechanisms that regulate this gene pool. Promiscuously expressed genes display two prominent features: they are highly clustered in the genome and show a preference for TRAs. To link these features it was set out to precisely define the genomic organization of this gene pool in mouse, rat and human. In particular, we probed to what extent and according to which rules predefined genomic clusters of TRAs are transcribed in mTEC subsets (immature and mature mTECs). Our analysis proceeded from the bioinformatic definition of TRA clusters, gene clustering and homology mapping via gene expression analysis using whole genome arrays to the in depth analysis of selected TRA clusters by RT-PCR at the population level.

Promiscuous genes expressed in single mTECs is to some degree stochastic with a heterogeneous pattern, that in sum all patterns add up resulting in a constant, complete representation at the population level. Hence, to elucidate: what dictates the pool of pGE at the single cell level, whether it was constraint or random, studies were performed on single mTECs. Gene expression and chromosomal co-localization studies of single mTECs expressing a particular antigen (like Mucin1, MUC1) were carried out. Patterns emerging from these combined studies could yield insights into the evolutionary mechanisms responsible for selecting this gene pool. Conceivably, positional clues in the genome and/or particular properties of self-antigens (e.g. immunogenicity) could have been driving forces during the co-evolution of pGE and adaptive immunity.

2. Materials and Methods

2.1. Materials

2.1.1. Chemicals

Table 2.1: Overview of chemicals

Product	Supplier
Acetone	Riedel-de Haën
Agarose	Invitrogen
Citrate, sodium salt	Merck
Diethylpyrocarbonate (DEPC)	Sigma
Ethylenediaminetetraacetic acid (EDTA)	Sigma
Ethanol (absolute)	Riedel-de Haën
Ethidium Bromide (10 g/l)	Roth
Fetal calf serum (FCS)	Biochrom
Fixogum	Marabu
Formaldehyde	Merck
Formamide	Merck
Glycerol	Merck
HCl (1 M)	J.T. Baker
HEPES	Invitrogen/Gibco
Hoechst 33342	Sigma
Isopropanol	Riedel-de Haën
Kaisers Glycerin gelatine	Merck
LPA	Ambion
β-Mercaptoethanol	Invitrogen/Gibco
Methanol	Merck
Sodium Azide (NaN_3)	Merck
Sodium Chloride (NaCl)	Fluka
Sodium hypochlorite (bleach)	Roth
10x Phosphate Buffered Saline (PBS)	Biochrom
PFA (Paraformaldehyde)	Merck
Percoll™	Amersham
Penicillin/Streptomycin	PAA
Poly-L-Lysine, 0.01 %	Sigma
ProLong® Gold	Invitrogen

Product	Supplier
Propidium Iodide	Sigma
RPMI 1640	Invitrogen/Gibco
TetraSpeck™ beads, 0.2 µm	Invitrogen
Tissue-Tek®	Sakura
Triton-X-100	Merck
Trizol®	Invitrogen
Trypan Blue	Merck
Tween 20	Gerbu

2.1.2. Buffers, solutions and media

All solutions were prepared with double distilled water purified by Millipore Milli-Q Plus (Millipore, Billerica, USA). Reagents were sterilized by autoclaving.

2.1.2.1. General buffers and stock solutions

DEPC Water (RNase free)	0.1 % (v/v) DEPC in water. Dissolved over-night under the hood and then autoclaved.
1x TE Buffer	Invitrogen
PBS	136 mM NaCl 2.56 mM KCl 10 mM Na2HPO4 1.76 mM KH2PO4 pH 7.2-7.4

2.1.2.2. Immunohistology

PBS/Tween 20	0.1 % (v/v) Tween 20 in 1x PBS, pH 7.2-7.4

2.1.2.3. Agarose gel electrophoresis

Agarose	1.5 % (w/v) Agarose in 100 ml 1x TAE 5 µl Ethidium Bromide (10 mg/ml)
TAE Buffer	40 mM Tris/Acetate 1 mM EDTA pH 7.5-8.0

2.1.2.4. Isolation of TECs

RPMI 1640 Medium	5 % Fetal Calf Serum (FCS) 10 mM HEPES 2 mM Glutamine 50 µM β-Mercaptoethanol 50 µg/ml Streptomycin 50 U/ml Penicillin
Serum-free RPMI Medium	Same supplements as above only without FCS
Collagenase Solution	0.2 mg/ml Collagenase IV 10 mM HEPES 2 % FCS (v/v) in RPMI 1640 medium pH 7.3 (Stored at -20 °C; thawed for the experiment and warmed)
Collagenase/Dispase Solution	0.2 mg/ml Collagenase IV 0.2 mg/ml Dispase Grade I 25 µg/ml DNase 10 mM HEPES 2 % FCS (v/v) in RPMI 1640 medium pH 7.3 (Stored at -20 °C; thawed for the experiment and warmed)

Trypsin Solution	0.05 % Trypsin 0.5 mM EDTA 0.3 % BSA 50 µg/ml DNase in PBS, pH 7.3 (Stored at -20 °C; thawed for the experiment and warmed)
Percoll Stock	9 parts Percoll (ρ 1.13 g/cm^3) 1 part 10x RPMI/HEPES (ρ 1.00 g/cm^3) gives ρ 1.117 g/cm^3
FACS Buffer	3-5 % FCS (v/v) 0.1 % NaN_3 in PBS, pH 7.2-7.4
Trypan Blue	0.2 % Trypan Blue 150 mM NaCl pH 7.0
MACS Buffer	0.5 % BSA (v/v) 5 mM EDTA in PBS, pH 7.2-7.4

2.1.2.5. Illumina expression profiling whole genome BeadArrays

Reagents as described in company protocol (performed by Genomics and Proteomics Core Facility - Dr. B. Korn).

2.1.2.6. µMACS™ SuperAmp™ Technology for Illumina BeadArrays

Reagents as described in TechNote (Pinto *et al.*, 2009).

2.1.2.7. Fluorescence *in situ* hybridization

20x SSC	3 M sodium chloride 300 mM trisodium citrate pH 7.0
0.3x PBS	150 ml 1x PBS 500 ml autoclaved Millipore water pH 7.0
4 % Paraformaldehyde/0.3x PBS	4 g PFA 0.3x PBS pH 7.0
0.5 % Triton-X-100/PBS	1 ml Triton-X-100 500 ml 1x PBS
20 % Glycerol/PBS	25 ml Glycerol 500 ml 1x PBS (Store at 4 °C)
0.1 N HCl/H_2O	50 ml 1 N HCl 500 ml 1x PBS
50 % Formamide/2x SSC	100 ml Formamide (v/v) 200 ml 2x SSC pH 7.4 (Store at 4 °C)
70 % Formamide/2x SSC	140 ml Formamide (v/v) 200 ml 2x SSC pH 7.0 (Store at 4 °C)
0.2 % Tween 20/4x SSC	1 ml Tween 20 500 ml 4x SSC

2.1.3. Enzymes and proteins

Table 2.2: Overview of enzymes and proteins

Product	Supplier
AmpliTaq Gold	Applied Biosystems
BSA	Sigma
Collagenase Type IV	Worthington
Dispase Grade I (neutral Protease)	Worthington
DNase (for collagenase/dispase and trypsin Mix)	ICN
DNase I (1U/µl) with 10x buffer and 25 mM EDTA	Invitrogen
DNAaway	MβP
Electro Zap	Ambion
FCS	Biochrom
MuLV Reverse Transcriptase	Applied Biosystems
Mouse Serum	Dianova
Power SYBR Green Master Mix	Applied Biosystems
Proteinase K	Merck
RedTaq™ DNA Polymerase (1 U/µl) with 10x buffer	Sigma
RNase Block Ribonuclease Inhibitor	Stratagene
RNase H (2 U/µl)	Fermentas
RNA Zap	Ambion
Superase•In (20 U/µl)	Ambion
SuperScript II™ Reverse Transcription (200 U/µl) with 5x buffer and 100 mM DTT	Invitrogen
T4gp32	USB
Trypsin (2.5 %)	ICN
Uracil-DNA Glycosylase (1 U/µl)	Eurogentec

2.1.4. Antibodies, secondary reagents

Table 2.3: Overview of primary and secondary antibodies used for FACS

Antigen	Clone	Species/ Isotype	Conjugate	Reference/ Supplier
CD45	30-F11	Rat IgG2b, κ	PerCP	Pharmingen
CD45	2D1	Mouse IgG1, κ	PerCP	Pharmingen
CD45	OX-1	Mouse IgG1, κ	PE-Cy5	Pharmingen
CD80	16-10A1	Hamster IgG2, κ	PE	Pharmingen
EpCAM	GZ1	Mouse IgG1	Alexa 488	BioVendor Laboratory Medicine Inc.
EpCAM	HEA125	Mouse IgG1	Biotin	G. Moldenhauer, DKFZ Heidelberg
FcR (FcγIII/IIR)	2.4G2	Rat IgG2b, κ	Supernatant	AG Altevogt, DKFZ Heidelberg
$F(ab')_2$ anti-Mouse	-	Goat IgM (μ chain specific)	RPE	SouthernBiotech
gp40 (EpCAM/ Tacstd1)	G8.8	Rat IgG	Cy5	(Farr *et al.*, 1991)
His38	-	Mouse IgM	Ascites	Jan Rozing, University of Groningen
HLA-DR	L243	Mouse	Alexa 647 Alexa 680	G. Moldenhauer, DKFZ Heidelberg
Ly51 (6C3/BP-1 Antigen/Enpep)	6C3	Rat IgG2a, κ	FITC	Pharmingen
MHC Class II (I-A/I-E)	2G9	Rat IgG2a, κ	PE	Pharmingen
MUC1	214D4	Mouse IgG1	Alexa 647	Upstate
MUC1	214D4	Mouse IgG1	Alexa 647	University of Maastricht
RT1B	OX-6	Mouse IgG1, κ	Purified	Pharmingen
Streptavidin	-	-	PE	Pharmingen
TEZ	CDR2	Mouse IgG2b	Alexa 488	AG Kyewski, DKFZ Heidelberg

Table 2.4: Overview of primary and secondary antibodies used for immunohistology

Antigen	Clone	Species/ Isotype	Conjugate	Reference/ Supplier
Keratin 14	AF64	Rabbit	Purified	Covalence
Goat IgG	-	Rabbit	Cy3	Jackson Research

2.1.5. MicroBeads used for MACS purification

Table 2.5: Overview of MACS beads used for cell separation

Name	Company
Anti-CD45-Microbeads (Human)	Miltenyi Biotech
Anti-CD45-Dynal Beads (Human)	Invitrogen

2.1.6. Conventional PCR

All primers were HPSF-purified and obtained from MWG-Biotech. Almost all primers were designed to cross intron-exon boundaries.

2.1.6.1. Primers for conventional PCR

Table 2.6: Overview of primers for conventional PCR

Primer Name	Primer Sequence
Mouse/Rat ß-Actin Primer (348 bp)	
Forward	5'- TGG AAT CCT GTG GCA TCC ATG AAA C -3'
Reverse	5'- TAA AAC GCA GCT CAG TAA CAG TCC G -3'
Annealing-Temperature	55 °C
Human ß-Actin Primer (208 bp)	
Forward	5'- CGT GGA CAT CCG TAA AGA CC -3'
Reverse	5'- ACA TCT GCT GGA AGG TGG AC -3'
Annealing-Temperature	58 °C

2.1.6.2. Real-time PCR primers

Mouse gene expression analysis:

Table 2.7: Overview of primers for mouse gene expression analysis with real-time PCR

Primer Name and Conc. (µM/µM)	Primer Sequence
5430425J12Rik (300/300)	
Forward	5'- CAC CCT TGA GAA CCA ACT TTC C -3'
Reverse	5'- TGC CCT AGG CCC ACT TTG -3'
Aire (300/900)	
Forward	5'- GTA CAG CCG CCT GCA TAG C -3'
Reverse	5'- CCC TTT CCG GGA CTG GTT TA -3'
Brd9 (900/300)	
Forward	5'- AGT GAG AGC CTG CCG AAC AC -3'
Reverse	5'- CTC TGT AGC TGG CGG AGG AA -3'
Cep72 (900/900)	
Forward	5'- GAG TCT GACT ACC GCC TGT TTG T -3'
Reverse	5'- TTC TCT CAC AGG ACG GTC ATC TAG -3'
Clptm1l (900/900)	
Forward	5'- CCA ACT GCA TCC AGC CCT AT -3'
Reverse	5'- GAC CGT GTG GTG GTG TAA ACA C -3'
Csnb (300/900)	
Forward	5'- TGT GCT CCA GGC TAA AGT TCA CT -3'
Reverse	5'- GGT TTG AGC CTG AGC ATA TGG -3'
Ins2 (300/300)	
Forward	5'- CAC CAG CCC TAA GTG ACT CG -3'
Reverse	5'- ATC CAC AGG GCC ATG TTG AA -3'
Irx1 (300/50)	
Forward	5'- ACC CTC ACA CAG GTC TCC AC -3'
Reverse	5'- TCG ATG TCA ATG CTC TCC AG -3'
Irx2 (50/300)	
Forward	5'- GAA CAC CGA AAG AAC CCG TA -3'
Reverse	5'- CAT CCT GTG CCT TGT CTG AA -3'
Irx4 (900/900)	
Forward	5'- CCC GTC TAC TGC CCT GTC TA -3'
Reverse	5'- TCC TTG GAC TCG AAG CTG TT -3'

Primer Name and Conc. (µM/µM)	Primer Sequence
Lpcat1 (300/300)	
Forward	5'- TGG AGG AAG GTC GTG GAC TT -3'
Reverse	5'- GAA GCC GCC AGC AAA CC -3'
Mrpl36 (900/900)	
Forward	5'- GAG GTG CGC TCA GTT CTC TGT -3'
Reverse	5'- TTG ATG ACA CCT TTG GTT TTG AA -3'
Ndufs6 (900/900)	
Forward	5'- TTG TAG ATC GTC AGA AAG AGG TGA A -3'
Reverse	5'- GCG GTG CTC CAC CTC ATT -3'
Nkd2 (900/300)	
Forward	5'- CCT GAT GCA CAC CAT CTA CG -3'
Reverse	5'- CAA TCT CTG TTC TGC CAC GA -3'
Slc12a7 (900/900)	
Forward	5'- GCG TCC ACG CTT CAA GTT C -3'
Reverse	5'- CAG CGC GAG GCA GAG ACT -3'
Slc6a18 (900/900)	
Forward	5'- TTT GAG GGT ATC CCG CTT TTC -3'
Reverse	5'- GCC TAC GCC ACC GAG GTA -3'
Slc6a19 (900/900)	
Forward	5'- CAT CAG TGA CTC AGG CTC CA -3'
Reverse	5'- CCA CGG ATG AGA AAG ATG GT -3'
Slc6a3 (900/900)	
Forward	5'- TGG CTT CGT TGT CTT CTC CT -3'
Reverse	5'- CAG CTG GAA CTC ATC GAC AA -3'
Tert (900/900)	
Forward	5'- TGT TGG TGA CGC CTC ACT TG -3'
Reverse	5'- CAT ACT CAG GAA CGC CAT GGA -3'
Tppp (900/300)	
Forward	5'- TCT CTG GCG TCA CGA AAG CT -3'
Reverse	5'- TTG GTC GAA ACG CTC CTT GT -3'
Trip13 (900/900)	
Forward	5'- TTC CTG GCT CAT GCT CTC TAC A -3'
Reverse	5'- TGT TTG TCC ACT GCC AGA GAT AG -3'
Ubc (300/900)	
Forward	5'- CAC CAG CCC TAA GTG ACT CG -3'
Reverse	5'- ATC CAC AGG GCC ATG TTG AA -3'

Primer Name and Conc. (µM/µM)	Primer Sequence
Zdhhc11 (50/50)	
Forward	5'- CGA CAG GTC CAA ACA CAC AC -3'
Reverse	5'- ACA CCA AGA ATC CCA ACT GC -3'

Rat gene expression analysis:

Table 2.8: Overview of primers for rat gene expression analysis with real-time PCR

Primer Name and Conc. (µM/µM)	Primer Sequence
Aire (900/300)	
Forward	5'- TCT GGC CTC AAA GAG CAT CTC T -3'
Reverse	5'- TTG CCC TCT GGC TTC TTA GG -3'
Hprt (900/900)	
Forward	5'- GCC CTT GAC TAT AAT GAG CAC TTC A -3'
Reverse	5'- TCT TTT AGG CTT TGT ACT TGG CTT TT -3'
Ins2 (900/900)	
Forward	5'- GCC CAG GCT TTT GTC AAA CA -3'
Reverse	5'- TCC CCA CAC ACC AGG TAG AGA -3'

Human gene expression analysis:

Table 2.9: Overview of primers for human gene expression analysis with real-time PCR

Primer Name and Conc. (µM/µM)	Primer Sequence
AC007405.6-202 (50/900)	
Forward	5'- AAG AAT ACT CAG GCC CCA CTA GAG -3'
Reverse	5'- CCT TGG CCT CAG GAT TTT CTG -3'
ACBD5 (900/300)	
Forward	5'- TGA AGT CAA GCA TGG AGG AGA A -3'
Reverse	5'- CAA GTG TTG CAT CCT ATG TCC TCT T -3'

Primer Name and Conc. (µM/µM)	Primer Sequence
AIRE (900/900)	
Forward	5'- CTG ATG AGA GAG TGC TGA GAA GGA -3'
Reverse	5'- GTT TAC AGC CGA GCA CTG ACA A -3'
APBB1IP (300/900)	
Forward	5'- CTG GGA GAG ATG GAT CTT CTG ACT -3'
Reverse	5'- TTC CAG TGC ATT TAA GGA CTC ATT T -3'
ANKRD26 (900/900)	
Forward	5'- GAG AGG CTA GCA GAG GTC AAC AC -3'
Reverse	5'- CAC ACA AGG TGG CTC CAT GA -3'
CEACAM3 (900/900)	
Forward	5'- CAG CCT CAC TTC TAA ACT TCT GGA A -3'
Reverse	5'- TGA GCG GCA TGG ATT CAA TA -3'
CEACAM4 (900/900)	
Forward	5'- ACT GCC AGA TCG ACC ACA AAG -3'
Reverse	5'- ACG CTC CAT CAA CCC ACA A -3'
CEACAM5 (300/300)	
Forward	5'- TCC AGA ACT CAG TGA GTG CAA AC -3'
Reverse	5'- CTC CCG AAA GGT AAG ACG AGT C -3'
CEACAM6 (300/900)	
Forward	5'- ATA TGT GCC AAG CCC ATA ACT C -3'
Reverse	5'- AGC TGA GAG GAC AGG AGC ACT T -3'
CEACAM7 (900/900)	
Forward	5'- CTG CTC ACA GCC TCG CTT TTA A -3'
Reverse	5'- GAA CGG CAC GAC ATC AAT ATT G -3'
GAD65 (300/300)	
Forward	5'- GCA ATT AAA ACA GGG CAT CCT AGA -3
Reverse	5'- ATG TTA GTA TTT GCT GTT GAT GTC A -3'
GAD67 (300/50)	
Forward	5'- TTT GAT CGC TCC ACC AAG GT -3'
Reverse	5'- TCC AAG TTG AAG CCC TCC AT -3'
GAPDH (900/900)	
Forward	5'- TCG ACA GTC AGC CGC ATC T -3'
Reverse	5'- CCG TTG ACT CCG ACC TTC A -3'
Probe	5'- CGT CGC CAG CCG AGC CAC AT -3'
GORASP2 (300/900)	
Forward	5'- CGC CCA TTT GAG GAA GGA A -3'
Reverse	5'- TGG ACC TCT GTA AAC CCA TCT TTA A -3'

Primer Name and Conc. (µM/µM)	Primer Sequence
GPR158 (900/900)	
Forward	5'- CCG ATC TGG ATC CTA CCT GA -3'
Reverse	5'- CGT AAT GCG TCT CAT GAT GG -3'
HMG1L4P (900/900)	
Forward	5'- AAC TTG TCG GGA GGA GTG TAA GAA -3'
Reverse	5'- ATG GCC TTC CAC CTC TCT GA -3'
INS (900/300)	
Forward	5'- GCA GCC TTT GTG AAC CAA CA -3'
Reverse	5'- GTG TGT AGA AGA AGC CTC GTT CC -3'
PDSS1 (300/900)	
Forward	5'- GCA CAC TAC CTT GAG AAG ACA TTC A -3'
Reverse	5'- ACA TCC TAG AAC AGA GAC ATA CTG CTT T -3'
MASTL (900/300)	
Forward	5'- CGT TGA TGA TGG GCG AAT TC -3'
Reverse	5'- TTC TGG CCA AGG GAT ATC ATG -3'
METTL8 (50/300)	
Forward	5'- TGA TGT ATG TGA TGA TGG CTT ACC T -3'
Reverse	5'- TTA CAA CAC CTT GCA TCC TGT CA -3'
MUC1 (300/300)	
Forward	5'- CTT TCT TCC TGC TGC TGC TCC T -3'
Reverse	5'- AGC CGA AGT CTC CTT TTC TCC A -3'
Probe	5'- AGC TTG CAT GAC CAG AAC CTG TAA CAA CTG T -3'
MUC4 (900/300)	
Forward	5'- AGA GGT ATC GCC CTG ATA GAT TCC -3'
Reverse	5'- ACG GTA GTT GGG CCT TTC TTC -3'
MYH6 (900/300)	
Forward	5'- TTC TCC GTG AAG GGA TAA CC -3'
Reverse	5'- CGT CTT CCC ATT CTC GGT TTC AGC -3'
MYH7 (900/900)	
Forward	5'- GGC CCC TTT CCT CAT CTG TAG -3'
Reverse	5'- CGG TCA CTG TCT TGC CAT ACT CAG -3'
MYO3A (300/50)	
Forward	5'- CTA GCT GAC CTT CAT CCC ATG AG -3'
Reverse	5'- GAA GTC ATT GAA TTC TGC TGA CCA T -3'

Primer Name and Conc. (µM/µM)	Primer Sequence
MYO3B (900/50)	
Forward	5'- CTG ATA AAA GTG AGG TGC CCA AT -3'
Reverse	5'- CCC GGG TGA CCA CAC AGT -3'
SP5 (900/50)	
Forward	5'- TCT TCT GCG GGA AGA GCT T -3'
Reverse	5'- TGG TGA GTC TTG ACG TGC TT -3'
SSH3BP (900/900)	
Forward	5'- GAT GTG GGC CAT GGT GTC A -3'
Reverse	5'- TGT TCT CGA CAG TGT GCC AGT T -3'
TLK1 (900/300)	
Forward	5'- TGT ATG GTC GGT TGG AGT CA -3'
Reverse	5'- GCC TTG GCT TCA CTG CTT AC -3'
YME1L1 (900/900)	
Forward	5'- CTG AAA GCT CAA GCA CTC ACA CA -3'
Reverse	5'- GCA GCA GAA CGA AGA GAA TCA GA -3'

SC-PCR

Table 2.10: Overview of primers for human SC-PCR

Primer Name	Primer Sequence
MUC1 A2	5'- GGT ACC ATC AAT GTC CAC GA -3'
MUC1 B2	5'- ACG GAA GCA GCC TCT CGA TA -3'
MUC1 C2	5'- GAC AGC CAA GGC AAT GAG AT -3'
CEA A2	5'- TGG CTA CTG GCC GCA ATA AT -3'
CEA B2	5'- CAT GAT TGG AGT GCT GGT TG -3'
CEA C2	5'- CCA AGC CCA GCT CAT TTT TG -3'
CEACAM6 A	5'- TTC CAT GTA TAC CCG GAG CT -3'
CEACAM6 B	5'- CCT GTG GTG GGT AAA TGG TC -3'
CEACAM6 C2	5'- GGT AAT TGG CCT TTG AGG GG -3'
CEACAM3 A	5'- AAG AAC CAG CAT CCA GCG TG -3'
CEACAM3 B	5'- AGC TCT GCC TTC TCG ATG TC -3'
CEACAM3 C	5'- GCG GAA GCT AAG AAG CCA CT -3'
MUC4 A	5'- GGA GTT TCC CTC TTC CCC TA -3'
MUC4 B	5'- TTC ACC TCC CCA CTC TTC AA -3'
MUC4 C	5'- AAG TCA GCA TCG TCC CAG AA -3'

Primer Name	Primer Sequence
EpCAM A2	5'- TGA GCG AGT GAG AAC CTA CTG -3'
EpCAM B	5'- CGG ACT GCA CTT CAG AAG GA -3'
EpCAM C	5'- CCC CAT TTA CTG TCA GGT CC -3'

2.1.7. Nucleotide and nucleic acids

Table 2.11: Overview of DNA, nucleotides and oligonucleotides

Product	Supplier
BAC clone- RP11-263K19-Gold Cyanine-3 UTP	Empire Genomics
BAC clone- RP11-343B1 Green 5(6)-Rhodamine Green dUTP	Empire Genomics
dNTP Set (100 mM)	GE Healthcare
dNTP-Mix (10 mM)	MBI Fermentas
dNTP-Mix (2 mM)	MBI Fermentas
GeneAmp 10mM dNTP Mix with dTTP	Applied Biosystems
Human COT-1 DNA	Invitrogen
Oligo $(dT)_7$ Primer	DKFZ Heidelberg
Oligo (dT)20 (500 µg/ml)	DKFZ Heidelberg
Salmon Sperm DNA	Invitrogen
Total Organ RNA from different mouse and human organs	Stratagene

2.1.8. Microarrays, kits and standards

Table 2.12: Overview commercial kits

Product	Supplier
Alexa Fluor® 488 Protein Labeling Kit	Molecular Probes
Alexa Fluor® 647 Monoclonal/Protein Labeling Kit	Molecular Probes
Alexa Fluor® 680 Protein Labeling Kit	Molecular Probes
Expression BeadChip, Whole Genome Gene Expression Analysis	Illumina

Product	Supplier
GeneRuler™ 100 bp DNA Ladder plus (0.5 µg/µl)	MBI Fermentas
High Pure RNA Isolation Kit	Roche
Illumina® TotalPrep RNA Amplification Kit	Ambion
Power SYBR Green	Applied Biosystems
qPCR™ Core Kit for SYBR™ Green I	Eurogentec
qPCR™ Core Kit	Eurogentec
RNeasy® Mini Kit	Qiagen

2.1.9. Instruments

Table 2.13: Overview of equipment

Product	Supplier
Agilent 2100 Bioanalyzer	Agilent Technologies
AutoMACS™ Pro Separator	Miltenyi Biotech
BD FACSAria™ (SOP) Cell Sorter	Becton Dickinson
BD FACSCanto™ Flow Cytometer	Becton Dickinson
BD FACSVantage™ SE Cell Sorter	Becton Dickinson
CCD Camera (Cosmicar)	Pentax
Centrifuge Rotatanta 460 R	Hettich
Cryostat (CM 3050 S)	Leica
Gel electrophoresis Camera	AGS
GeneAmp® 7300 Sequence Detector	ABI
GeneArray Scanner	Hewlett-Packard
Heating Block	Grant/Eppendorf
Homogenisator (Ultra-Turrax® T25)	IKA
Incubator HeraCell 240	Heraeus
Leica CM 1900 Cryostat	Leica
Leica TCS SP5	Leica
Magnetic bar (MR 2000)	Heidolph
Microscope Axio Imager.Z1	Zeiss
Nano Drop® 1000 photometer	Thermo Scientific
PCR-Machine (PTC-100™)	MJ Research
Power Supply (EPS 500/ 400)	Pharmacia

Product	Supplier
Quadro MACS® separator	Miltenyi Biotech
Sterile Hood HeraSafe Typ KS12	Kendro
Table Centrifuge (Biofuge fresco)	Heraeus
UV Table	Konrad Benda
Water Bath (Thermomix® M)	Braun
Zeiss Axio Imager.Z1 fluorescence microscope	Zeiss

2.1.10. Consumables

Table 2.14: Overview of consumables

Product	Supplier
ABI PRISM 96-well Optical Reaction Plate and Optical Caps	Applied Biosystems
AutoMACS columns	Miltenyi Biotech
Cell-Strainer-Cap-Tubes (5 ml)	Becton Dickinson
Centrifuge tubes (15 ml and 50 ml)	TPP
Coverslips, all sizes	Lankenbrinck
Filter tipps (10 µl, 20 µl, 200 µl and 1000 µl)	Starlabs
Gauze (PA-60 Nybolt)	Eckert
Glass slides (Histobond)	Marienfeld Laborglas
MicroAmp Optical Adhesive Film	Applied Biosystems
MicroSpin™ G-50 columns	Amersham
Multi-pipets (0.1 ml, 0.2 ml, 0.5 ml, 2.5 ml and 5 ml)	Eppendorf
Neubauer chamber	Blau Brand
Pasteur pipets	WU-Mainz
PCR reaction tubes (200 µl)	Biozym
Petri dishes (all sizes)	TPP
Round-bottom screw-cap tube (sterile)	Nunc
Round bottom tubes (13 ml)	Becton Dickinson
Safe-Lock reaction tubes (0.5-2 ml)	Eppendorf
Sterile filters (0.2 µm and 0.45 µm)	Millipore
Strips of 8 thermo tubes-Ultra Clear Cap Strips	Abgene

Product	Supplier
Strips of 8 tubes, thin wall micro test tubes, 0.2 ml and Domed cap for thin wall micro test tubes 0.2 ml, stripes of 8 caps	Nerbe
Syringes (10 ml and 50 ml)	Terumo
Thermo-Fast® 96 Detection Plate	Abgene

2.1.11. Software

Table 2.15: Overview of software used

Software	Company
AxioVision 4.5	Zeiss
Amplify 3.1.4	Freeware
BD FACSDiva	Becton Dickinson
BeadStudio 3.1	Illumina
Bioconductor	Freeware
ChromasLite	Freeware
ClustalW	Freeware
EditSeq 5.06	DNAStar
FlowJo 8.6	Tree Star
GeneAmp 7300 SDS Software	Applied Biosystems
Image J	National Institutes of Health, USA
LAS AF Lite	Leica
LinRegPCR	LinRegPCR
MatLab	The MathWorks Inc.
Microsoft Office	Microsoft
Primer Express™ 1.0 Applied Biosystems	Applied Biosystems
Primer Express™ 2.0 Applied Biosystems	Applied Biosystems
R Project	Freeware

2.1.12. Mouse, rat and human material

C57BL/6 mice and SD rats were bought from Charles River Wiga (females, 3-4 weeks old) and were used for organ preparations at the age of 5-6 weeks.

The Aire knock-out (KO) mice were bred in the barrier of the central animal facility at the DKFZ. The mice were originally from Peltonen's lab. All mice were kept under specific pathogen-free conditions at the animal facility of the German Cancer Research Center.

Human thymus samples for this study were obtained in the course of corrective cardiac surgery at the Department of Cardiac Surgery, Medical School, University of Heidelberg headed by Prof. Dr. med. Matthias Karck. This study has been approved by the Ethics Committee of the University of Heidelberg.

Table 2.16: List of individuals from which thymic samples were studied

Human Sample Number	Gender	Age
14	male	4 months
24	female	2 months
32	male	2 months
53	male	2 months
55	male	7 days
59	male	7 days
72	male	5 days
74	female	3 years
76	male	6 months
77	male	4 months
83	male	7 months
87	female	4 months
88	female	3 months
89	male	7 days
92	male	5 months
93	female	8 months
94	male	2 months
96	female	3.5 months
97	female	4 months
101	female	5 months
102	female	10 months
103	female	3 months

Human Sample Number	Gender	Age
104	male	3 days
105	female	7 days
106	male	9 months
108	male	7 days
109	male	14 days

2.2. Methods

2.2.1. Antibody labeling

Table 2.17: List of antibodies conjugated using labeling kits

Antibodies	Conjugate	Kits
anti-mouse EpCAM	Alexa 647	Alexa Fluor® 647 Protein Labeling Kit
anti-rat EpCAM	Alexa 488	Alexa Fluor® 488 Protein Labeling Kit
anti-rat MHCII	Alexa 647	Alexa Fluor® 647 Protein Labeling Kit
anti-human CDR2	Alexa 488	Alexa Fluor® 488 Protein Labeling Kit
anti-human HLA-DR	Alexa 647 Alexa 680	Alexa Fluor® 647 Protein Labeling Kit Alexa Fluor® 680 Protein Labeling Kit
anti-human MUC1	Alexa 647	Alexa Fluor® 647 Monoclonal Labeling Kit

All conjugations were performed using labeling kits from Invitrogen and according to the manufacturer's instructions, in which 1 mg/ml antibody was used for the protein labeling kit, while 100 µg/100 µl antibody was labeled using the monoclonal antibody kit.

2.2.2. Immunohistochemistry

2.2.2.1. Organ preparation for cryosections

After the removal of the thymus from the thorax of the mouse or rat, the organ was embedded in a plastic mold with *Tissue-Tek*® and gradually frozen on dry ice. The organ was then preserved at -80 °C until further use.

5 µm cryosections were cut at -22 °C to -24 °C using the Leica CM 1900 Cryostat. The sections were then dried over-night on *Histobond*® slides.

2.2.2.2. Immunohistochemical staining

The tissue sections were fixed with Acetone (-20 °C) for 10 min at room temperature. Subsequently they were air dried and encircled using a Pap pen. The slides were then washed for 5 min in 1x PBS pH 7.4 at room temperature and blocked with 3 % BSA/1x PBS for 20 min at room temperature in a humidity chamber. After washing the slides with 1x PBS/0.1 % Tween for 10 min at room temperature, the primary antibody (diluted with PBS and centrifuged) was added and incubated for 30 min at 37 °C and then 30 min at room temperature in a humidity chamber. The slides were then washed once in 1x PBS/0.1 % Tween for 5 min and twice in 1x PBS pH 7.4 for 5 min each and then briefly rinsed in distilled water. The secondary antibody was treated in the same way as the primary antibody. After incubation for 30 min at 37 °C and 30 min at room temperature in a dark humidity chamber, the slides were washed as prior. In some cases, the sections were counter stained with Hoechst 33342 for 2 min and washed as mentioned above. All samples were embedded with warm Kaiser's Glycerol Gelatine and covered with coverslips. Images were taken with a Zeiss Axio Imager Z.1 fluorescence microscope. Immunohistochemical staining was performed to establish the staining of the anti-His38 ascites and anti-MHCII on rat thymus (Figure 4).

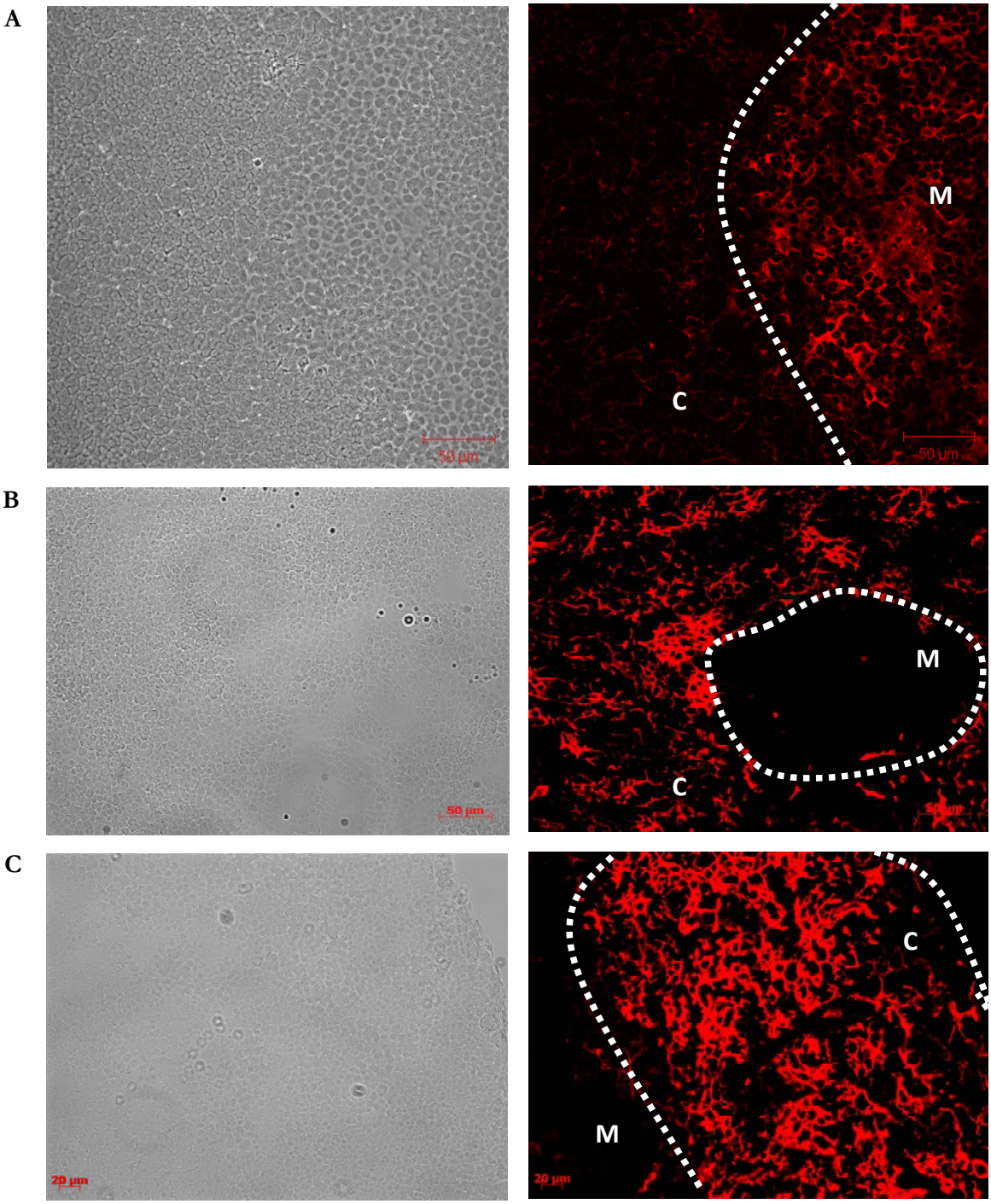

Figure 4

Immunohistochemical staining with the anti-His38 ascites and anti-MHCII mAb on rat thymus

(A) MHCII antibody labeled with Alexa 647 stained the rat medulla more intensely than the cortex (40x).

(B) His38 ascites-Cy3 stained the rat thymic cortex and the outer cortex (C) just below the thymic capsule (20x). Marking: M = medulla; C = cortex.

2.2.3. Isolation of thymic epithelial cells

2.2.3.1. Isolation of mouse thymic epithelial cells

2.2.3.1.1. Enzymatic digestion of mouse thymic tissue

Mice were killed with CO_2 and the thymi were removed from the thorax into a petri plate filled with RPMI 1640 medium (containing 5 % FCS) on ice. Residual fat and connective tissue if any were removed from the thymi. The thymi were then cut into small pieces and stirred in a round-bottom tube containing ~20-25 ml medium at low speed on a magnetic stirrer for 10-15 min at room temperature. The supernatant containing thymocytes was decanted and the remaining tissue was further digested until complete dissociation into a single cell suspension. The tissue was digested thrice with 10 ml collagenase for 15 min each at 37 °C, thrice with collagenase/dispase for 25 min each at 37 °C and two-three rounds of trypsin for 20 min each at 37 °C in a water bath with magnetic stirring. During the digestion steps, the tissue was agitated regularly with a pasteur pipet. After each digestion step, the supernatant was collected separately on ice and washed in RPMI 1640 medium containing 5 % FCS (1400 rpm for 5 min at 4 °C). The cell pellet was then resuspended in 10 ml RPMI 1640 medium containing 5 % FCS and kept on ice. The cells from each fraction were then counted and depending on the cell count, usually from the 2nd collagenase/dispase fraction till the last trypsin fraction, were pooled and filtered through 60 μm gauze.

2.2.3.1.2. Enrichment of mouse TECs using density gradients

In order to enrich for TECs, density gradients were used, as described below.
After pooling the digestion fractions the cells were washed twice (1400 rpm for 5 min at 4 °C) in RPMI 1640 medium without FCS. In the meanwhile, the various density solutions were prepared as described in Table 2.18. The cell pellet was then suspended in Percoll stock/RPMI, ϱ = 1.07 g/cm^3, over which, the other two gradient layers (6 ml of Percoll stock/RPMI, ϱ = 1.045 g/cm^3 and 6 ml of medium (-FCS), ϱ = 1.00 g/cm^3) were carefully added using a glass pasteur pipet. Not more that 5 x 10^8 cells were used for one gradient. The gradients were then centrifuged at 4000 rpm (3500 g, *Hettich Rotanta 460R*; without breaks) at 4 °C for 30 min.

Table 2.18: Different density gradient solutions for the isolation of mouse and rat thymic epithelial cells

Density (g/cm^3)	RPMI Medium without FCS (ml)	Percoll Stock (ml)
1.0	6 (normal pH)	0
1.045	3.69 (pH 6.5)	2.31
1.07	2.41 (pH 6.5)	3.59

Percoll stock: 9 parts Percoll (Amersham Biosciences, ϱ = 1.13 g/cm^3) + 1 part RPMI/HEPES (10x) (ϱ = 1.00 g/cm^3). This gives a density of ϱ = 1.117 g/cm^3.

RPMI medium (-FCS) with normal pH 6.5 was prepared by adjusting the pH with 1 M HCl (until it turns yellow).

After centrifugation, the cells were collected in a 50 ml Falcon containing RPMI 1640 medium (with FCS) from both interphases using a pasteur pipet. The cells were then washed twice (1600 rpm for 8 min at 4 °C) in medium. At the end, the cell pellet was resuspended in RPMI 1640 medium or FACS buffer (5 % FCS) and counted. Following which, they were stained for FACS (Section 2.2.3.1.3).

2.2.3.1.3. Staining of mouse TECs

For cell staining, firstly the cells were blocked with 1 ml (for every 1 x 10^8 cells) of anti-Fc-receptor supernatant (2.4G2) for 15 min on ice. The cells were then washed (1400 rpm for 5 min at 4 °C) and stained with an antibody cocktail (Table 2.19) for 15 min on ice in FACS buffer. After staining, the cells were washed, filtered through 35 μm filters and stained with PI directly prior to sorting. Cell populations were sorted on a *BD FACSDiVa* (Becton Dickinson) on purity mode under medium pressure (Figure 5).

Table 2.19: Overview of different antibody combinations used for mouse TEC cell sorting

TEC Populations Sorted	Antibodies used	Dilution
MHCII^{hi}/MHCII^{lo} mTEC and cTEC	anti-Ly51-FITC	1:100
	anti-CD45-PerCP	1:100
	anti-EpCAM-Alexa 647	1:100
	anti-MHCII-PE	1:2000
	PI (1 mg/ml)	1:1000

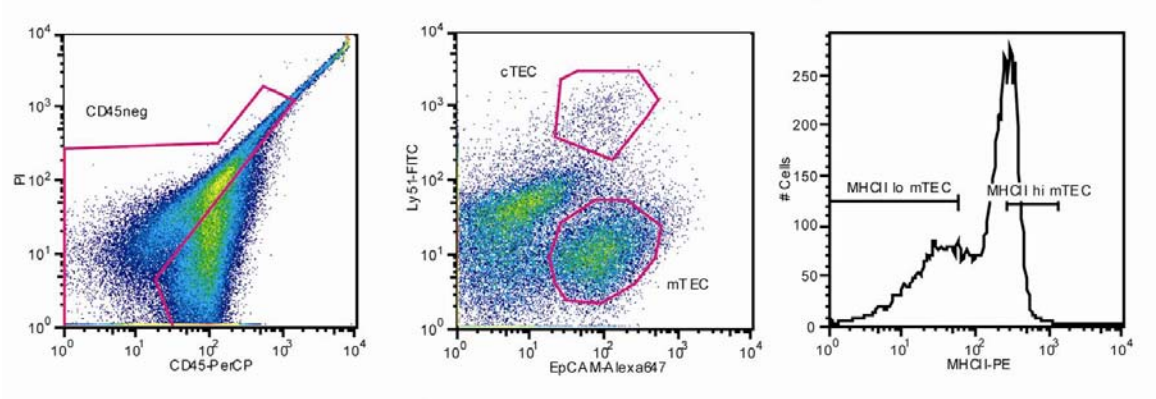

Figure 5

Sort gates for the isolation of mouse MHCII^{hi} and MHCII^{lo} mTECs

The mouse mTEC and cTEC cell populations were separated using anti-Ly51 and anti-EpCAM mAbs. The mTECs were further differentiated into mature and immature subsets using anti-MHCII mAbs.

2.2.3.2. Isolation of rat thymic epithelial cells

2.2.3.2.1. Enzymatic digestion of rat thymic tissue

Rats were killed with CO_2 and the thymi were removed from the thorax into a Petri plate filled with RPMI 1640 medium (containing 5 % FCS) on ice. The digestion steps for the isolation of thymic epithelial cells from rat were the same as performed in mice (Section 2.2.3.1.1).

2.2.3.2.2. Enrichment of rat TECs using density gradients

For the enrichment of rat TECs, density gradients were used as those in mice (Section 2.2.3.1.2), only that separate gradients were performed for the collagenase/dispase and trypsin fractions. Depending on the cell number, either both or the upper interphase of the collagenase/dispase gradients were added to both interphases of the trypsin gradients.

2.2.3.2.3. Staining of rat TECs

The cell staining was performed as described in Table 2.20. Cells were washed, filtered through 35 µm filters and stained with PI directly prior to sorting. Cell populations were sorted on a *BD FACSDiVa* (Becton Dickinson) on purity mode under medium pressure (Figure 6).

Table 2.20: Overview of blocking/staining scheme and different antibody combinations used for rat thymus cell sorting

	Steps			
	1	**2**		**3**
Block Goat Serum	His38 Ascites 1:500 for 30 min	Goat anti-mouse IgM-PE (1:200)	Block Mouse Serum	anti-EpCAM-Alexa 488 (1:100) anti-CD45-CyChrome (1:100) anti-MHCII-Alexa 647 (1:1500) PI (1 mg/ml, 1:1000)

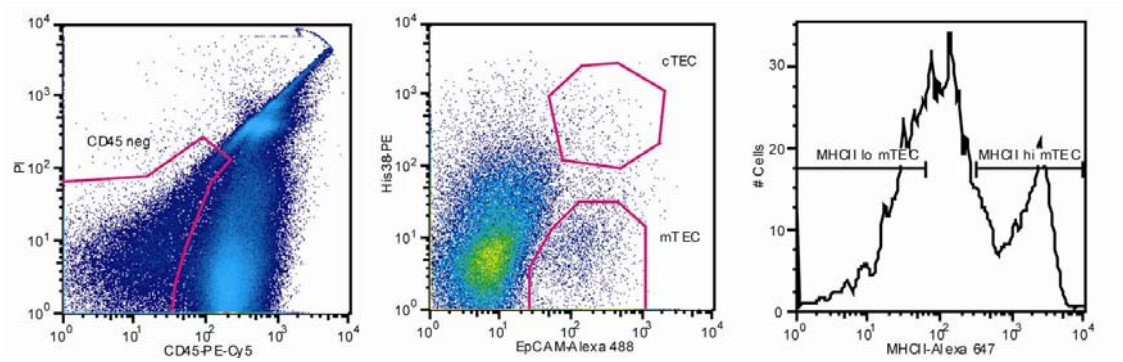

Figure 6

Sort gates for the isolation of rat MHCII^{hi} and MHCII^{lo} mTECs

The rat mTEC and cTEC cell populations were separated using anti-His38 ascites and anti-EpCAM mAbs. The mTECs were further differentiated into mature and immature subsets using anti-MHCII mAbs.

2.2.3.3. Isolation of human thymic epithelial cells

2.2.3.3.1. Enzymatic digestion of human thymic tissue

Human thymus samples for this study were obtained in the course of corrective cardiac surgery at the Department of Cardiac Surgery, Medical School, University of Heidelberg headed by Prof. Dr. med. Matthias Karck. This study has been approved by the Ethics Committee of the University of Heidelberg. The age of the children for this study ranges from 3 days to 3 year.

The thymus samples directly after removal were slit (to facilitate oxygenation) and transported in RPMI 1640 medium (containing 5 % FCS) on ice. The tissue was then cut into small pieces and stirred in a 250 ml conical flask containing ~50-60 ml RPMI 1640 medium at low speed on a magnetic stirrer for 10 min at 4 °C. This step was repeated twice, after each step the supernatant containing thymocytes was decanted. The remaining tissue was divided into two 100 ml conical

flasks and digested until complete dissociation into a single cell suspension. To do so, the tissue was digested thrice with 10 ml collagenase/dispase for 20 min each at 37 °C and three-four rounds of trypsin for 10 min each at 37 °C in a water bath with magnetic stirring. During the digestion times, the tissue was agitated regularly with a broken glass pasteur pipet. After each digestion step, the supernatant was collected separately on ice and washed in RPMI 1640 medium containing 5 % FCS (1400 rpm for 5 min at 4 °C). The cell pellet was then resuspended in 10 ml RPMI 1640 medium containing 5 % FCS and kept on ice. The cells from each fraction were then counted and depending on the cell count, usually from the last collagenase/dispase and all trypsin fractions were pooled and filtered through 60 μm gauze.

In order to enrich for TECs, either density gradients (Section 2.2.3.3.2) or *Anti-CD45-Dynal beads* (Invitrogen; Section 2.2.3.3.3) or *Anti-CD45-Microbeads* (Miltenyi Biotech; Section 2.2.3.3.4) were used.

2.2.3.3.2. Enrichment of human TECs using density gradients

For density gradients, after pooling the digestion fractions, the cells were washed (1400 rpm for 5 min at 4 °C) in RPMI 1640 medium without FCS. In the meanwhile, the various density solutions were prepared as described in Table 2.21. The cell pellet was then taken up in Percoll stock/RPMI, ϱ = 1.07 g/cm^3, over which, the other three gradient layers (6 ml of Percoll stock/RPMI, ϱ = 1.045 g/cm^3; 6 ml of Percoll stock/RPMI, ϱ = 1.03 g/cm^3 and 6 ml of medium (-FCS), ϱ = 1.00 g/cm^3) were carefully added using a glass pasteur pipet. Not more that 5 x 10^8 cells were used for one gradient. The gradients were then centrifuged at 4000 rpm (3500 g, *Hettich Rotanta 460R*; without breaks) at 4 °C for 30 min.

Table 2.21: Different density gradient solutions for the isolation of human thymic epithelial cells

Density (g/cm^3)	RPMI Medium without FCS (ml)	Percoll Stock (ml)
1.0	6 (normal pH)	0
1.03	4.46	1.54
1.045	3.69 pH 6.5	2.31
1.07	2.41	3.59

Percoll stock: 9 parts Percoll (Amersham Biosciences, ϱ = 1.13 g/cm^3) + 1 part RPMI/HEPES (10x) (ϱ = 1.00 g/cm^3). This gives a density of ϱ = 1.117 g/cm^3.

RPMI medium (-FCS) with normal pH 6.5 is prepared by adjusting the pH with 1 M HCl, until it turns yellow.

After centrifugation, the cells were collected in a 50 ml Falcon containing RPMI 1640 medium (with FCS) from the upper two interphases using a pasteur pipet. The cells were then washed twice (1600 rpm for 8 min at 4 °C) in medium. At the end, the cell pellet was resuspended in RPMI 1640 medium or FACS buffer (5 % FCS) and counted. Following which, the cells were stained for FACS (Section 2.2.3.3.5).

2.2.3.3.3. Enrichment of human TECs using Anti-CD45-Dynal beads

For TEC enrichment using *Anti-CD45-Dynal beads* (Invitrogen), the cells corresponding to ~ 2 x 10^9 cells (from the pooled trypsin factions) were washed (1400 rpm for 5 min at 4 °C) in FACS buffer. The cell pellet was taken up in 10 ml FACS buffer and incubated with *Anti-CD45-Dynal beads* (4 x 10^8 beads/ml) in a 1:1 ratio for 20 min at 4 °C. Prior to incubation, the beads (~ 3 ml) were washed thrice in 20 ml FACS buffer and incubated for 5-10 min on the magnet till the solution was clear. The solution was decanted.

After incubation, the cell-bead mix was placed on the magnet and the clear solution containing the $CD45^-$ cells was collected. The beads were washed (1400 rpm for 5 min at 4 °C) twice in 15 ml FACS buffer and placed on the magnet. After each wash, the clear solution containing the $CD45^-$ cells was collected and washed with FACS buffer (1400 rpm for 5 min at 4 °C). The cell pellet was resuspended in RPMI 1640 medium or FACS buffer (5 % FCS) and counted, following which, the cells were stained for FACS.

2.2.3.3.4. Enrichment of human TECs using Anti-CD45-Microbeads

For the use of *Anti-CD45-Microbeads* (Miltenyi Biotech) to enrich for TECs, the cells corresponding to ~ 2-3 x 10^9 cells (from the pooled trypsin factions) were washed (1400 rpm for 5 min at 4 °C) in GM buffer and taken up in 20 ml FACS buffer. The cells were then incubated with a 1:35 dilution of *Anti-CD45-Microbead* for 20-30 min at 4 °C. After incubation, the cell-bead mix was washed with GM buffer (1400 rpm for 5 min at 4 °C). The cell pellet was resuspended in 10 ml GM buffer and filtered through 70 μm gauze. After which, they were aliquoted in ten 15 ml tubes each having ~2 x 10^8 cells/ml. The $CD45^+$ cells were then depleted using the *autoMACS™ Pro Separator* (Miltenyi Biotech), "Depletion program" as per the manufacturer's recommendations. The collected $CD45^-$ cell fractions were pooled, washed, resuspended in FACS buffer (5 % FCS) and counted, following which, the cells were stained for FACS.

2.2.3.3.5. Staining of human TECs

For cell staining, firstly the cells were blocked with 5 % mouse serum in FACS buffer (1 ml for every 1 x 10^8 cells) for 15 min on ice. For MUC1 antigen sorts, 5 % BSA solution was used for

blocking. The cells were then washed (1400 rpm for 5 min at 4 °C) and stained with an antibody cocktail (Table 2.22) for 15 min on ice in FACS buffer. After staining, the cells were washed (1400 rpm for 5 min at 4 °C), filtered through 35 µm filters and stained with PI directly prior to sorting. Cell populations were sorted on a *BD FACSDiVa* or BD FACSAria™ (SOP) Cell Sorter (Becton Dickinson) on purity mode under medium pressure (Figures 7 and 8).

Table 2.22: Overview of different antibody combinations used for human TEC cell sorting

TEC Populations Sorted	Antibodies used	Dilution
MHCII^{hi}/MHCII^{lo} mTEC and cTEC	anti-CDR2-Alexa 488	1:100
	anti-CD45-PerCP	1:5
	anti-EpCAM-Biotin	1:100
	Sav-PE	1:100
	anti-HLA-DR-Alexa 647	1:500
	PI (1 mg/ml)	1:1000
MUC1^{+} and MUC1^{-} mTEC	anti-CDR2-Alexa 488	1:100
	anti-CD45-PerCP	1:5
	anti-EpCAM-Biotin	1:100
	Sav-PE	1:100
	anti-HLA-DR-Alexa 680	1:100
	anti-MUC1-Alexa 647	1:100
	PI (1 mg/ml)	1:5000

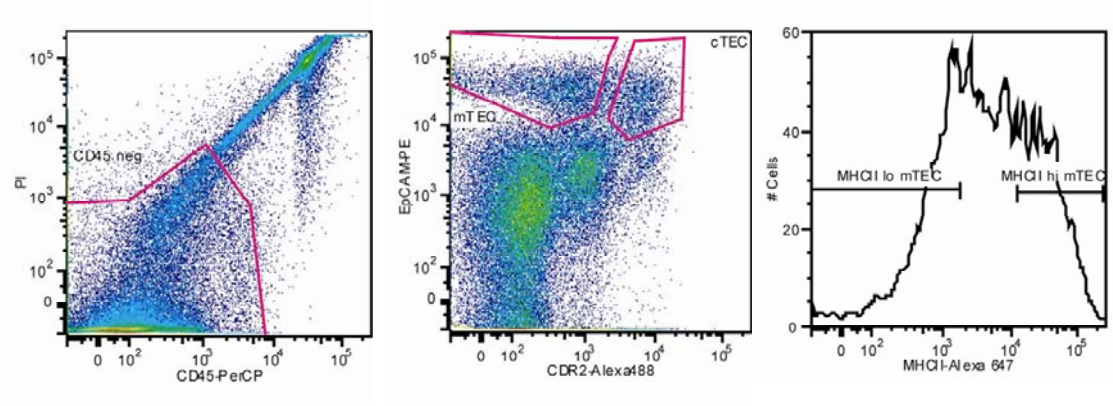

Figure 7

Sort gates for the isolation of human mTECs using *Anti-CD45-Microbeads*

The human mTEC and cTEC cell populations were separated using anti-CDR2 and anti-EpCAM mAbs. The mTECs were further differentiated into mature and immature subsets using anti-MHCII mAbs. The MHCII profile varied between the different human thymus samples.

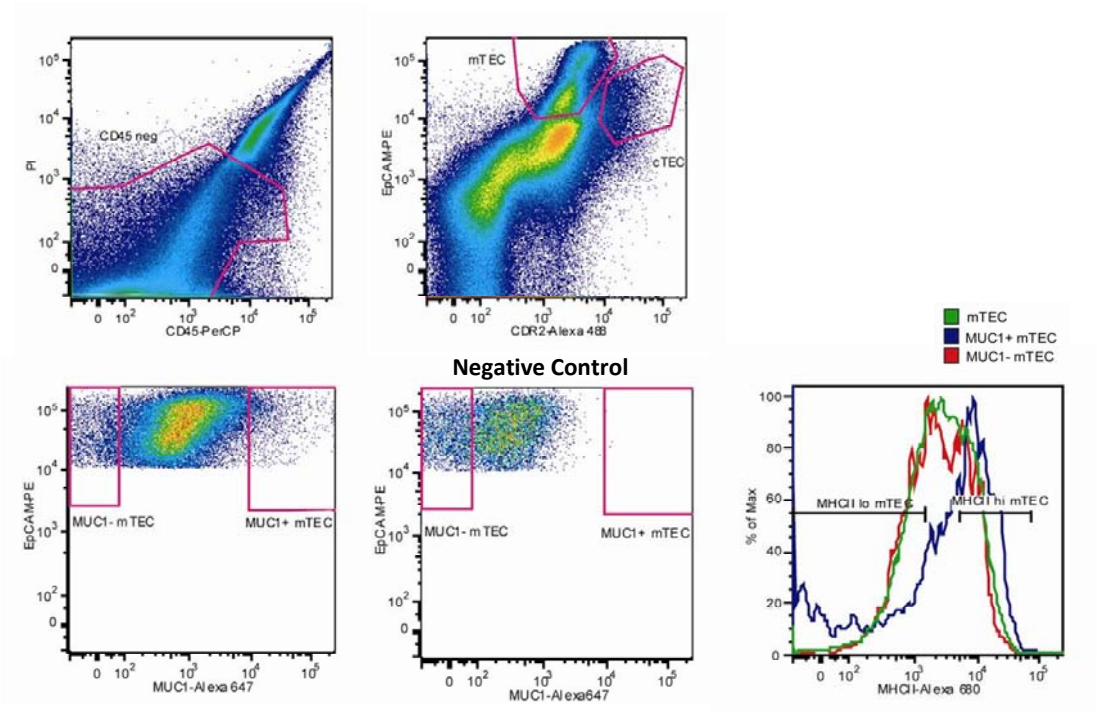

Figure 8

Sort gates for the isolation of MUC1 antigen specific mTECs using *Anti-CD45-Microbeads*

The human MUC1 expressing mTECs were stained and sorted for their MUC1 expression versus that of the negative control, without MUC1 antibody.

2.2.4. Counting of live cells

Cells were mixed in various dilutions with trypan blue and counted in a Neubauer counting chamber using a tabletop light microscope. The dead cells take up the trypan blue dye due to their disrupted cell membrane and appear blue, thus being able to be distinguished from their translucent live counterparts.

2.2.5. RNA isolation

Total cellular RNA was isolated using the *High Pure RNA Isolation Kit* (Roche) according to the manufacturer's instructions, from 2 x 10^4-10^6 cells.

2.2.6. RNA precipitation and RT-PCR

2.2.6.1. RNA precipitation

Total RNA eluted in 50 µl Elution buffer was precipitated if need be, depending on the concentration as measured using the *Nano Drop® 1000* photometer. The precipitation was performed over-night at -20 °C using 5 µg LPA and 2.5x sample volume of absolute ethanol (-20 °C), after which, the samples were centrifuged at 13,000 rpm for 30 min at 4 °C, then washed with 70 % ethanol (-20 °C) and re-centrifuged for 13 min. The pellet was then air-dried and re-suspended in 8-16 µl of RNase free water and either stored at -80 °C or directly used for RT-PCR.

2.2.6.2. RT-PCR

Genomic DNA was digested using 1 µl DNAse I (1 U/µl) for 30 min at 37 °C, followed by heat inactivation of the enzyme at 65 °C for 10 min. Subsequently, the RT-PCR was performed using the SuperScript II ™ RT (Invitrogen) as described in the manual.

For lower RNA amounts an alternative protocol was used, which is as follows:

To 4.5 µl RNA add 100 ng (200 ng/µl) (dT) - T7 primer, incubate at 70 °C for 10 min in a PCR block. To this add 4.5 µl ice-cold RT mix (2 µl 5x First Strand Buffer, 0.5 µl dNTP (10 mM), 0.5 µl T4gp32 (8 mg/ml, USB), 0.5 µl SuperaseIN, 1 µl H_2O). Incubate the mixture at 50 °C for 2 min. After which, 0.5 µl SuperScript II ™ RT enzyme (Invitrogen) was added. The reaction was incubated for 60 min at 50 °C.

The resulting cDNA from either protocol was purified on gel chromatography columns (*MicroSpin™ G50* columns) according to manufacturer's specifications, in order to remove excess nucleotides and oligonucleotides.

2.2.7. Conventional PCR

For 25 µl reaction of a conventional PCR:

Reagents	End Concentration	Volume
Forward Primer	250 nM	2.5 µl
Reverse Primer	250 nM	2.5 µl
dNTPs	200 µM	2.5 µl
10x Reaction Buffer	1x	2.5 µl
RedTaq® DNA-Polymerase	0.125 U	1 µl
cDNA	-	2 µl
H_2O	-	12 µl
Total Volume	**-**	**25 µl**

The following PCR cycle parameters were used for the thermocycler:

Steps	Time	Temperature	
Denaturation	3 min	94 °C	
Denaturation	1 min	94 °C	40 cycles
Annealing	1 min	55 or 58 °C	
Elongation	2 min	72 °C	
Elongation	3 min	72 °C	
	∞	4 °C	

The conventional PCR was used to control the success of the cDNA synthesis using β-Actin as a house-keeping gene. Since the β-Actin primers were intron spanning, the cDNA template gave a shorter product of 348 bp for mouse and rat cDNA using agarose gel electrophoresis. For human cDNA, the primers gave a product of 208 bp and had an annealing temperature of 55 °C.

2.2.8. Quantitative PCR (qPCR)

For quantitative gene expression analysis, real-time PCR was performed using the *GeneAmp® 7300 Sequence Detector*. Each primer pair was titrated for the optimum concentration, as mentioned in Tables 2.7-2.9.

Each reaction volume of 25 µl contained:

- Optimum primer concentration
- *Power SYBR® Green PCR Master Mix* (Applied Biosystems)/ *qPCR™ Core Kit for SYBR™ Green I* (Eurogentec)
- Template cDNA

The reaction mix was either pipetted as triplicates or duplicates in a *Thermo-Fast® 96 Detection Plate* (Abgene).

The following reaction parameters were used:

Steps	**Time**	**Temperature**
Activation*	2 min	50 °C
Activation of Hot GoldStar Polymerase	10 min	95 °C
Denaturation	15 s	95 °C } 40 or 45 cycles
Annealing and Elongation	1 min	60 °C }

* Activation step was always performed, but was usually for the activation of UNG for *qPCR™ Core Kit for SYBR™ Green I*.

The melting curves were compared to positive controls to ensure specificity of the PCR amplification. In some case, probes were used (with *qPCR™ Core Kit*) to increase the specificity of the PCR reaction. Relative quantification of gene expression was performed using the ΔΔCt (threshold value), with Ubc (for mouse), Hprt (for rat) and GAPDH (for human) as a house-keeping gene for normalization. ΔΔCt-method according to ABI User Bulletin #2; can be obtained under www.appliedbiosystems.com. Real-time PCR was performed to validate the sorted samples from all species (mouse, rat and human) for a set of known differentially expressed genes (Figure 9).

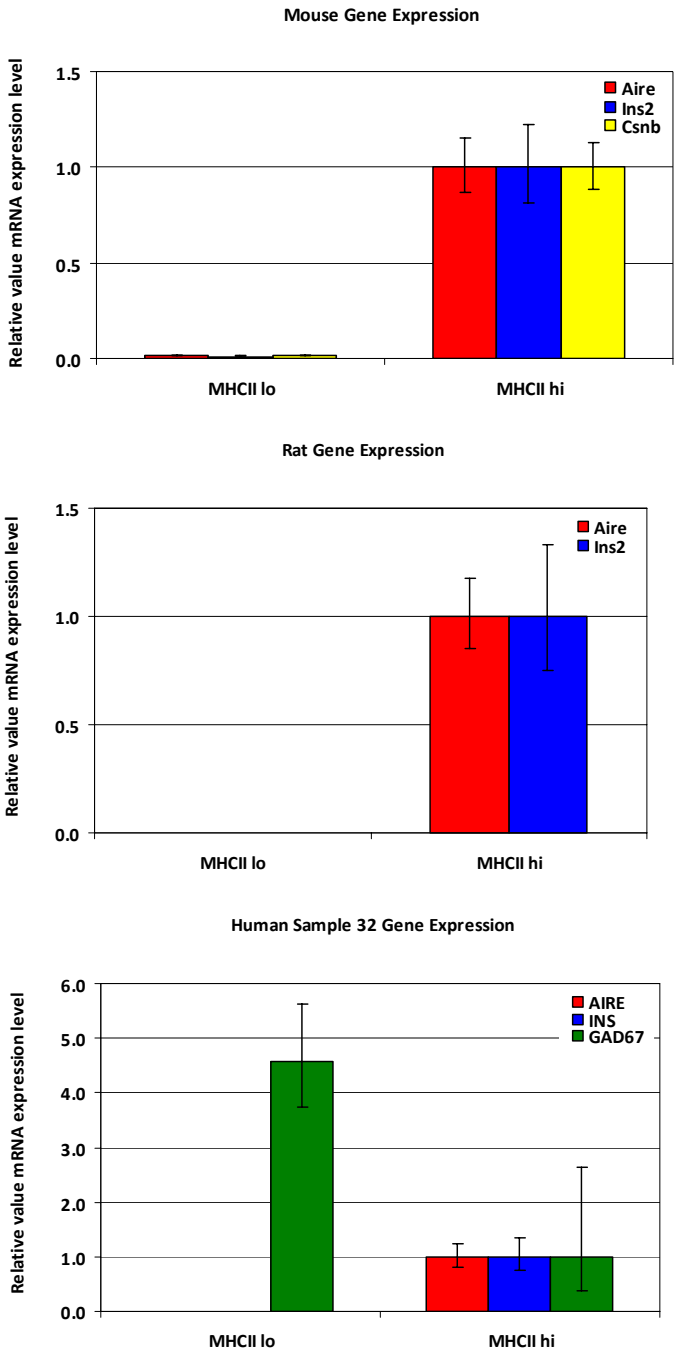

Figure 9

qPCR analysis of sorted samples from mouse, rat and human

Real-time PCR was performed to validate the sorted samples of all species (mouse, rat and human), prior to microarray hybridization for a set of known differentially expressed genes. One example from each sort for each of the species studies is shown. The MHCII^{hi} mTECs in all sepcies are enriched for pGE. The genes were normalized using a house-keeping gene (Ubc for mouse, Hprt for rat and GAPDH for human) and the expression was calculated using the ΔΔCt-method relative to the MHCII^{hi} mTECs. Genes tested: Aire-Autoimmune regulator; Ins-Insulin; Csnb-Casein beta; GAD67-glutamic acid decarboxylase 67.

2.2.9. Microarrays

Illumina expression profiling whole genome BeadArrays was used and the protocol followed was as described in the company manual (performed by the Genomics and Proteomics Core Facility of the DKFZ- Dr. B. Korn). For analysis of the array results, *BeadStudio 3.1* (Illumina Inc.) was used to obtain the raw data which were further analyzed using R project and Perl software.

2.2.10. µMACS™ SuperAmp™ Technology for Illumina BeadArrays

The *µMACS™ SuperAmp™* protocol (Miltenyi Biotec) is a recently established method for RNA amplification of small/rare cell populations. The amplified cDNA can be labelled and hybridized to microarrays for gene expression profiling. This technology was used and the samples were hybridized on Illumina's expression profiling whole genome BeadArrays. Technical details were established and performed as described in a TechNote (Pinto *et al.*, 2009).

2.2.11. Single-cell PCR (SC-PCR)

SC-PCR is a technique used to analyse the transcriptome of a single cell for up to 20 genes of interest and was essentially performed as described by Peixoto *et al.* (Peixoto *et al.*, 2004).

The different steps of the SC-PCR were performed on separate benches with dedicated pipets, ice-boxes, etc. The benches and ice-boxes were cleaned with sodium hypochlorite and *DNAaway* prior to starting the experiment to prevent cross-contamination. All reactions were performed on ice. Throughout the experiment, the same machines (the same order of heating blocks) were used.

2.2.11.1. Primer design, dilution and storage

Primers for SC-PCR were designed with the Amplify 3 program to be 20mers with a preferable GC content of 50 %. All primers were spanning exon-intron boundaries. Generation of primer dimers and potential cross priming was tested *in silico*. The primers were routinely tested by BLAST search for specificity. Lyophilized primers were resuspended in 1x TE buffer at 1 mM final concentration. From these stock solutions 100 µM aliquots were prepared (in water) and both solutions were stored at -80 °C. Working solutions of 25 µM or 12.2 µM were prepared from the 100 µM solutions with water. The working solutions were stored at -20 °C. No solution used in SC-PCR had gone through more than three freeze/thaw cycles.

2.2.11.2. Efficiency and competition primer tests

Each primer pair (primer pairs A-C and B-C from all genes of interest) was tested with the same template and the qPCR efficiency was assessed using the LinRegPCR program ("Efficiency test") (Figure 10A). In order to test the primer competition in the multiplex PCR, the first PCR was performed on the same template using: 1) a mix of all the A-C primer pairs (all genes); 2) an individual A-C primer pair (for each gene). The second PCR was a qPCR, using the first PCR as a template for each B-C primer pair (for each gene). Ct values and PCR efficiencies were compared between individual and multiplex PCRs to assess the degree of primer competition ("Competition test") (Figure 10B).

2.2.11.3. Cell sorting and storage

Cell sorting was performed with a *BD FACSDiVa* (Becton Dickinson) at 16 psi in single cell mode using the automatic cell deposition unit. Cells were collected in 5 µl PBS-DEPC (0.1 %) in 0.2 ml PCR 8-well stripes arranged in 96 well format, frozen in liquid nitrogen and stored at -80 °C. Routinely, positive and empty wells were included in the plates to check the specificity of the reaction. Each experiment was independently tested for instrument precision by sorting fluorescent beads and visually inspecting their deposition in a target area corresponding to the surface area of the 5 µl cell collecting volume.

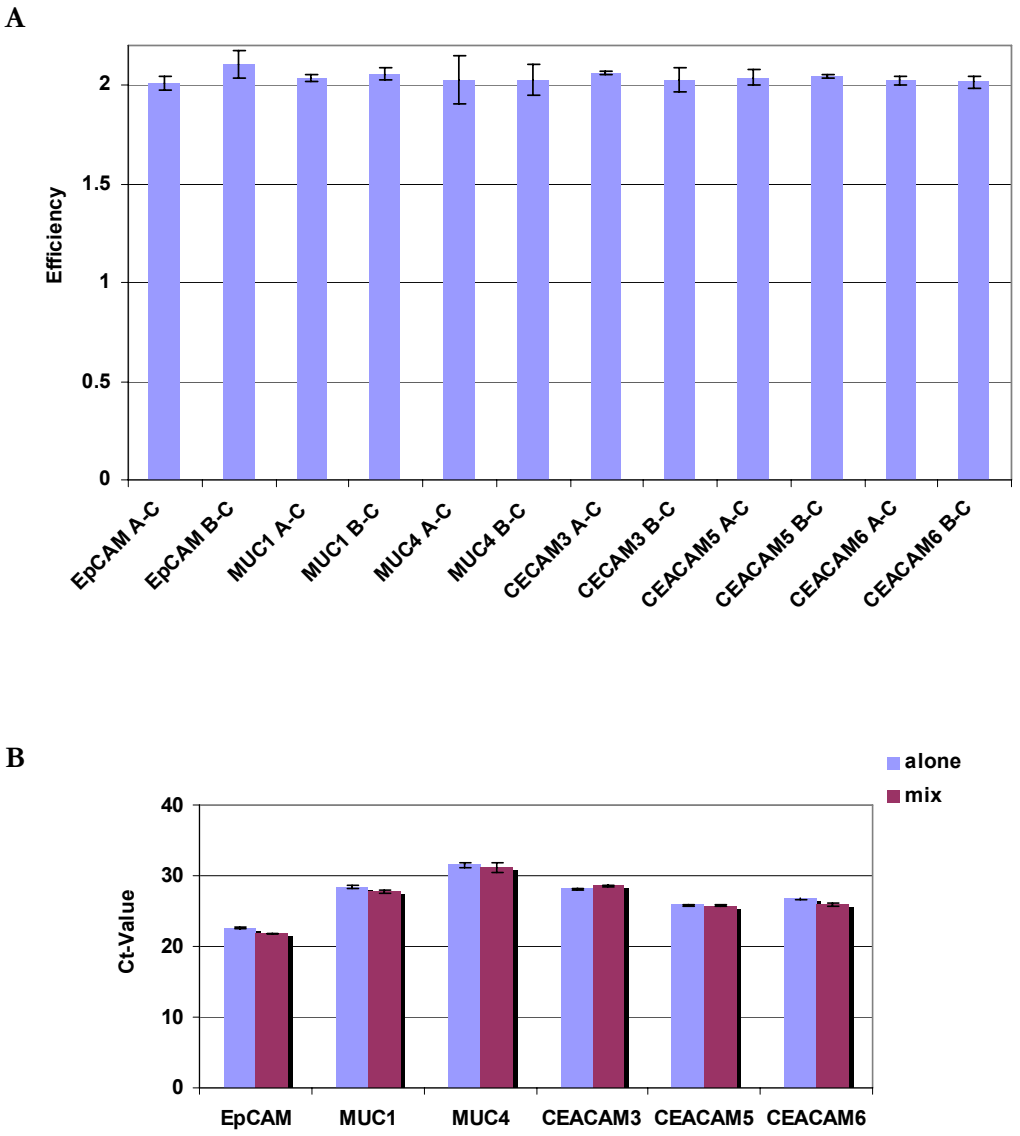

Figure 10

Efficiency and competition test of SC-PCR primers

(A) Efficiencies between the individual primer pairs tested did not vary significantly, primer pairs A-C and B-C were tested in sequential PCR reactions.

(B) Primer competition in the multiplex PCR, the first PCR was performed on the same template using: 1) a mix of all the A-C primer pairs (all genes); 2) an individual A-C primer pair (for each gene). The second PCR was a qPCR, using the first PCR as a template for each B-C primer pair (for each gene). There was no significant competition between the primer pairs as both "alone" and "multiplex" reactions achieved the same Ct values in the second amplification round.

2.2.11.4. Lysis of cells, reverse transcription and PCRs

Cell Lysis, reverse transcription, first PCR amplification and real-time quantitative PCR were performed using *DNA Engine Dyad* (MJ Research) and *7300 Real Time PCR System* (Applied Biosystems) instruments. The cycle number for the first PCR reaction was lowered from 15 to 14 and 50 cycles for the second round real-time quantitative PCR, since we observed an improved correlation between input cDNA and resulting threshold cycle (Ct) values.

The RT-PCR and the following gene expression studies of each sorted single cell were performed in the same tube. SC-PCR was highly sensitive and specific, as first a multiplex PCR was performed with outer primer pairs of all genes of interest (primers A and C) for 14 cycles and then a 50 cycle second round amplification-nested real-time PCRs were performed with the inner primer pairs (primers B and C) for each gene individually, using the first PCR as a template (Figure 11).

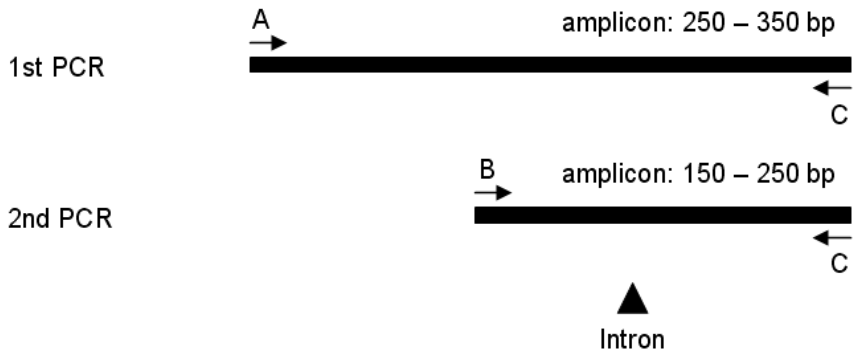

Figure 11

Schematic representation of the two amplification rounds performed in SC-PCR

14 cycles pre-amplification was performed in multiplex PCR with an outer primer pair, the second step amplification was performed as real-time PCR with a single inner primer pair.

Cells were lysed in the plate for 2 min at 65 °C in the PCR machine. 10 µl RT-Mix was added and reverse transcription performed in the PCR machine as below:

1x RT-Mix	
H_2O	2.34 µl
PCR buffer II (10x)	1.5 µl
$MgCl_2$	2 µl
dNTPs (10mM each)	1.5 µl
Oligos "C" (12.2 µM each)	0.16 µl x 6 (no. of oligos)
RNase Block	1 µl
MuLV	0.7 µl
Total	10 µl

PCR program for RT	
37 °C	60 min
95 °C	10 min
4 °C	∞

70 µl first PCR Master Mix was then added and the PCR was carried out in the PCR machine.

1x Master Mix 1st PCR	
H_2O	46.3 µl
PCR buffer II (10x)	8.5 µl
$MgCl_2$	7 µl
dNTPs (2.5 mM each)	7 µl
Oligos (25 µM each of "A" and "C")	0.05 µl x 2 x 6 (2 x no. of genes)
AmpliTaq Gold	0.6 µl
Total	70 µl

PCR program for 1st PCR		
95 °C	10 min	
94 °C	45 sec	10 cycles
60 °C	1 min	
72 °C	1 min 30 sec	
72 °C	10 min	

From the resulting 85 µl template, 4 µl/well were transferred to an *ABI PRISM 96-well Optical Reaction Plate* (Applied Biosystems) for individual gene qPCR with specific inner primers (primer pair B-C).

1x Master mix for 2nd PCR (qPCR)	
H_2O	7.52 µl
Primer "B" (25 µM)	0.24 µl
Primer "C" (25 µM)	0.24 µl
Power SYBR Green Mix	12 µl
Total	20 µl

PCR program for 2nd PCR (qPCR)		
95 °C	10 min	
95 °C	30 sec	50 cycles
60 °C	30 sec	
72 °C	45 sec	
Melting curve analysis		

Our data were analyzed in a qualitative fashion, since the PCR efficiency varied among cells for the same and different genes. In case of an atypical melting curve, the product from the respective well was re-amplified by the appropriate primer combination for 15 cycles with "conventional" PCR, analyzed on an agarose gel, purified with QIAquick PCR Purification Kit and sequenced in house.

Expression frequencies and co-expression patterns were tested for significance with the Chi-Square Test. Co-expression studies were tested for significance with the Jonckheere-Terpstra Test.

2.2.12. Fluorescence *in situ* hybridization (FISH)

2.2.12.1. FISH probes

Labelled FISH probes BAC clone- RP11-263K19-Gold Cyanine-3 UTP and RP11-343B1 Green 5(6)-Rhodamine Green dUTP were ordered from Empire Genomics.

2.2.12.2. Cell fixation

Slides were coated with 0.1 mg/ml Poly-L-Lysine for 1 hour at room temperature and then washed twice in water and air-dried. The FACS cells (in 50 µl 50 % RPMI/ 50 % FCS) were then dropped onto the coated slides and allowed to settle for 1 hour at 37 °C. The slides were washed for 1 min in 0.3x PBS and fixed for 10 min in 4 % PFA/0.3x PBS. Thereafter, the slides were washed thrice for 5 min each in 1x PBS. The nuclear membrane was permeabilised for 20 min in 0.5 % Triton-X-100/PBS, following which, they were washed thrice for 3 min each in 1x PBS. The samples were immersed in 20 % Glycerol/PBS as a cryo-preservative and left to equilibrate

for 1.5 h at room temperature or over-night at 4 °C. The samples were then subjected to 4 freeze/thaw cycles in liquid nitrogen, then washed thrice for 5 min each in 1x PBS and incubated for 7.5 min in 0.1 N HCl/H_2O. After which the slides were washed three times for 5 min each in 2x SSC. They were then equilibrated in 50 % formamide/2x SSC over-night at 4 °C and stored in this solution at 4 °C for up to three months.

2.2.12.3. *In situ* hybridization (ISH)

For ISH, both the cellular DNA as well as the probe DNA were denatured, combined together and renatured allowing the single stranded probe DNA to bind to single strands of the genomic DNA. The probes (2 µl of each probe, 1 µl human COT-1, 1 µl Salmon Sperm, 6 µl probe buffer) were denatured at 78 °C for 7 min and partially renatured for 20 min at 37 °C. In the meanwhile, the PFA-fixed cells (cellular DNA) were denatured at 72 °C for 3 min, immediately thereafter the probes were dropped onto 18 x 18 mm cover slips and combined with the denatured cell nuclei on the slides. The coverslips-slides were then sealed with rubber cement (Fixogum) and left to renature over 2 nights in a moist chamber at 37 °C in the dark. During the entire preparation of PFA-fixed nuclei it was crucial to keep samples wet at all times as drying would lead to a collapse of the 3D architecture of the nucleus.

After renaturation, the cover slips were removed and excess probe was washed off thrice for 5 min each in 0.5 % Tween 20/4x SSC at 42 °C followed by three washes of 5 min each with 1x SSC at 60 °C. Then the slides were dipped in 0.5 % Tween 20/4x SSC, equilibrated in PBS for 5 min and stained with HOECHST 33342 (1:1000 of 1 mg/ml stock) for 3-4 min. Slides were washed twice for 3 min each in 1x PBS and embedded on to 22 x 22 mm coverslips in 15 µl ProLong Gold (Invitrogen). The ProLong Gold was left to harden over 1-2 nights before images were taken.

2.2.12.4. Image acquisition and analysis

Z-stack images were acquired at the Microscopy Core Facility, DKFZ, Heidelberg, with a Leica TCS SP5 Confocal Microscope using the 63x oil objective.

Image analysis was performed using a custom-made ImageJ plugin. In order to exclude false-positive spots, the position and the slices of appearance of the FISH probes were manually selected in the ImageJ software. FISH probes were confirmed to be sphere-shaped in 3D by determining the area of the (2D) spots of a FISH probe across confocal slices (Figure 12). In the ImageJ plugin the distance between FISH probes was then calculated as the 3D Euclidean

distance between the spot centres of the confocal slices with the largest area for each FISH probe, which was considered as the probe (sphere) centre (Figure 13). An output file consisting of the x, y and z co-ordinates of sphere centres of each FISH probe and distance measurements (four distances per cell) were generated for each image and the co-localization of the two chromosomes was studied.

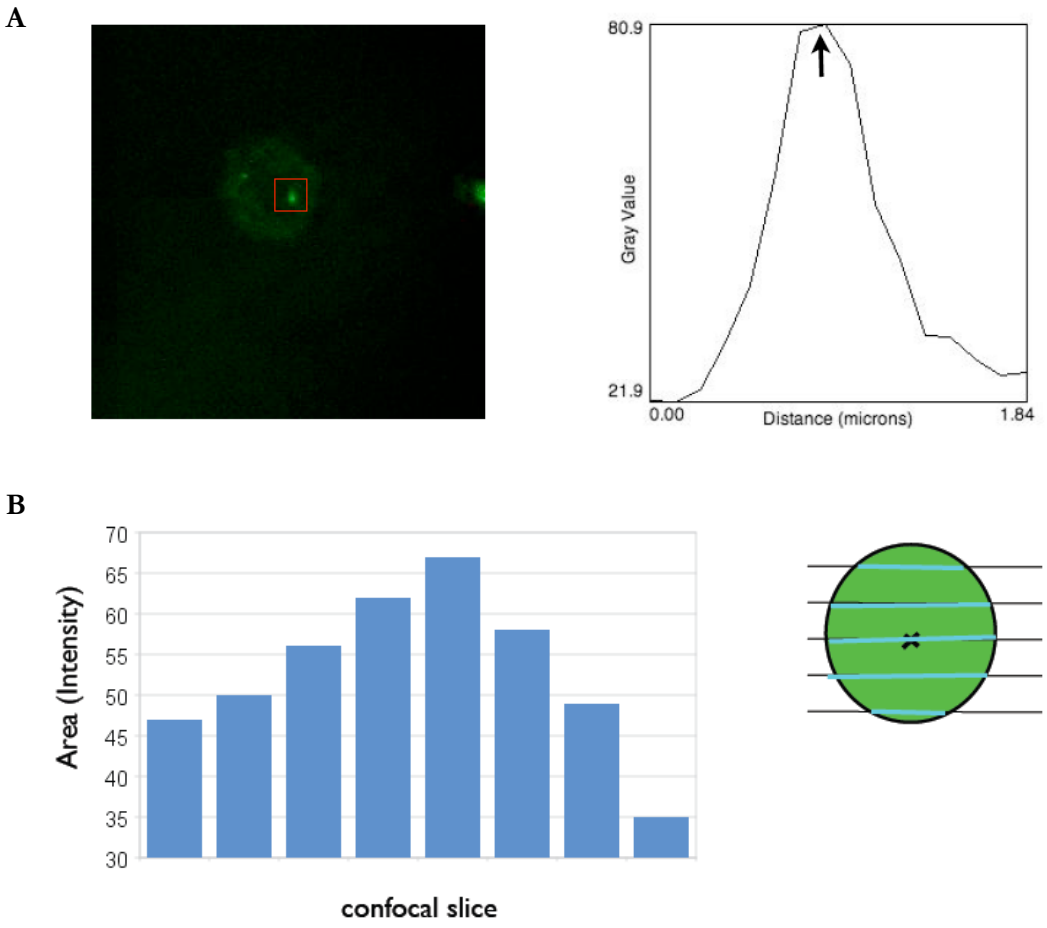

Figure 12

Intensity measurements for the FISH probes

(A) Example of green FISH probe and a plot of it's intensity. The arrow indicates the point of maximum intensity.

(B) A plot of the confocal slices versus intensity of a FISH probe. Each FISH probe appears and disappears over certain slices and there is always a slice where the probes intensity is maximum. This slice was considered as its z-position of the FISH probe. A sketch of a FISH probe was drawn, with the cross in the centre representing the slice of maximum intensity.

In order to set a threshold for the minimum distance between the FISH probes, which we would consider to be co-localized, we estimated the radius of the sphere described by a FISH probe in two different ways, which both yielded the same result. First, we determined the typical diameter of the (2D) spot with maximum area of a FISH probe (Figure 14A). This was found to be 1.3 µm, yielding a radius R of 0.65µm. In a second estimate of the sphere radius, we measured the average number of slices in which the probes appear as 6. With a distance of 0.21 µm between consecutive confocal slices, this yields a diameter of 6 x 0.21 = 1.26 µm and a radius of 0.63 µm (Figure 14B), which is similar to the first estimate.

If two FISH probes are adjacent or over-lapping then the 3D distance between probe centres should be less than or equal to the sum of the radii of both probes (Figure 14A). Taken together, we considered 1.2 µm to be the maximum distance for co-localization between any two FISH probes. Using the Matlab software the plots of distance measurements between the FISH probes for each human sample were generated.

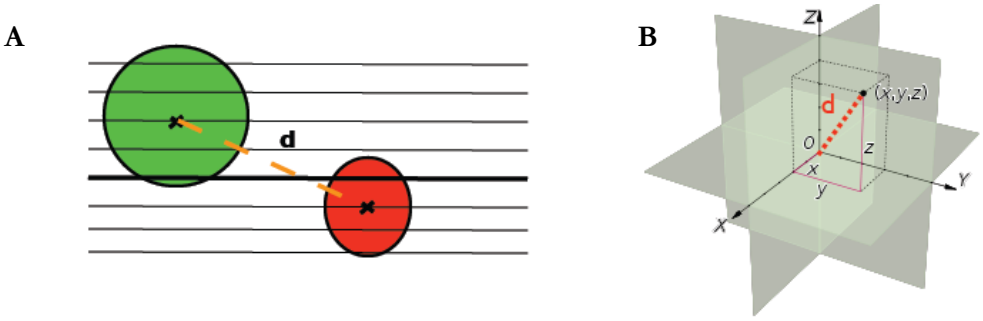

Figure 13

3D Euclidean distance measurements between the FISH probes

(A) A sketch of the distance (d) between two FISH probes as calculated using the slice of maximum intensity for each probe in the z-plane.

(B) The 3D Euclidean measurements used to calculate the distance between the FISH probes.

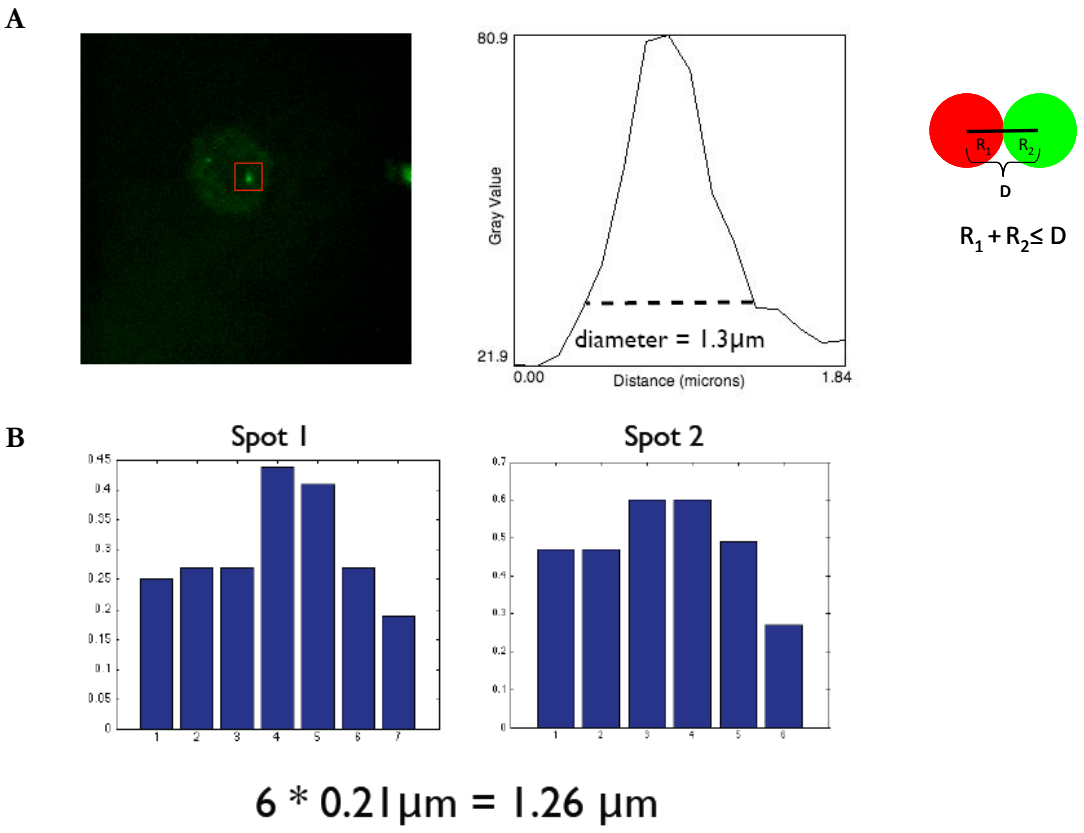

Figure 14

Estimations used to set the threshold for the minimum distance between the FISH probes

(A) First an estimation was used to set a threshold for the minimum distance between the FISH probes, which we would consider to be co-localized. The typical diameter (D) of the FISH probes was found to be 1.3 µm, yielding a radius (R) of 0.65µm. Hence, if two FISH probes are adjacent or over-lapping then the sum of the radius (R) for both probes should be less than or equal to the diameter ($R_1+R_2 \leq D$).

(B) The second criterion we considered was the average number of slices in which the probes appear as 6 and 0.21 µm as the distance between consecutive confocal slices. This yields a diameter of 6 x 0.21 = 1.26 µm and a radius of 0.63 µm. Together; we considered 1.2 µm to be the maximum distance for co-localization between any two FISH probes.

3. Results

3.1. Expression patterns and evolutionary conservation of promiscuous gene expression (pGE)

The scope of promiscuous gene expression (pGE) largely determines the extent of central T-cell self-tolerance. Global gene expression patterns among thymic stromal cells clearly singled out mTECs as a cell type specialized in expressing TRAs (Derbinski *et al.*, 2001; Anderson *et al.*, 2002; Gotter *et al.*, 2004; Derbinski *et al.*, 2005). MTECs are a heterogeneous population with regards to their phenotype, expressing varying levels of co-stimulatory molecules like CD80, CD86 and MHCII, which denotes progressive maturation. The complete representation of pGE requires differentiation steps as shown previously in murine and human mTECs whereby the majority of promiscuously expressed genes is up-regulated in a subset, characterized by high level expression of MHCII, CD80/86 in addition to the expression of Aire (Nelson *et al.*, 1993; Derbinski *et al.*, 2005; Derbinski and Kyewski, 2005; Taubert *et al.*, 2007). Hence, to affirm previous observations showing a correlation between promiscuous gene expression and induction of these differentiation markers we chose to separate mTECs according to their relative expression levels of MHCII (into immature, $MHCII^{lo}$ and mature, $MHCII^{hi}$ mTECs). More so, we sought to gain a comprehensive insight into: firstly to what extent is the genome represented in the thymus, secondly to decipher underlying mechanisms/parameters/rules governing pGE and thirdly to study the evolutionary conservation of pGE. This study focused on mTEC subsets in different species (i.e. mouse, rat and human) and the phenomenon of pGE at a global level.

We could have opted for the separation of complete mTECs from cTECs in order to get an insight into the above queries. But since they represent two distinct lineages, it would include the expression of lineage-specific genes. Hence, we decided to study gene expression within the mTEC cell-lineage focusing on its two different subsets of immature and mature mTECs. The MHCII molecule is well characterized in mice, rats and humans, thus in this study mTECs were separated into mature and immature subsets based on MHCII expression. The lower and upper 30 % of $MHCII^{lo}$ and $MHCII^{hi}$ expressing mTECs from each species were enriched by density gradients/magnetic beads and sorted by FACS (Section 2.2.3, Figures 5, 6 and 7). RNA was isolated and part of the RNA was used for cDNA synthesis to perform a control qPCR to validate the quality of the sorts using a set of known differentially expressed genes (Section 2.2.5 - 2.2.8 and Figure 9).

A RNA collection of 3 mouse sorts (20 female mice each, in the range of 6-8 weeks of age), 5 rat sorts (5-6 female rats each, in the range of 7-9 weeks of age) and 11 human sorts (ranging from 3 days to 3 years of age) were *in vitro* transcribed into labeled cRNA (Illumina® TotalPrep RNA

Amplification Kit, Ambion) and hybridized onto Expression BeadChip, Whole Genome Gene Expression Arrays (Illumina). The data were then further processed using Bead Studio 3.1 (Illumina), R and Bioconductor packages.

3.1.1. Estimation of the number of differentially expressed genes between MHCII^{lo} and MHCII^{hi} mTECs

The probes on the arrays were annotated based on Ensembl genes. After Quantile normalization of the microarray data, the differentially expressed genes between MHCII^{lo} and MHCII^{hi} mTECs of each species were estimated using the criteria of $p \leq 0.01$ and Fc (fold-change) greater/lesser than or equal to 2 ($Fc \geq 2$ or $Fc \leq 2$).

	Mouse	Rat	Human
Differentially expressed genes	1889	700	2000-3000 (2205)
Up-regulated genes	1263	360	~1226
Down-regulated genes	626	340	~980

Table 3.1

Comparison of differentially expressed, up-regulated and down-regulated genes between MHCII^{lo} and MHCII^{hi} mTECs from mouse, rat and human thymus

Data represent 3 mouse sorts, 5 rat sorts and 11 human sorts. Values for humans are an estimation owing to the large inter-individual differences.

The number of differentially expressed, up- and down-regulated genes between the three species was rather similar (Table 3.1), taking into consideration that the number of probes on the rat microarrays were half compared to mouse and human (22,000 probes for rat vs. 45,000 probes for mouse and 48,000 probes for human).

In addition, the autoimmune regulator (Aire) dependency was also studied in mouse where the KO strain was available. Microarrays of MHCII^{lo} and MHCII^{hi} mTECs from Aire$^{-/-}$ female mice (3 sorts, 6-7 female mice each), were performed. Aire has been shown to control pGE at least partially by regulating the expression of numerous genes in mTECs with a predilection for TRAs (Anderson *et al.*, 2002; Derbinski *et al.*, 2005). This issue is of particular importance in the pathophysiology of the human autoimmune polyglandular syndrome type 1 (APS-1). APS-1 is a rare recessive, autosomally inherited monogenic disease, which is caused by mutations in the *AIRE* gene (Pitkanen and Peterson, 2003). This disease is modeled in Aire$^{-/-}$ mice and offers valuable information to study tolerance mechanisms since thymi of APS-1 patients are not

available for study (Anderson *et al.*, 2002; Ramsey *et al.*, 2002). From the microarray data the Aire-dependent genes were defined as those genes whose: 1) difference in average expression of $MHCII^{hi}$ - $MHCII^{lo}$ mTECs in WT mice was significantly different from the difference in average expression of $MHCII^{hi}$ - $MHCII^{lo}$ mTECs in KO mice; 2) fold change was greater/lesser than or equal to 2 between $MHCII^{hi}$ and $MHCII^{lo}$ mTECs in WT mice and greater than the fold change in KO mice.

Criteria for defining Aire-dependent genes:

1. [avg. exp. $MHCII^{hi}$ mTECs - avg. exp. $MHCII^{lo}$ mTECs] in WT mice - [avg. exp. $MHCII^{hi}$ mTECs - avg. exp. $MHCII^{lo}$ mTECs] in KO mice

2. [Fc ≥ 2 or Fc ≤ 2 between $MHCII^{hi}$ and $MHCII^{lo}$ mTECs] in WT mice > [Fc ≥ 2 or Fc ≤ 2 between $MHCII^{hi}$ and $MHCII^{lo}$ mTECs] in KO mice

Using the above criteria, global analysis in $Aire^{-/-}$ female mice showed that a large number of genes were Aire-dependent in the up-regulated gene set. Yet, a large number of genes were also observed to be Aire-independent, thus confirming that Aire regulates only a part (~36 %) of genes that are differentially expressed in $MHCII^{hi}$ vs. $MHCII^{lo}$ mTECs (Table 3.2).

	Up-regulated genes	**Down-regulated genes**
Aire-dependent genes	455	32
Aire-independent genes	808	594

Table 3.2

Set of Aire-dependent and -independent up-regulated and down-regulated genes

Data is a compilation of 3 $Aire^{-/-}$ mouse sorts.

The human data showed large inter-individual variability, to such an extent that a common set of differentially expressed genes cannot be deduced. Table 3.5A shows the estimated number of up- and down-regulated genes within and between each patient.

Extrapolating from the gene array analysis, we estimate that ~10 % of all known genes are turned on in mature $MHCII^{hi}$ mTECs in addition to differentiation-dependent genes. This however is an under-estimate due to a methodological limitation, as the currently available genome-wide screening microarray platform has low sensitivity. Use of most modern Deep Sequencing technology may ultimately precisely define the promiscuously expressed gene pool.

3.1.2. Linking features of promiscuous gene expression

After having defined the pools of differentially expressed genes in the different species, further studies into the properties of these genes were carried out. Anderson *et al.* first showed that genes expressed in mTECs are enriched for TRAs (Anderson *et al.*, 2002). Subsequently our working group (Gotter *et al.*, 2004; Derbinski *et al.*, 2005) as well as Johnnidis' (Johnnidis *et al.*, 2005) described the bulk of promiscuously expressed genes that are turned on in the mature mTEC subset to be: 1) enriched in TRAs and 2) tend to co-localize in clusters in the genome. A direct link between these two features i.e. enrichment for TRAs and clustering had not been formally shown (Figure 15). How are these two features linked? One possibility is that TRAs are clustered in the genome irrespective of functional or structural relatedness. PGE would project onto such TRA clusters to various extents in mTECs. In order to test this notion, TRAs were operationally defined, their genomic position deduced and genome-wide analysis of gene clusters was performed.

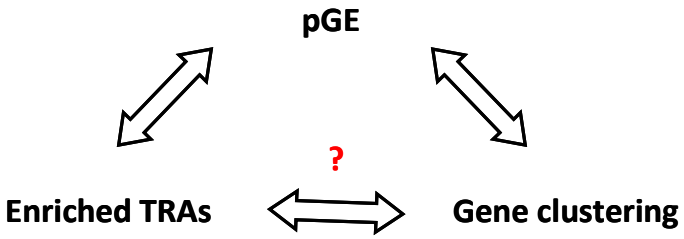

Figure 15

Linking features of pGE

PGE is known to enrich for TRAs and clustered genes. How do these features link?

3.1.2.1. Defining tissue-restricted antigens (TRAs)

Gene expression data from the public database at *http://symatlas.gnf.org* (Su *et al.*, 2004) were taken for the identification of tissue-restricted genes. This database contains expression assignments for many different tissues and cell types derived by gene array analysis. A gene was defined as a TRA, if its expression was above 5X the median (the median expression over all tissues) in less than five tissues. From the database in mouse, 61 different tissues were listed. The gene expression data for 20,000 non-redundant annotated genes were analyzed over 61 tissues. By these criteria, 5000 genes in the mouse genome were defined as TRAs (Figure 16).

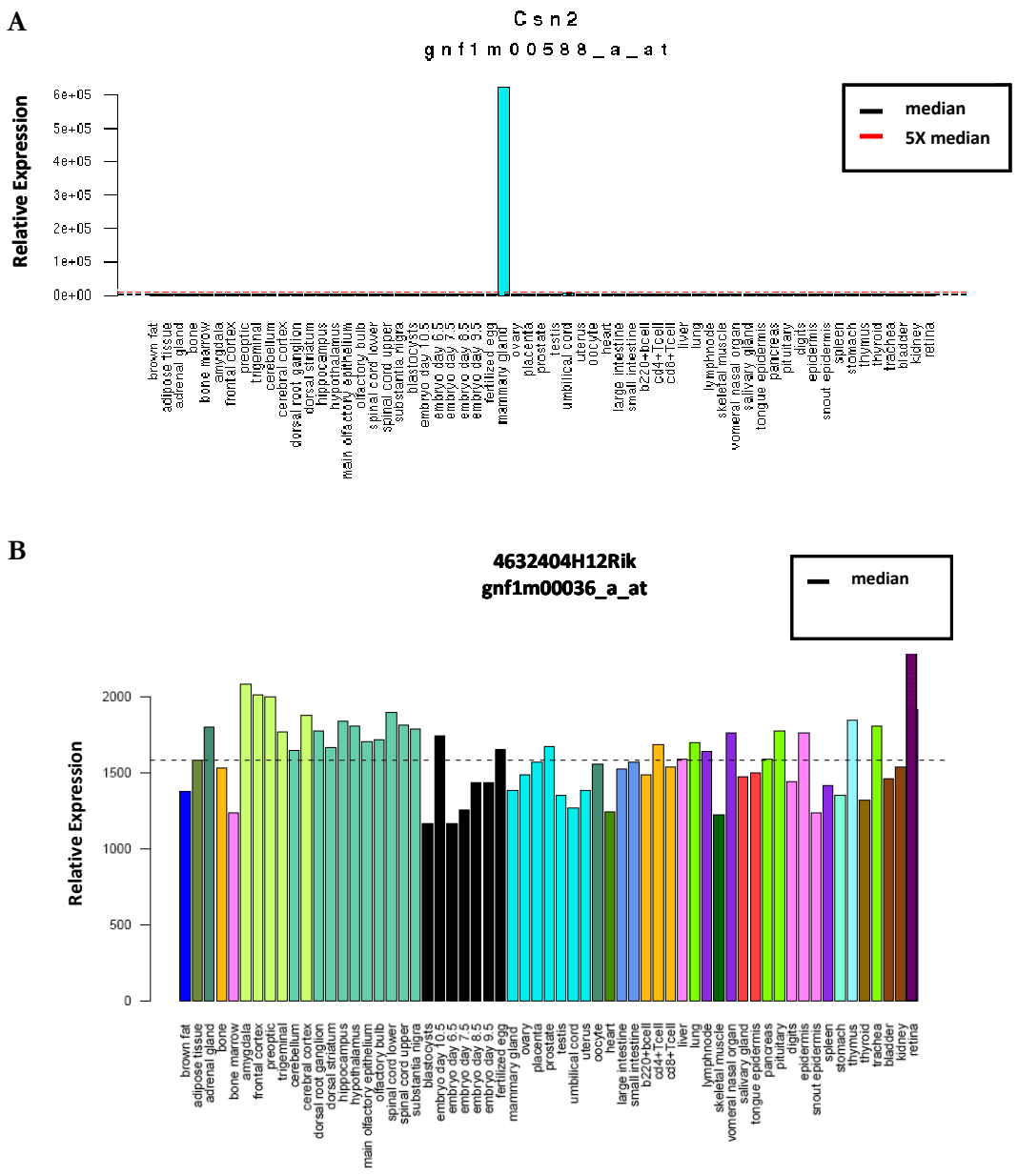

Figure 16

Defining TRAs in mouse

The public database *http://symatlas.gnf.org* (Su *et al.*, 2004) was used to identify tissue-restricted antigens (TRAs). Array expression data of each gene was plotted across the various tissues. The median expression was set across all tissues and a gene was defined as a TRA, if its expression was above 5X the median in less than five tissues.

(A) Example of a TRA, Casein beta (Csn2) exclusively expressed in the mammary gland. Note that Csn2 is not detected in the thymus, though it is known to be expressed as a TRA in the thymus. This is due to 3 reasons: 1) pGE tested by PCR is 10,000 or more fold lower in mTECs than in the respective tissue cell type (J. Derbinski unpublished data); 2) here the expression is tested in complete thymus and not purified mTECs; 3) the array data is of lower sensitivity than PCR, hence making Csn2 too low to score.

(B) Example of a non-TRA, 4632404H12Rik, which is widely expressed across all tissue.

The same method was used to define TRAs in human over 57 tissues listed in the database. A total of 3294 TRAs are present in the human genome from 22,284 non-redundant annotated genes (Figure 17).

A

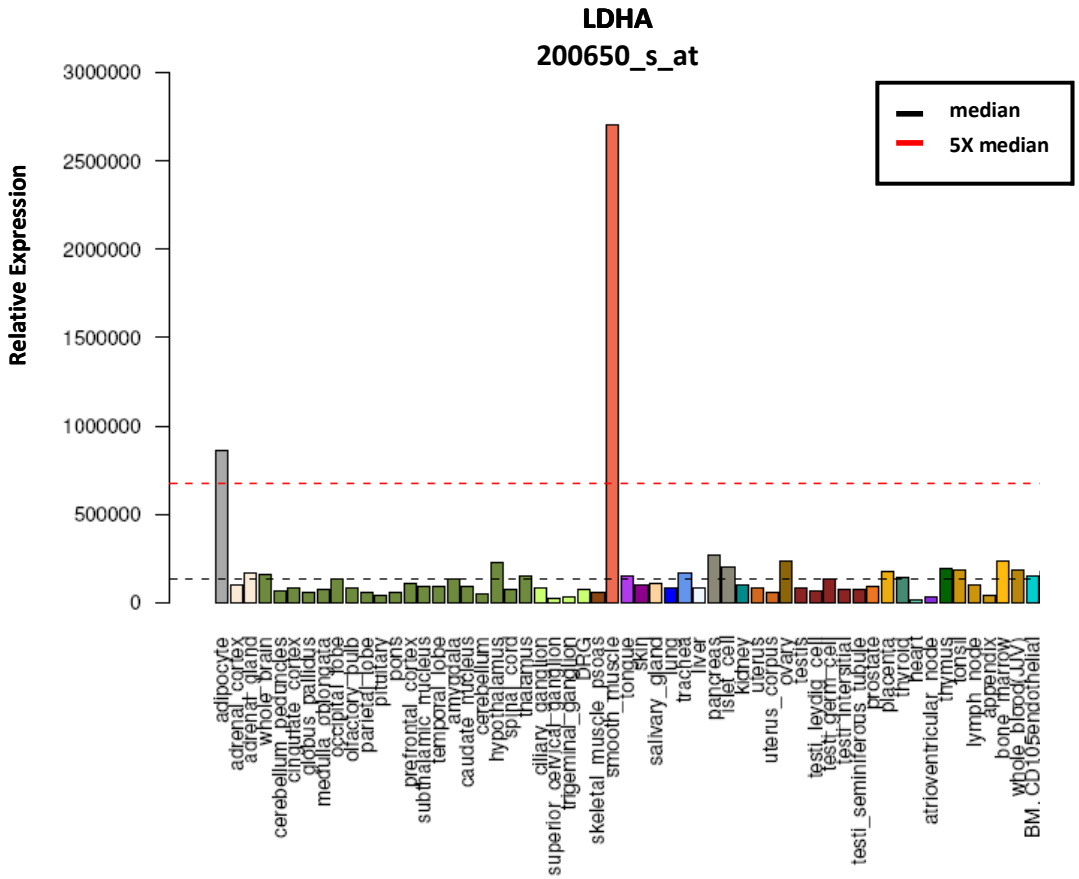

B

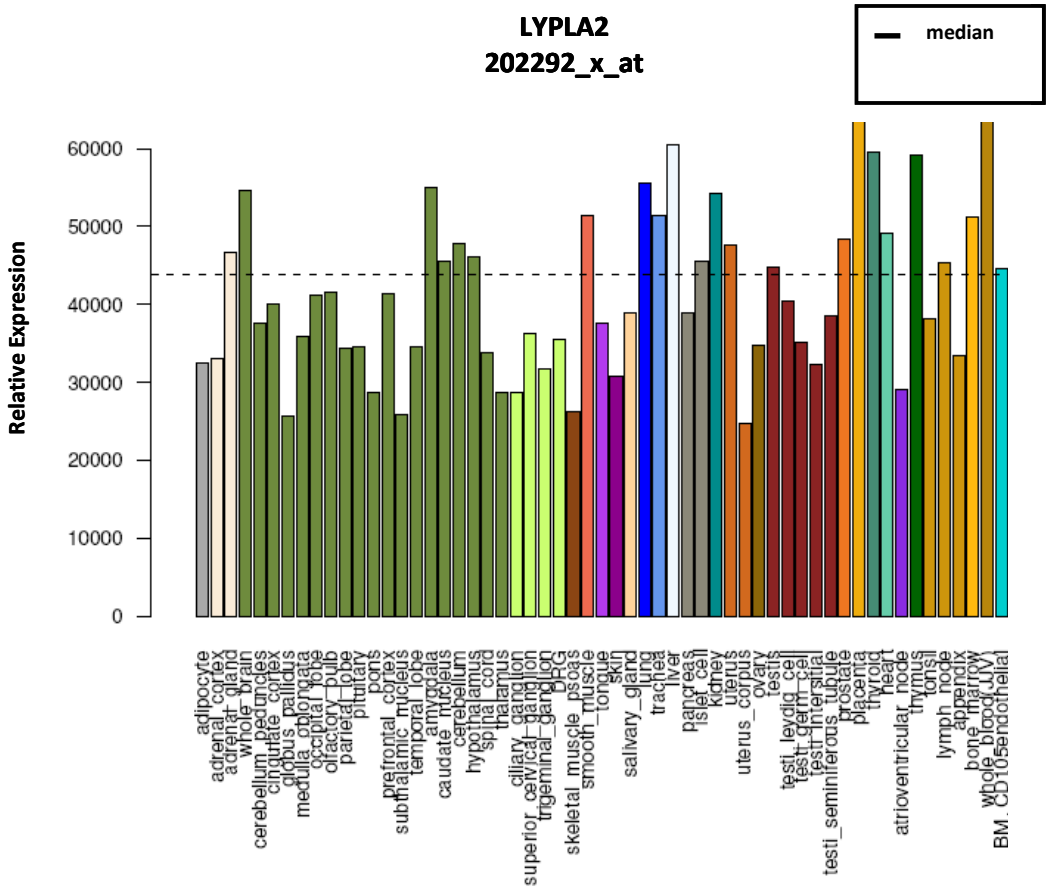

Figure 17

Defining TRAs in human

The public database *http://symatlas.gnf.org* (Su *et al.*, 2004) was used to identify tissue-restricted antigens (TRAs) in human just as described above for mouse.

(A) Example of a TRA, L-lactate dehydrogenase A chain (LDHA) primarily expressed in smooth muscle.

(B) Example of a non-TRA, Lysophospholipase II (LYPLA2), which is widely expressed across all tissues.

Owing to the lack of sufficient information in the *Symatlas* database as well as in the annotation of the rat genome, only 12 different tissues could be defined. Since this would create a bias while calculating the median expression over these tissues, TRAs in rat were defined using mouse orthologs. Next we analyzed whether these defined TRAs are randomly distributed or clustered in the genome.

3.1.2.2. Gene clustering

In order to analyze gene clustering independent of gene density, a 10-gene sliding window approach was used as described by Derbinski *et al.* (Derbinski *et al.*, 2005). In this method, a sliding 10-gene window is used to count for the number of TRAs within 10 consecutive genes on each chromosome (Figure 18). Firstly, the physical position of the non-redundant annotated genes was designated on their chromosomes using the Ensembl database. Then, the 10-gene sliding window clustering algorithm was run and the cluster size was recorded. As it turned out that in some cases, immediately neighbored clusters were < 10 genes apart, an assembly step was appended to the algorithm to combine such clusters. The significance of the clustering was determined by repeating the same procedure 1,000 times in each case with a list of random genes of the same size as the experimental dataset and the results were compared with the number of clusters found.

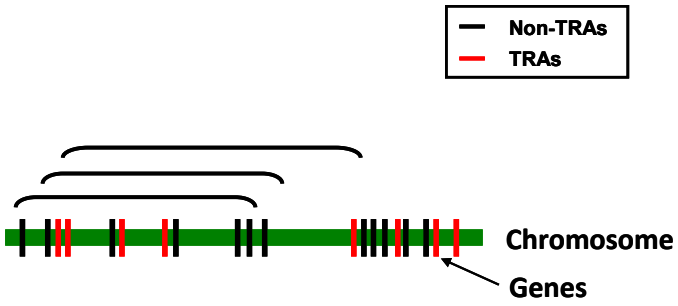

Figure 18

10-gene sliding window clustering algorithm

To analyze gene clustering, a 10-gene sliding window was used to count for the number of TRAs within 10 consecutive genes on each chromosome. Then the window was moved to the adjacent gene and the same procedure was performed over all chromosomes, to finally give a cluster plot, described in Figure 19. For immediately neighbored clusters which were < 10 genes apart an assembly step was appended to the algorithm to combine such clusters.

Preferential chromosomal localization has been reported for genes co-expressed in certain cell lineages and serving a common function (Wang *et al.*, 2001; Ramalho-Santos *et al.*, 2002; Hurst *et al.*, 2004). We analyzed, if TRAs *per se* are clustered in the genome. Indeed, in all three species it was observed that TRAs tend to co-localize in clusters, the largest comprising up to 117 genes in mouse (Figure 19A), 130 genes in rat (Figure 19B) and 63 genes in human (Figure 19C). This clustering of more than 4 TRAs was highly significant when compared with random distributions of genes. Taken together, TRAs are clustered in the genome in the studied species, this is highly significant and the degree of clustering is similar between all three species.

A

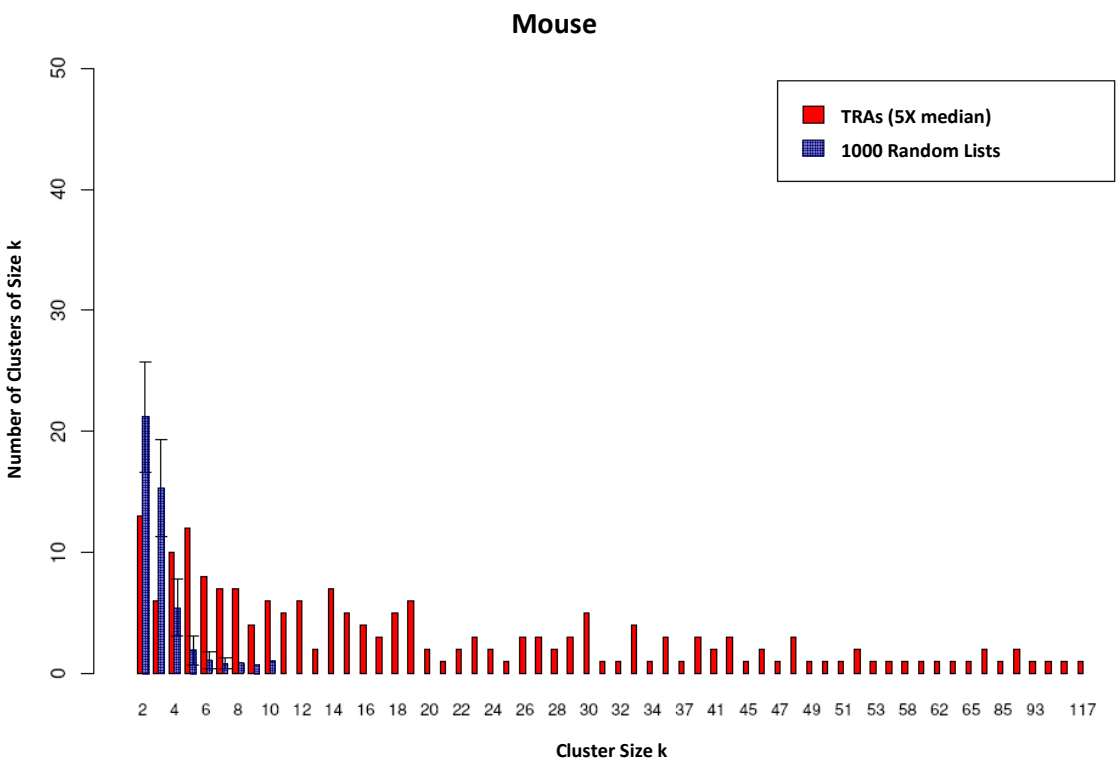
Mouse
TRAs (5X median)
1000 Random Lists
Number of Clusters of Size k
0
10
20
30
40
50
2 4 6 8 10 12 14 16 18 20 22 24 26 28 30 32 34 37 41 45 47 49 51 53 58 62 65 85 93 117
Cluster Size k

B

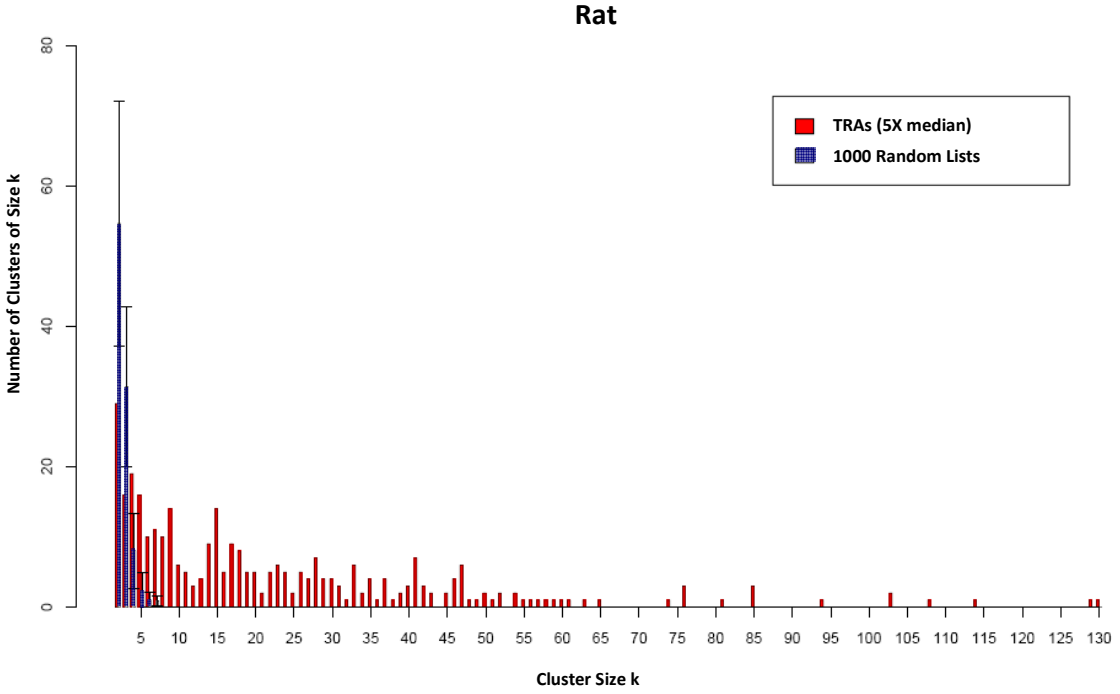
Rat
TRAs (5X median)
1000 Random Lists
Number of Clusters of Size k
0
20
40
60
80
5 10 15 20 25 30 35 40 45 50 55 60 65 70 75 80 85 90 95 100 105 110 115 120 125 130
Cluster Size k

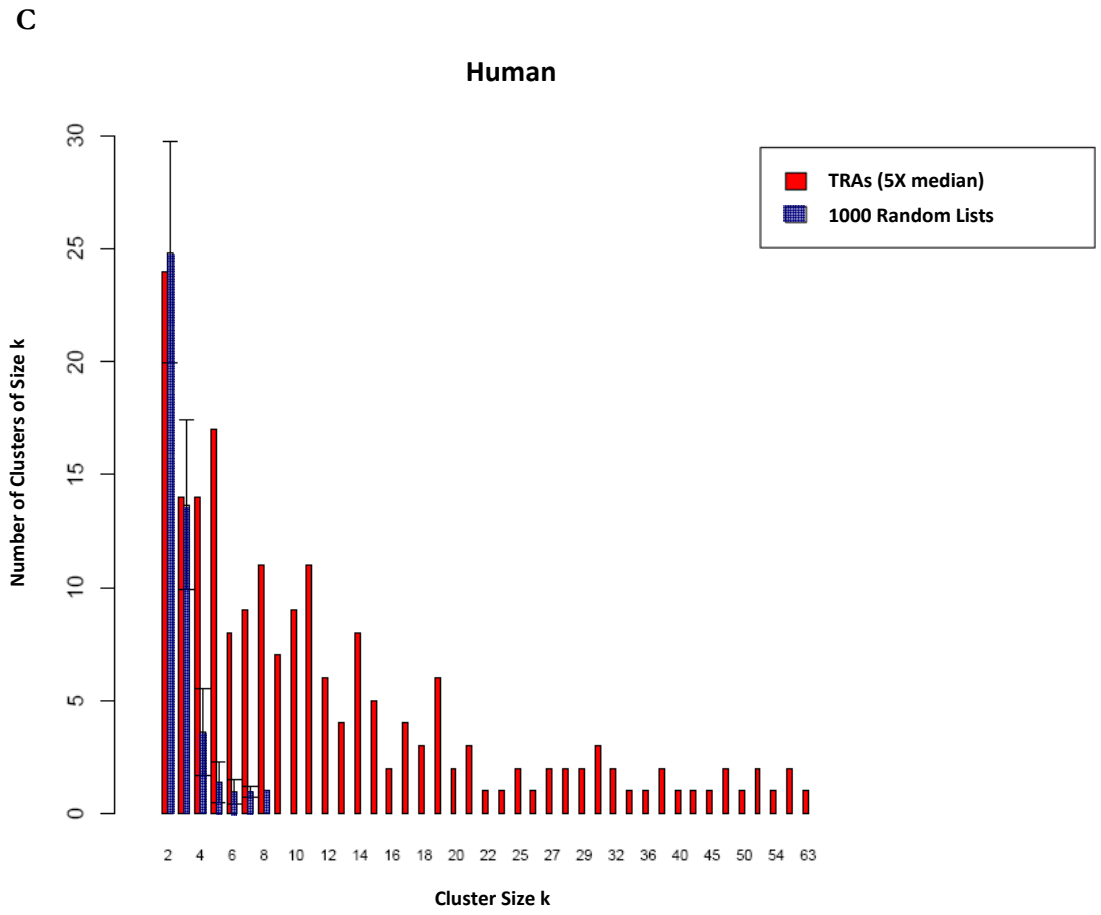

Figure 19

Genome-wide TRA cluster maps in mouse, rat and human

After running the 10-gene sliding window clustering algorithm, the cluster size k (number of TRAs in a cluster, x-axis) is plotted versus the number of clusters of a particular size (k; y-axis). The significance of clustering was determined by repeating the same procedure 1,000 times in each case with a list of random genes of the same size as the experimental dataset (violet bars).

(A) Mouse genome-wide TRA clusters show that TRAs are significantly clustered in the genome, with the largest cluster comprising 117 TRAs.

(B) Rat genome-wide TRA clusters show that TRAs are significantly clustered in the genome, with the largest cluster comprising 130 TRAs.

(C) In human, the same was observed; TRAs are significantly clustered in the genome, with the largest cluster comprising 63 TRAs.

In all cases clusters >4 TRAs are significantly different from the random samples.

3.1.3. Gene clusters are present in syntenic regions across species

Since TRAs in all three species are clustered in the genome, it was of interest to know if they are localized within certain conserved regions i.e. syntenic regions on the same or on different chromosomes of the different species. Hence, matching of orthologous gene TRA clusters in the mouse and human genome was performed based on *HomoloGene* (NCBI).

It was observed that most of the clusters were localized in syntenic regions conserved between mouse and human (Figure 20). The gene order in these clusters in both species was mostly conserved, i.e. a co-linear relationship was observed (Figure 20A). In some cases, the gene order was inverted (Figure 20B). The gene density of TRAs in the clusters was generally higher in mouse than in human. This analysis was not performed in rat due to the poor annotation of the rat genome.

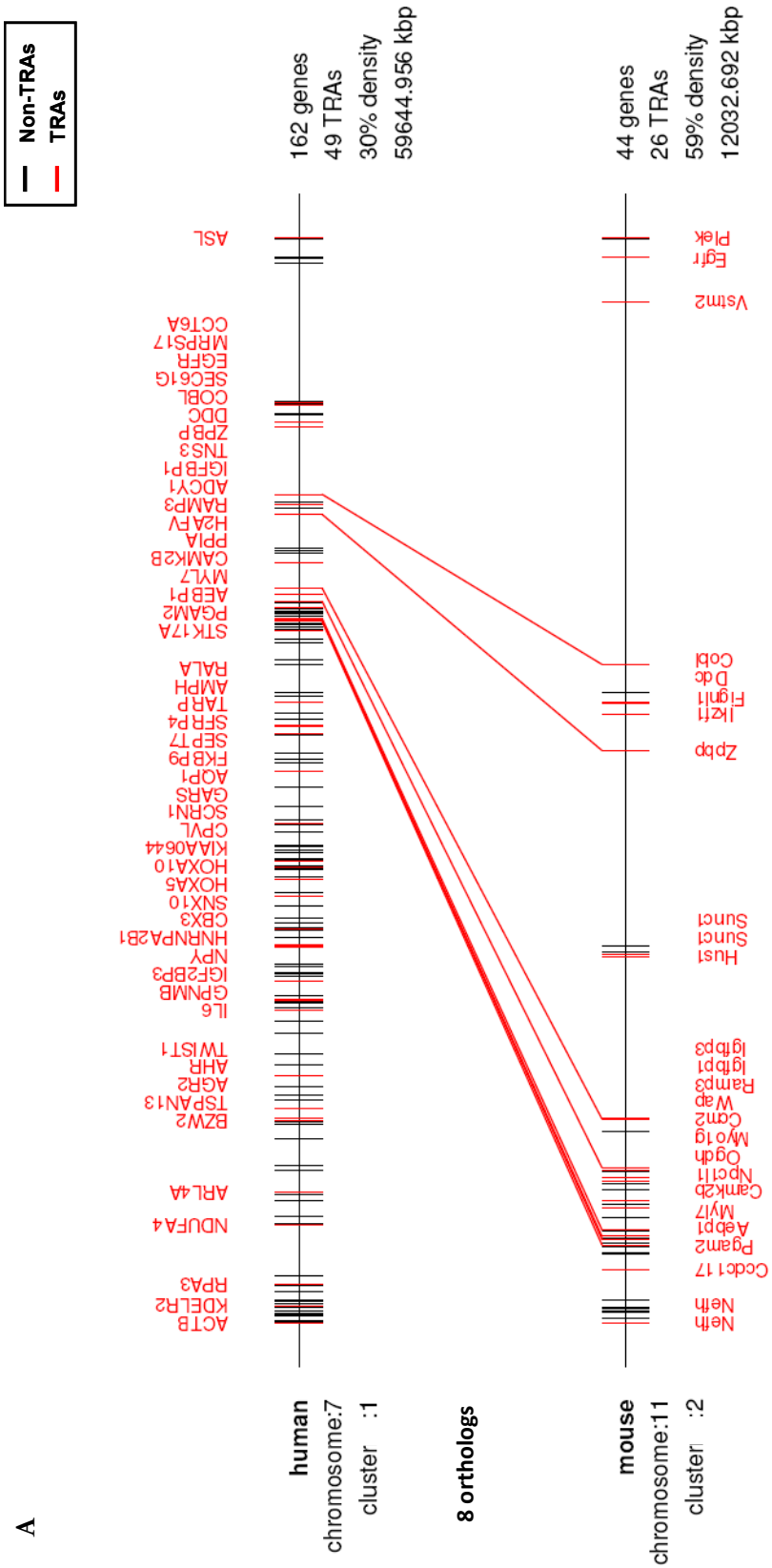
A
Non-TRAs
TRAs
human
chromosome:7
cluster :1
162 genes
49 TRAs
30% density
59644.956 kbp
8 orthologs
mouse
chromosome:11
cluster :2
44 genes
26 TRAs
59% density
12032.692 kbp
ASL
ACTB
KDELR2
RPA3
NDUFA4
ARL4A
BZW2
TSPAN13
AGR2
AHR
TWIST1
IL6
GPNMB
IGF2BP3
NPY
HNRNPA2B1
CBX3
SNX10
HOXA5
HOXA10
KIAA0644
CPVL
SCRN1
GARS
AOP1
FKBP9
SEPT7
SFRP4
TARP
AMPH
RALA
STK17A
PGAM2
AEBP1
MYL7
CAMK2B
PPIA
H2AFV
RAMP3
ADCY1
IGFBP1
TNS3
ZPBP
DDC
COBL
SEC61G
EGFR
MRPS17
CCT6A
Nefh
Nefh
Ccdc117
Pgam2
Aebp1
Myl7
Camk2b
Npc1l1
Ogdh
Myo1g
Cgn2
Wap
Ramp3
Igfbp1
Igfbp3
Hust
Suncr1
Suncr1
Cobl
Ddc
Flgnl1
Ikzf1
Zpbp
Vstm2
Egfr
Plek

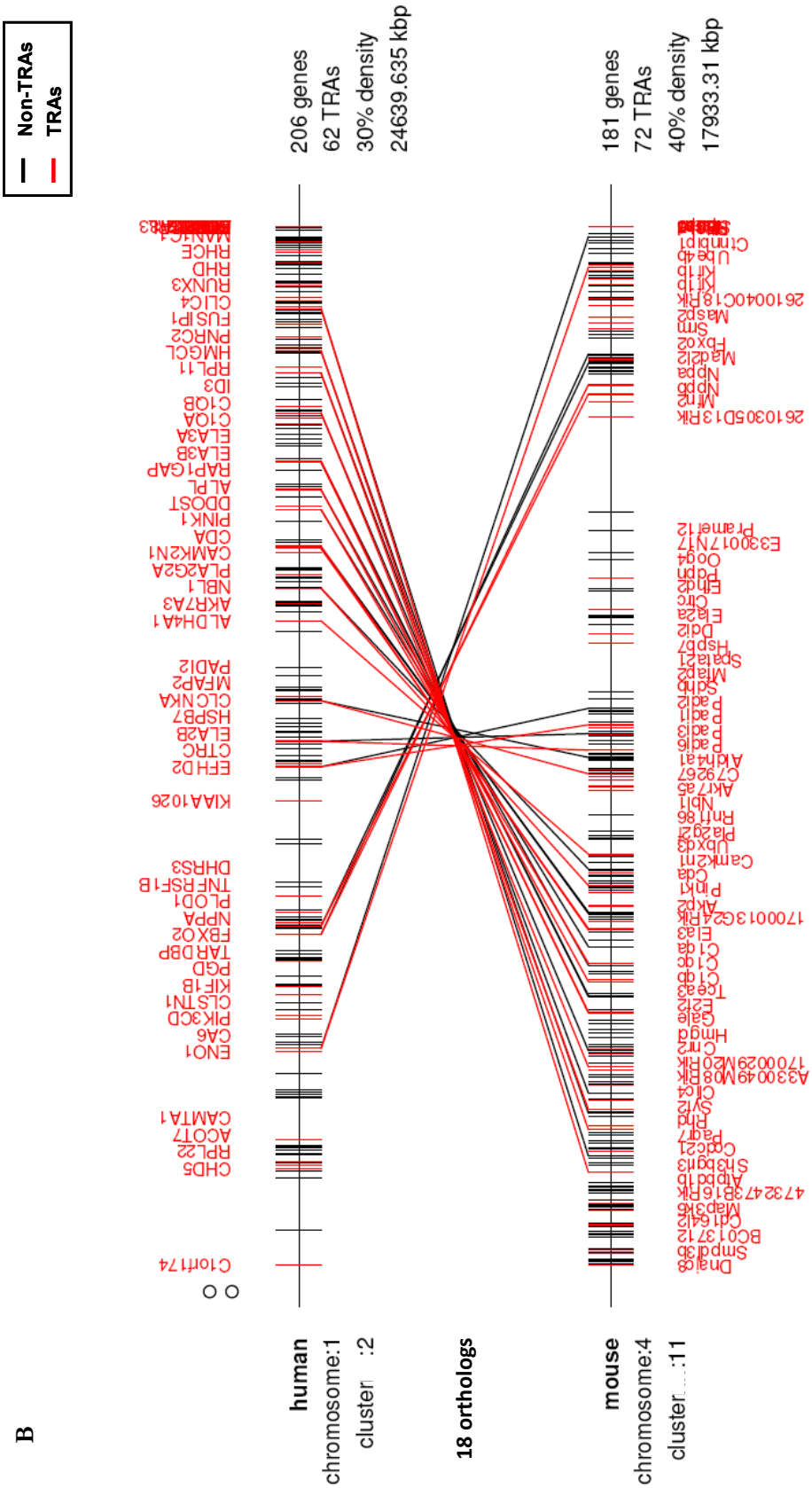
B
Non-TRAs
TRAs
206 genes
62 TRAs
30% density
24639.635 kbp
181 genes
72 TRAs
40% density
17933.31 kbp
human
chromosome:1
18 orthologs
mouse
chromosome:4

Figure 20

TRA cluster maps of syntenic regions

(A) An example of a co-linear syntenic cluster on mouse chromosome 11 and human chromosome 7 shows 8 orthologs. Clusters in both species have different gene density (30 % in human and 59 % in mouse) and numbers of TRAs (49 TRAs in human versus 26 TRAs in mouse). The gene order in both species was conserved.

(B) An example of an inverted syntenic cluster on mouse chromosome 4 and human chromosome 1 shows an overlap of 18 orthologs. Clusters in both species have different gene densities (30 % in human and 40 % in mouse) and numbers of TRAs (62 TRAs in human versus 72 TRAs in mouse). The gene order in both species was inverted in this case.

3.1.4. Gene homology within TRA clusters in the mouse genome

In order to investigate, if TRA clusters in the genome arose from gene duplication or are the result of co-localization of structurally and functionally related genes, a homology match was performed on the TRAs within each cluster. To do so, the nucleotide sequence of each particular TRA within a cluster was compared to the sequence of every other TRA within the same cluster. A homology plot denoting the percent sequence identity (% Id) of each such comparison within every cluster was plotted (Figure 21A). The percent identity of majority of the TRAs within clusters is ~30 %. The threshold probability of four nucleotides (ATGC) is 25 %. A few outliers (circles) having a high percent identity ~60-99 % are likely to be gene families (Figure 21A). For a set of random genes, the percent identity was in the range of 25-30 % homology (Figure 21B). Thus, the bulk of the TRA clusters contain structurally unrelated genes that do not insinuate a common deviation by gene duplication or gene conversion, which would explain their co-localization in the murine genome.

A

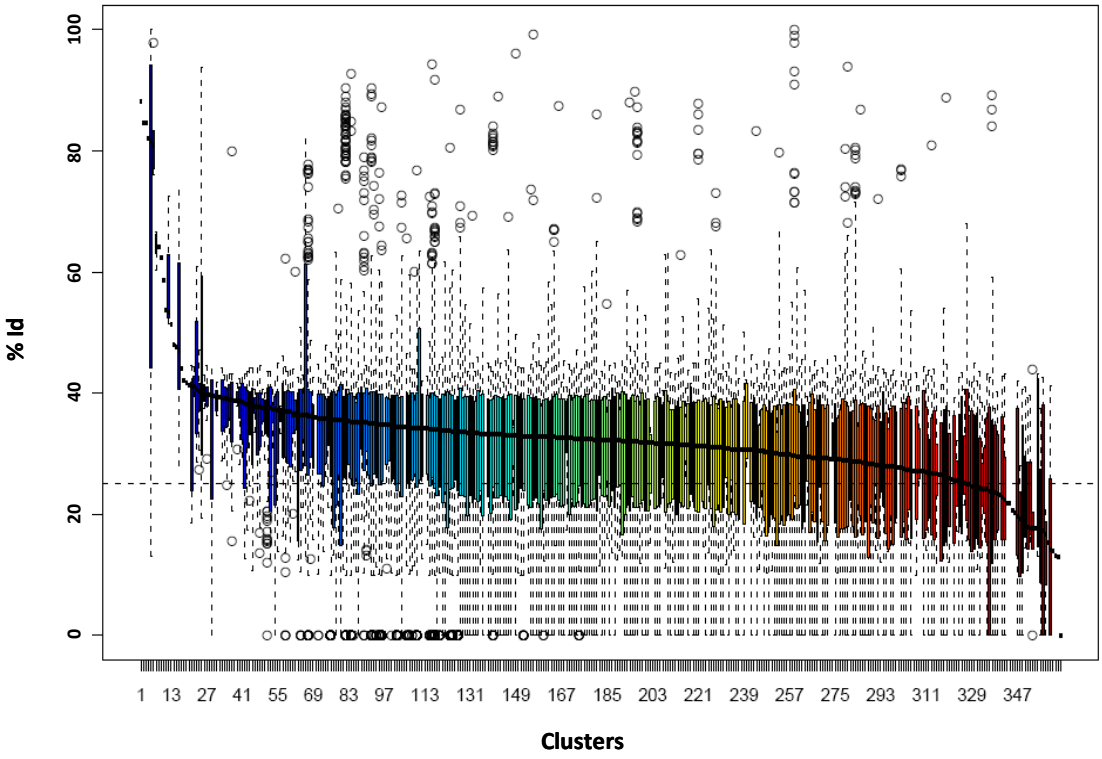
% Id
0
20
40
60
80
100
1 13 27 41 55 69 83 97 113 131 149 167 185 203 221 239 257 275 293 311 329 347
Clusters

B

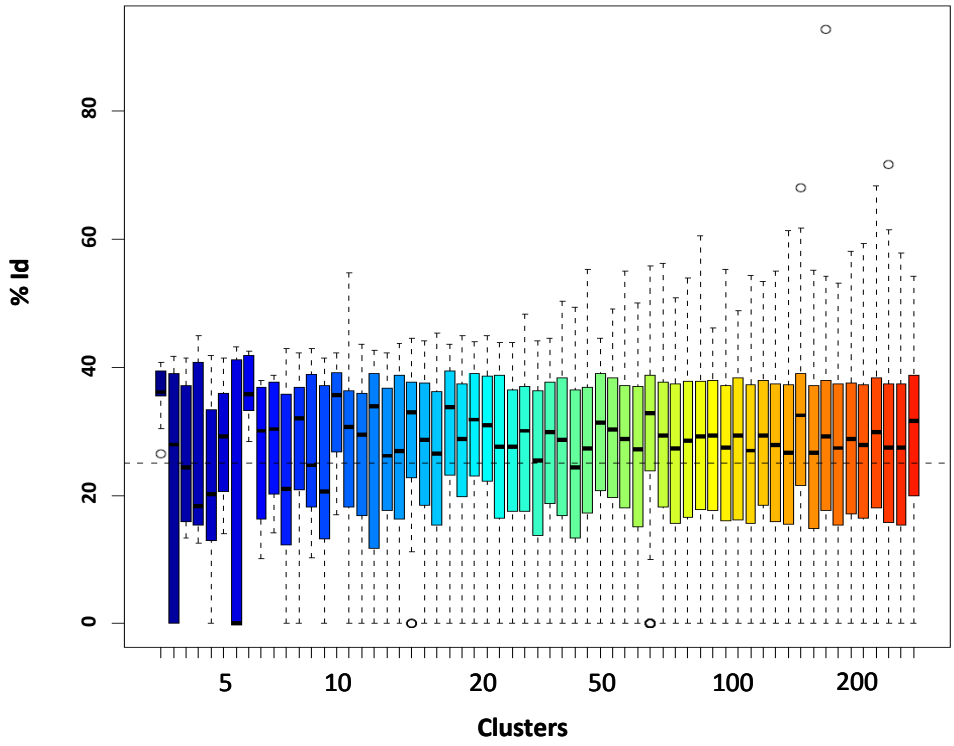
% Id
0
20
40
60
80
5 10 20 50 100 200
Clusters

Figure 21

Homology plot of mouse TRA clusters

The nucleotide sequence of each particular TRA within a cluster was compared to the sequence of every other TRA within the same cluster. A homology plot denoting the percent sequence identity (% Id) of each such comparison within all clusters was plotted.

(A) In mouse clusters, the %Id of majority of the TRAs is ~30 %, while the threshold probability of four nucleotides (ATGC) is 25 %. The circles represent outliers having a high percent identity, ~60-99 % which are likely gene families.

(B) In comparison, a homology analysis with a set of random genes was performed. The percent identity is also in the range of 25-30 % and very few high %Id genes pairs were detected compared to the mouse TRA clusters. Thus, the bulk of the mouse TRA clusters contain non-homologous genes.

3.1.5. Analysis of gene expression between immature and mature mTECs in the thymus

We defined TRAs, their genomic distribution and demonstrated that TRAs are clustered in the genome irrespective of structural relatedness or apparent immunological criteria. It was previously published that promiscuously expressed genes are enriched in TRAs (Anderson *et al.*, 2002; Gotter *et al.*, 2004; Derbinski *et al.*, 2005; Johnnidis *et al.*, 2005) and during progressive maturation, mTECs show an increased pGE, concomitant with Aire expression. Using a more complete second generation microarray platform, larger and better annotated genome database and robust computed TRA definition, we sort to reanalyze previous findings: 1) TRA enrichment and 2) Aire-dependency in mouse. Previous studies were performed on both (immature and mature) mTEC subsets in mouse and on complete mTECs in human; here our studies extend to these subsets in mouse, human and rat.

3.1.5.1. Analysis of the differentially expressed gene content in murine mTECs: TRAs and Aire dependency

PGE has been tightly correlated with the differentiation stage in mTECs i.e. mature mTECs (Derbinski *et al.*, 2005). In this study MHCII was chosen to separate mTECs into immature and mature stages of differentiation. Based on genome-wide TRA definition, the thymic differentially expressed genes ($MHCII^{lo}$ vs. $MHCII^{hi}$ mTECs) were designated as TRAs or non-TRAs. Due to the importance of Aire in regulating the expression of numerous genes in mTECs with a predilection for TRAs (Anderson *et al.*, 2002; Derbinski *et al.*, 2005; Johnnidis *et al.*, 2005) and the availability of $Aire^{-/-}$ mice, the Aire dependency was studied. To delineate the size and diversity of Aire-dependent vs. Aire-independent gene pool, genome-wide microarrays were performed using $Aire^{-/-}$ mice.

	Up-regulated genes	Down-regulated genes
Total gene number	1263	626
Aire-dependent genes	455 (240 TRAs, 53 %)	32 (17 TRAs, 50 %)
Aire-independent genes	808 (391 TRAs, 48 %)	594 (234 TRAs, 39 %)

Table 3.3

Comparing the percentage of Aire-dependent and -independent differentially expressed genes in murine thymus (between MHCII^{lo} and MHCII^{hi} mTECs)

The percentage of TRAs was calculated in each gene set.

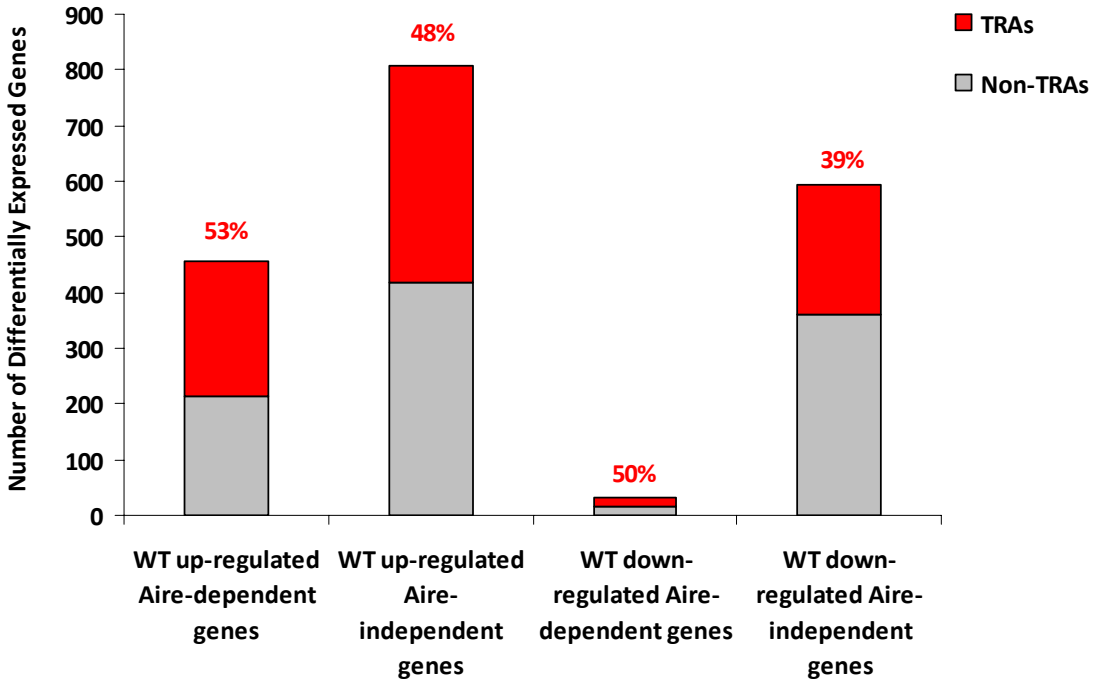

Figure 22

Representation of TRAs and Aire dependency in mouse thymic differentially expressed genes

The percentage of TRAs in up- or down-regulated Aire-dependent or -independent genes were plotted. It was observed that MHCII^{hi} mTECs have a large number of Aire-dependent and -independent genes. The down-regulated gene pool shows a small number of Aire-dependent genes, though 50 % are TRAs. Most of the down-regulated genes are Aire-independent. The plot corresponds to Table 3.3.

In mice, 1263 genes were up-regulated versus 626 genes which were down-regulated from 27,000 well annotated mouse genes. It was observed that MHCII^{hi} mTECs express a large number of Aire-dependent and -independent genes, both of which appeared to be enriched in TRAs. The up-regulated Aire-dependent genes showed 5 % more TRAs as compared to the Aire-independent gene set (Table 3.3 and Figure 22). The down-regulated gene pool showed a small number of Aire-dependent genes, though 50 % were TRAs (Table 3.3). Most of the down-regulated genes were Aire-independent, consisting of 39 % TRAs (Table 3.3 and Figure 22). Nonetheless both up- and down-regulated genes appeared to have similar percentages of Aire-dependent TRAs while the up-regulated gene pool had 9 % more Aire-independent TRAs. Thus, it appears that the maturation stage i.e. MHCII^{hi} mTECs and not Aire per se has an effect on both number and fraction of TRAs.

3.1.5.2. How is pGE projected onto pre-existing genome-wide mouse TRA clusters?

We affirmed previous observations that pGE in mTECs is enriched in TRAs and in part regulated by Aire while others are Aire-independent. The percentage of TRA content is far above the background of 10.8 % in the genome. Here we aimed at studying the projection of pGE onto pre-existing genome-wide TRA clusters that were defined in the previous chapter.

In the mouse genome, 364 gene clusters ranging from 4 - 117 TRAs were identified. The set of thymic differentially expressed genes (Aire-dependent and -independent genes) were plotted onto these clusters giving rise to cluster maps for each chromosome. It was observed that, promiscuously expressed TRAs tend to map to these clusters; within each cluster, TRAs were intermingled with non-TRAs. It was rather rare that a cluster comprised purely TRAs. Moreover Aire-dependent and -independent genes were interspersed among each other. Part of the genes within clusters was regulated during mTEC differentiation (Example Figure 23A).

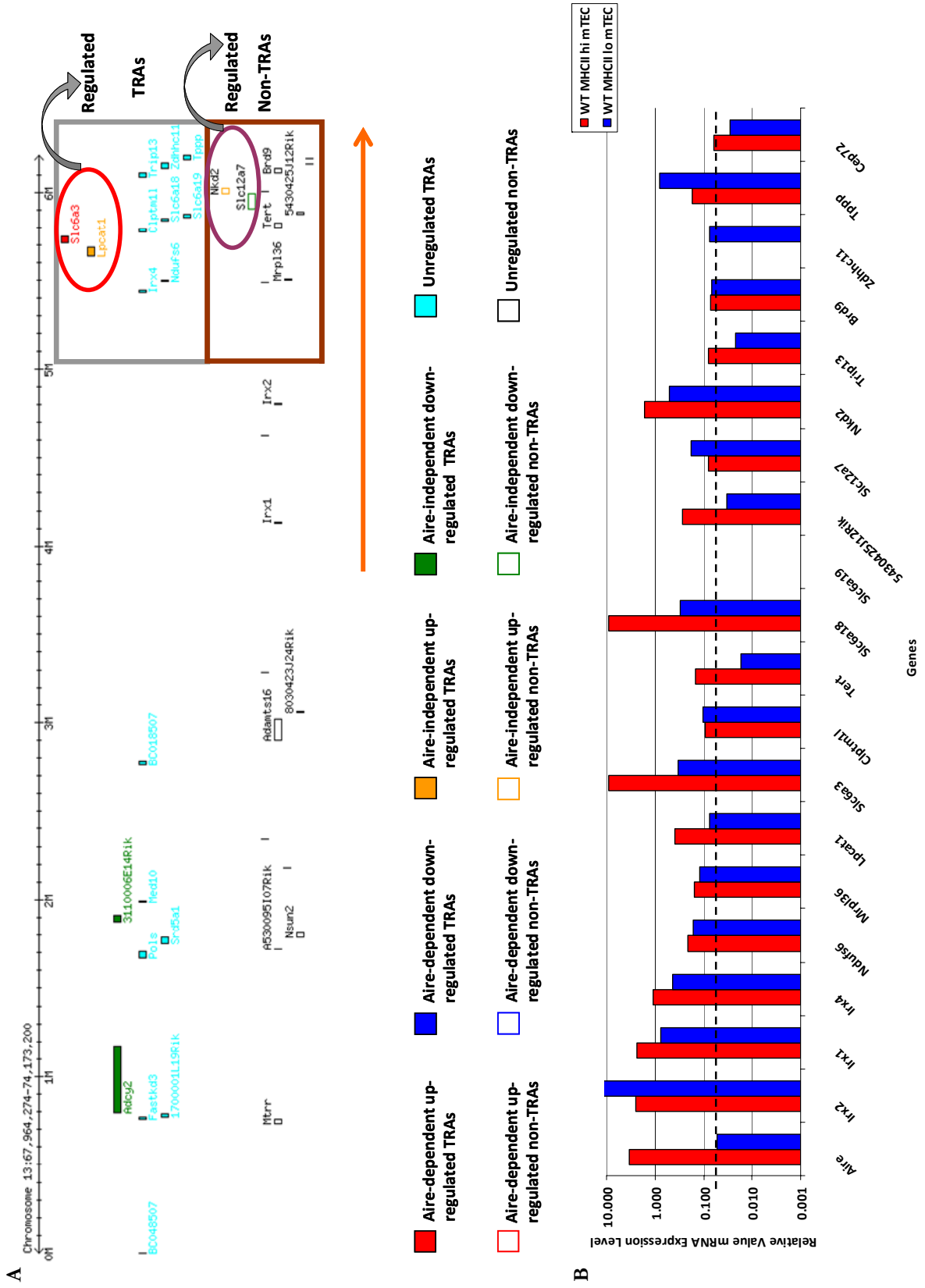
A
Chromosome 13:67,964,274-74,173,200
Regulated
TRAs
Regulated
Non-TRAs
Aire-dependent up-regulated TRAs
Aire-dependent down-regulated TRAs
Aire-independent up-regulated TRAs
Aire-independent down-regulated TRAs
Unregulated TRAs
Aire-dependent up-regulated non-TRAs
Aire-dependent down-regulated non-TRAs
Aire-independent up-regulated non-TRAs
Aire-independent down-regulated non-TRAs
Unregulated non-TRAs
B
WT MHCII hi mTEC
WT MHCII lo mTEC
Relative Value mRNA Expression Level
10.000
1.000
0.100
0.010
0.001
Genes
Aire
Irx2
Irx1
Irx4
Ndufs6
Mrpl36
Lpcat1
Slc6a3
Cliptm1l
Tert
Slc6a18
Slc6a19
5430425J12Rik
Slc12a7
Nkd2
Trip13
Brd9
Zdhhc11
Tppp
Cep72

Figure 23

Example of cluster 13 on mouse chromosome 13

(A) 364 clusters, ranging from 4 - 117 TRAs were identified. Here, an example of one such TRA cluster onto which the projection of mouse mTEC differentially regulated genes is depicted. Color code legend represents each type of gene set, Aire-dependent (red and blue boxes, filled colored boxes-TRAs; non-filled colored boxes-non-TRAs) and -independent (orange and green boxes; filled colored boxes-TRAs, unfilled colored boxes-non-TRAs) differentially regulated genes between $MHCII^{lo}$ and $MHCII^{hi}$ mTECs as well as remaining unregulated genes (cyan-TRAs and white-non-TRAs boxes). TRAs were intermingled with non-TRAs. No pure TRAs cluster was identified. Aire-dependent and-independent genes were interspersed among each other. The gray box depicts TRAs and the brown box represents the non-TRAs. While the red and maroon circles within these boxes represent the regulated TRAs or non-TRAs respectively. The orange arrow represents the region in which real-time PCR analysis was performed to confirm the gene regulation within a cluster.

(B) Real-time PCR analysis of a region (marked by orange arrow Figure 23A) of cluster 13 on chromosome 13 in WT $MHCII^{lo}$ and $MHCII^{hi}$ mTECs, normalized to Ubiquitin. It was observed that the genes detected by the microarray to be differentially expressed (either up- or down-regulated) between $MHCII^{lo}$ and $MHCII^{hi}$ mTECs reflect the same expression pattern using PCR. Dotted line represents the level of Aire expression in $MHCII^{lo}$ mTECs, which was considered as a minimal expression threshold.

The set of differentially expressed genes projected onto the genome-wide clusters are deduced from bioinformatic processing of the microarrays which is likely to be incomplete. Even though chips contain all known well annotated genes, array analysis is less sensitive than real-time PCR and promiscuously expressed genes are expressed at low levels. Therefore, the total number of differentially expressed promiscuous genes will be underestimated by at least a factor of two. Hence, to gain a more complete, true picture of gene regulation within clusters and to study if neighboring genes are regulated as a unit or whether individual genes are subjected to differential regulation as observed with the array data, we performed real-time PCR. A core region of cluster 13 on chromosome 13 was selected and differential gene expression within this region was analyzed using real-time PCR in $MHCII^{lo/hi}$ WT mTECs (Figure 23B; region marked orange arrow). It was observed that the genes depicted on the microarrays to be differentially expressed (either up- or down-regulated) between $MHCII^{lo}$ and $MHCII^{hi}$ mTECs reflect the same expression pattern using PCR (Figure 23B; Slc6a3, Lpcat1, Slc12a7 and Nkd2). Some, genes considered to be unregulated did not always follow the array expression and were differentially regulated (Figure 23B; e.g. Irx2, Tppp and Tert). Taking the level of Aire expression in $MHCII^{lo}$ mTECs as a minimal expression threshold, it was observed that several genes qualified as expressed and their expression was higher than that in microarrays. A three-log difference in expression was seen for certain genes (Figure 23B e.g. Slc6a3, Slc6a18). In addition, the Aire dependency of the genes within this cluster region was studied using Aire KO. Most of them had the same pattern of expression on both platforms i.e. array and PCR (data not shown).

Overall, a heterogeneous contiguous expression pattern was observed in mTECs at the qualitative level using real-time PCR (with the exception of Slc6a19, which was detected in complete thymus but not purified WT mTECs). Extrapolating from the gene array analysis, we estimate ~10 % of all known genes are turned on in mature MHCII^{hi} mTECs in addition to differentiation-dependent genes. This however is an under-estimate due to a methodological limitation, as the currently available genome-wide screening microarray platform has low sensitivity. Use of most modern Deep Sequencing technology may eventually precisely define the promiscuously expressed gene pool.

3.1.5.3. Are TRAs regulated over non-TRAs within gene clusters in murine mTECs?

Within each cluster, TRAs were intermingled with non-TRAs (Figure 23A). It was of interest to study, if the TRAs within clusters are preferentially regulated in mTECs over the non-TRAs. Hence, the proportion of regulated TRAs vs. regulated non-TRAs from each of the 364 clusters was statistically analyzed. Combined regulation within all 364 clusters showed that there was a higher tendency of the TRAs being regulated within the clusters versus that of the non-TRAs. 11.7 % TRAs versus 4.6 % non-TRAs were regulated (Figure 24). The preferential TRA regulation within clusters is highly significant ($p \leq 2.2 \times 10^{-16}$). The percentage of regulation of TRAs within clusters ranged from 0 to 50 %.

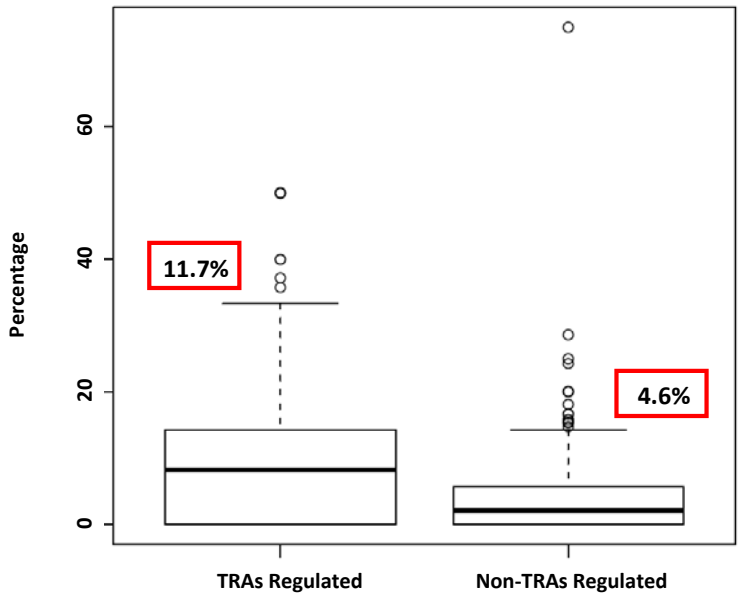

Figure 24

Preferential regulation of TRAs within clusters

Over the 364 clusters, the regulation of TRAs versus non-TRAs (e.g. red and maroon circles, Figure 23A) was plotted. The extent of the TRAs being regulated within the clusters was higher versus that of the non-TRAs. This difference is highly significant having a $p \leq 2.2 \times 10^{-16}$.

3.1.5.4. Analysis of the differentially expressed gene content in rat mTECs

In rat, the mTECs were separated into immature and mature cells based on MHCII as in mouse and human. 700 genes were found to be differentially expressed from 22,000 annotated rat genes. From these, 360 were up-regulated and 340 were down-regulated.

An ortholog match between rat and mouse using *HomoloGene* (NCBI), showed 624 mouse orthologs (from 700 differentially expressed genes), 94.4 % of which were also differentially regulated in mouse (589 genes) (Table 3.4). 75.7 % up-regulated and 64.3 % down-regulated genes followed the same regulation pattern in rat and mouse. Thus, there exists a large over-lap of promiscuously expressed genes between these two species, further corroborating the notion of an evolutionary conservation of pGE.

	Rat	Mouse Orthologs	Regulated in mouse	Percentage overlap - Regulated rat and mouse genes
Differentially expressed genes	700	624	589	94.4 %
Up-regulated genes	360	333	252	75.7 %
Down-regulated genes	340	291	187	64.3 %

Table 3.4

Set of rat differentially-, up- and down-regulated genes between MHCII^{lo} and MHCII^{hi} mTECs and their corresponding mouse orthologs

The regulation of the mouse orthologs and the percentage overlap between the two species are shown.

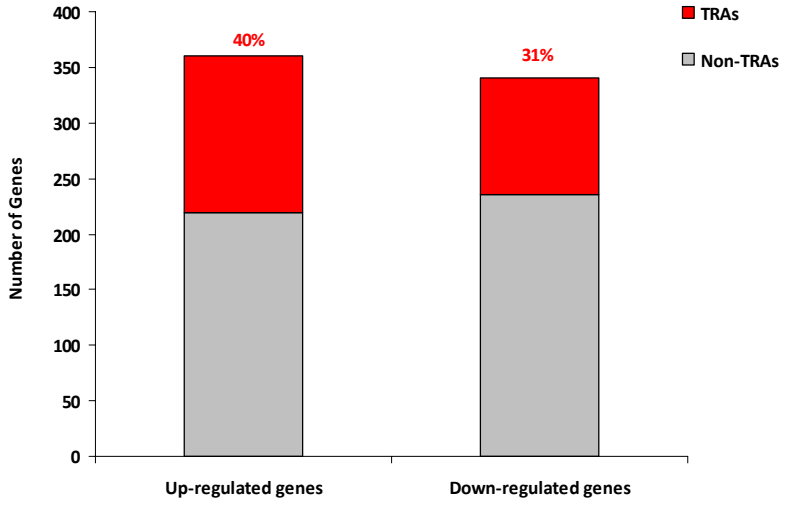

Figure 25

Percentage of TRAs within regulated rat genes

The percentage of genes up- or down-regulated in mature rat mTECs is shown. MHCII^{hi} mTECs are enriched in TRAs, having a higher percentage of TRAs than MHCII^{lo} mTECs (40 % TRAs vs. 31 % TRAs). The rat TRAs were defined using mouse orthologs.

Owing to the lack of sufficient information in the *Symatlas* database as well as in annotation of the rat genome, TRAs in rat were defined using mouse orthologs. Of 360 up-regulated genes in rat, 141 correspond to mouse TRA orthologs (~40 %). While in the set of 340 down-regulated genes in rat, 104 correspond to mouse TRA orthologs, (~31 %). MHCII^{hi} mTECs are enriched in TRAs versus MHCII^{lo} mTECs (Figure 25). The percentage of TRAs in rat is under-estimated as a number of genes will be missed by way of comparing the genomes between the two species; as observed it is lower than in mouse (Figure 22).

3.1.5.5. Analysis of the differentially expressed gene content in human mTECs

The immature and mature mTECs ($MHCII^{lo}$ and $MHCII^{hi}$ respectively) from 11 different individuals ranging from 3 days to 3 years of age were isolated from their thymus. The mTECs were enriched using three different methods (Density gradients, depletion of $CD45^{+}$ cells using either Dynal beads or Miltenyi beads) as described earlier (Section 2.2.3.3). Gene array results showed substantial variations in the number of differentially expressed gene between the different individuals. The number of differentially expressed genes ranged from ~700 to 6000 (Table 3.5A). Differences were observed irrespective of the different isolation methods used. Hence, it can be excluded that the variation arose due to the isolation methods used.

Seeking for a common set of differentially expressed genes between individuals we found a negative correlation between the number of individuals and the number of common/overlapping genes. The intersection interval which is the extreme point in the comparison containing genes that are differentially expressed in all 11 individuals showed only 24 common differentially expressed genes, 18 genes were up-regulated and 6 genes were down-regulated (Table 3.5B). AIRE can be considered as a measure for the degree of enrichment of $MHCII^{hi}$ mTECs of the individual samples. Since, AIRE is the driving force for many of the promiscuously expressed genes in the mature mTEC population, the correlation between the number of differentially expressed genes and fold change in AIRE expression was determined. There does exist a correlation between the fold change in AIRE expression (between $MHCII^{lo}$ and $MHCII^{hi}$ mTECs) and the number of differentially expressed genes, (correlation coefficient, $r = 0.5$), though two individual samples were outliers (Table 3.5C and Figure 26).

This is the first time that such striking inter-individual difference in pGE is found, though Taubert *et al.* also reported considerable variability in the expression of several target auto-antigens in mTECs (Taubert *et al.*, 2007). These variations could result from differences in the genetic background, environmental factors, disease/health condition of the individuals and pre-medication. The observed variations in antigen expression are likely to influence T-cell repertoire selection and thus tolerance thresholds in human provided they reflect steady state values.

Taken together, the results in the three species show that promiscuously expressed genes are enriched in TRAs that are partitioned into clusters and this phenomenon is conserved between species. Clusters harbor both TRAs and non-TRAs that are interspersed between each other. TRAs are preferentially regulated during mTEC differentiation. Moreover, genes within a particular gene cluster are subject to partial co-regulation. The bulk of the TRA clusters contain structurally unrelated genes. Based on these data, we propose these clusters to be the "operational genomic unit" of pGE in the thymus.

A

	Different methods of separation used to isolate human mTECs										
	Dynal Bead					Miltenyi beads (MACS)			Density Gradients		
Individuals	Ind. 14	Ind. 24	Ind. 32	Ind. 72	Ind. 74	Ind. 77	Ind. 89	Ind. 92	Ind. 53	Ind. 55	Ind. 59
Differentially expressed genes	1560	2153	2114	697	1003	706	1097	1674	5885	6383	984
Up-regulated genes	1081	1557	1306	426	657	391	472	972	2942	2937	706
Down-regulated genes	479	596	808	271	346	315	625	702	2943	3410	278

B

	Union	In at least 2 individuals	In at least 3 individuals	In at least 4 individuals	In at least 5 individuals	In at least 6 individuals	In at least 7 individuals	In at least 8 individuals	In at least 9 individuals	In at least 10 individuals	Intersection
Differentially expressed genes	13937	4400	2096	1257	878	616	420	312	199	108	24
Up-regulated genes	6805	2921	1331	798	558	394	269	194	128	67	18
Down-regulated genes	7132	1479	756	459	320	222	151	118	71	41	6

C

	Different methods of separation used to isolate human mTECs										
	Dynal Bead					Miltenyi beads (MACS)			Density Gradients		
Individuals	Ind. 14	Ind. 24	Ind. 32	Ind. 72	Ind. 74	Ind. 77	Ind. 89	Ind. 92	Ind. 53	Ind. 55	Ind. 59
AIRE fold change $MHCII^{hi}$ vs. $MHCII^{lo}$ mTECs	23.7	22.5	50.1	23.2	21.0	14.0	4.5	36.2	28.7	69.5	46.0

Table 3.5

Representation of gene expression data from different individual thymi

Human mTECs (MHCII^{lo} and MHCII^{hi}) were isolated from thymus samples for 11 different individuals ranging from 3 days to 3 years of age. The mTECs were enriched using three different methods (Density gradients, Dynal beads and Miltenyi beads) as described earlier (Section 2.2.3.3).

(A) Comparison of differentially-, up- and down-regulated genes between MHCII^{lo} and MHCII^{hi} mTECs from each individual thymus.

(B) Number of differentially-, up- and down-regulated genes expressed in at least "n" individuals, n = 2 to 10. Union and intersection intervals are the extreme points in the comparison: where union means all genes that are found to be differentially expressed in at least one individual; intersection contains genes that are differentially expressed in all 11 individuals.

(C) Fold change of AIRE expression between MHCII^{lo} and MHCII^{hi} mTECs from individual thymi.

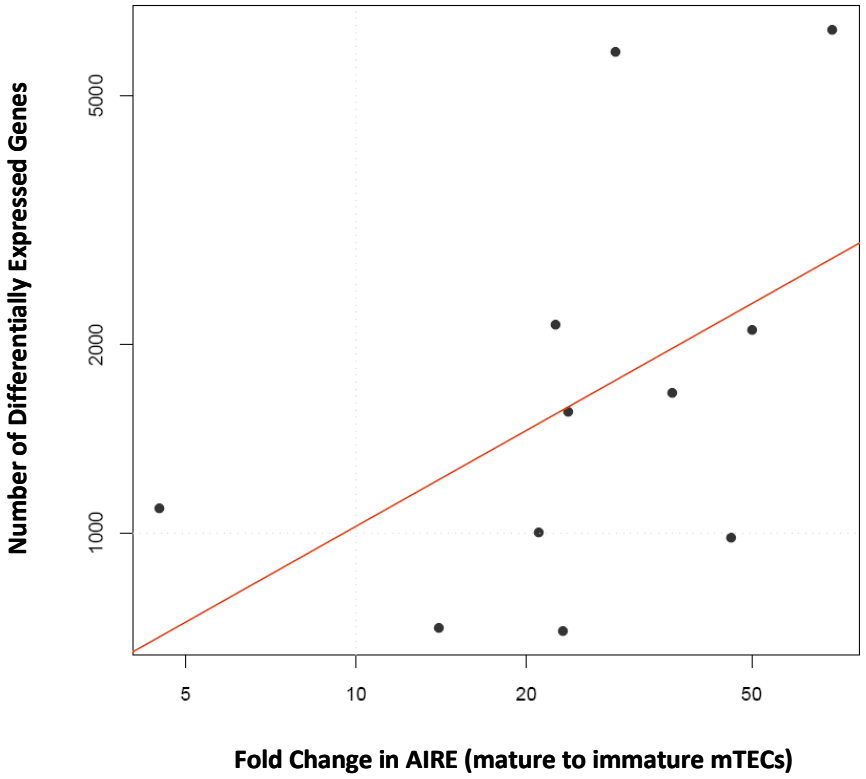

Figure 26

Correlation between number of differentially expressed genes and fold change in AIRE expression in the different individual thymi

Correlation plot of the number of differentially expressed genes and fold change in AIRE expression between MHCII^{hi} and MHCII^{lo} mTECs in the 11 individual samples, (correlation coefficient, r = 0.5). Two individual samples were outliers.

3.2. "Holes" in the thymic antigen repertoire: implications for central tolerance and autoimmunity

Genome-wide studies of pGE in mTECs showed a respectful representation of the genome in the thymic antigen repertoire, but this is not a complete representation. "Holes" or absence in expression of certain genes in the thymus, should lead to lack of central tolerance for particular antigens, therefore it would be a preferential target for autoimmune disease. An important question in organ-specific autoimmune diseases is: why the loss of self-tolerance is so selective that only certain tissues and auto-antigens are targeted?

Two prominent examples of target antigens in autoimmune diseases are: glutamic acid decarboxylase (GAD) involved in insulin-dependent diabetes (IDD) (Tisch, 1996; Yoon *et al.*, 2000; Lernmark, 2002) and cardiac myosin heavy chain (MyHC) involved in myocarditis (Wolfgram *et al.*, 1985; Neu *et al.*, 1987; Rose, 2000). Both cases involve two isoforms in which the expression of either one of the two is lacking in the thymus. This lack of expression may represent a "pitfall" of pGE. It is possible that the non-expressed isoform is embedded in a silent chromosomal context i.e. "region of closed chromatin". We started to investigate this possibility by analyzing the thymic expression of the flaking regions of these gene loci.

3.2.1. Regulation of the GAD65/GAD67 loci in human thymus

Glutamic acid decarboxylase (GAD), a target of both auto-antibodies and autoreactive T-cells in insulin-dependent diabetes (IDD), exists as two homologous forms, GAD65 and GAD67. GAD65 is predominantly expressed in human islets (pancreas) and recognized by auto-antibodies in IDD, but which form primarily elicits GAD autoimmunity is unknown. Gotter and colleagues showed that GAD65 is apparently absent from mTECs of healthy humans and thus is likely to be absent from the human thymus while GAD67 is present in the thymus (in mTECs). Its absence in the thymus, i.e. lack of central tolerance could explain the occurrence of specific autoantibodies in the course of IDD, as an inverse expression pattern is observed between occurrence of GAD65 antibodies and thymic expression (Gotter *et al.*, 2004). Why is GAD65 not expressed in the thymus? Are there certain molecular clues in terms of its genomic position? To answer the above questions the expression of the GAD65 locus spanning ~2 Mb was analyzed in the different mTEC subsets.

The GAD65 and GAD67 clusters are evolutionary conserved in human and mouse (Figures 27 and 28).

A

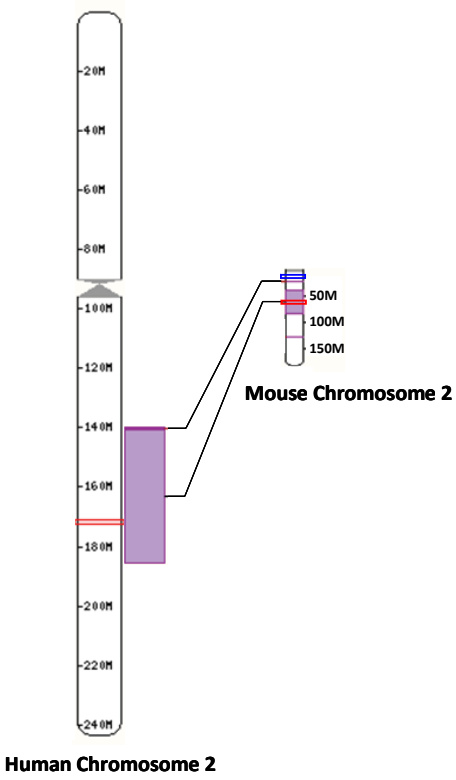
20M
40M
60M
80M
100M
120M
140M
160M
180M
200M
220M
240M
50M
100M
150M
Mouse Chromosome 2
Human Chromosome 2

B

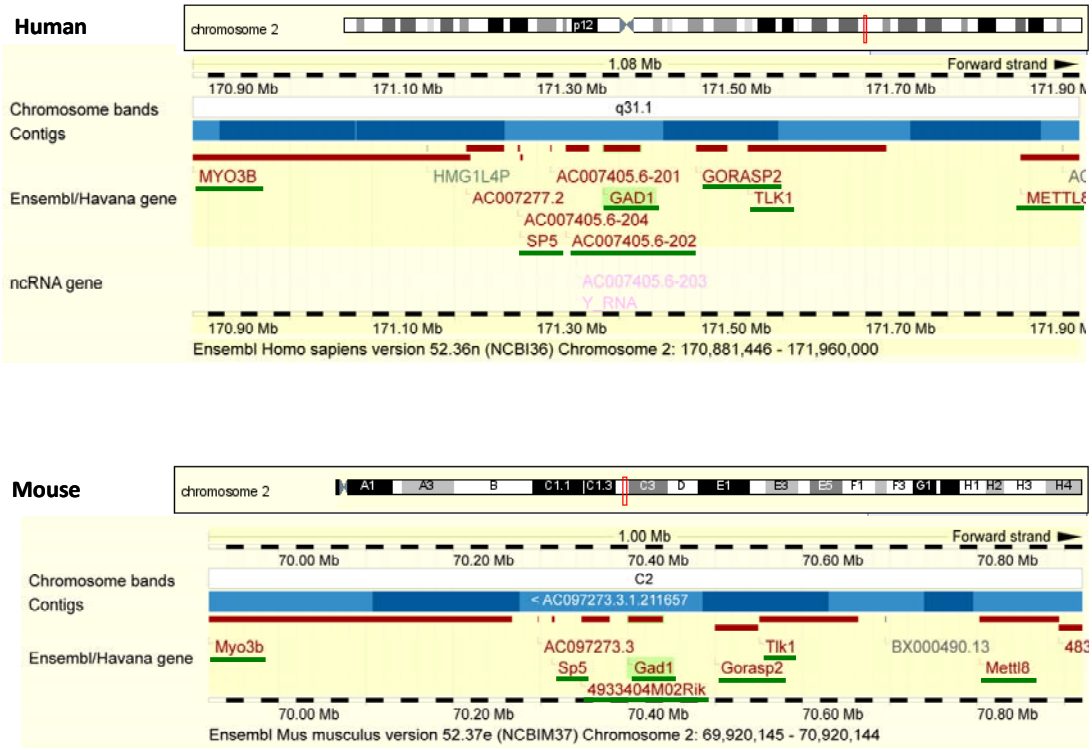

Figure 27

Comparison of genomic location of GAD1 (GAD67) in mouse and human

Red box depicts the location of GAD1 in each species.

(A) GAD1 is located on the same chromosome in human and mouse i.e. chromosome 2. Blue box on the mouse chromosome 2 represents the GAD65 gene.

(B) In depth view of the genomic location of GAD1 in human and mouse, showing the high degree of conservation of the gene cluster. Green lines indicate the common genes within this region, for which PCR was performed in human.

A

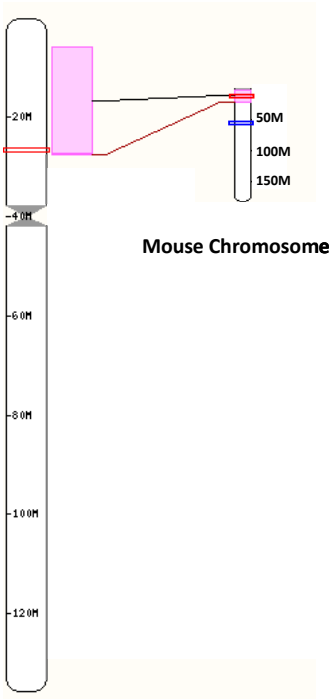

B

Human

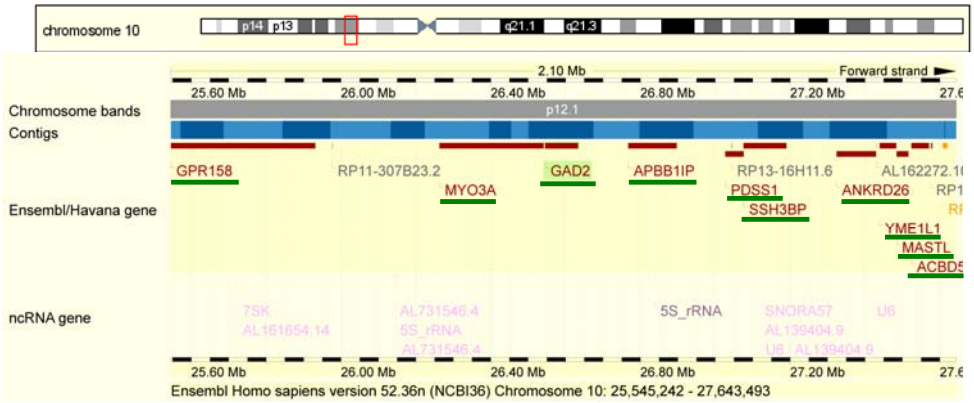

Mouse

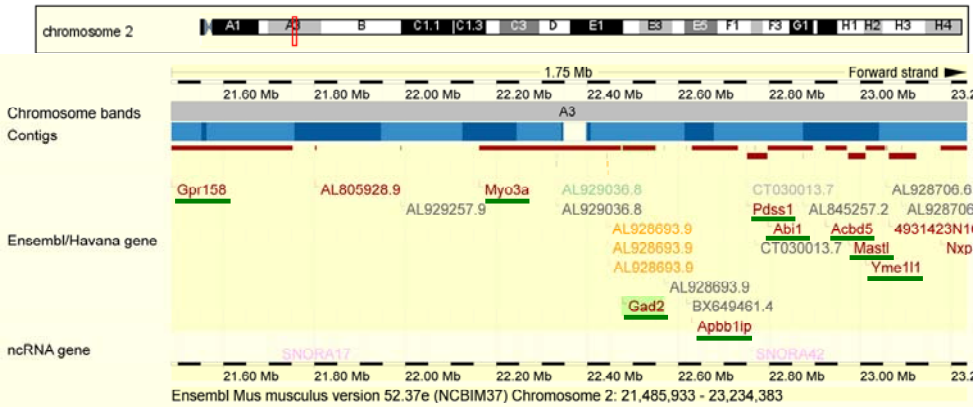

Figure 28

Comparison of genomic location of GAD2 (GAD65) in mouse and human

Red box depicts the location of GAD2 in each species.

(A) GAD2 is located on a different chromosome in human and mouse i.e. chromosome 10 in human and chromosome 2 in mouse, 47 Mb down-stream of GAD1. Blue box on the mouse chromosome 2 represents the GAD1 gene.

(B) In depth view of the genomic location of GAD2 in human and mouse, showing the high degree of conservation of the gene cluster. Green lines indicate the common genes within this region, for which PCR was performed in human. Even though the region is located on different chromosomes it is highly conserved, though the regulation differs in both species, that being expressed in mouse, while absent in human.

Real-time PCR analysis of both loci in human, showed that all genes within the GAD67 cluster were expressed in the thymus, GORASP2 showed the lowest expression. Most genes were not differentially regulated between MHCII^{hi} and MHCII^{lo} mTECs, except for SP5 and GAD67. The entire gene locus had a rather regular expression with genes 5' to GAD67 being more strongly expressed (Figure 29A; MYO3B, SP5, AC007405). Interestingly, in the GAD65 locus, most genes were expressed, though not differentially between the two mTEC subsets. Expression was however more variable than in the GAD67 locus, with low to almost absent levels of expression for GPR158 and GAD65 in the thymus or purified mTEC populations. Intriguingly, MYO3A that is located between these two genes was expressed at relatively high levels (Figure 29B). Moreover, genes immediately downstream 3' to GAD65 showed a lower expression (Figure 29B; APBB1IP, PDSS1, SSH3BP). Thus, the lack of expression of GAD65 may be related to the low overall transcriptional activity 3' to GAD65.

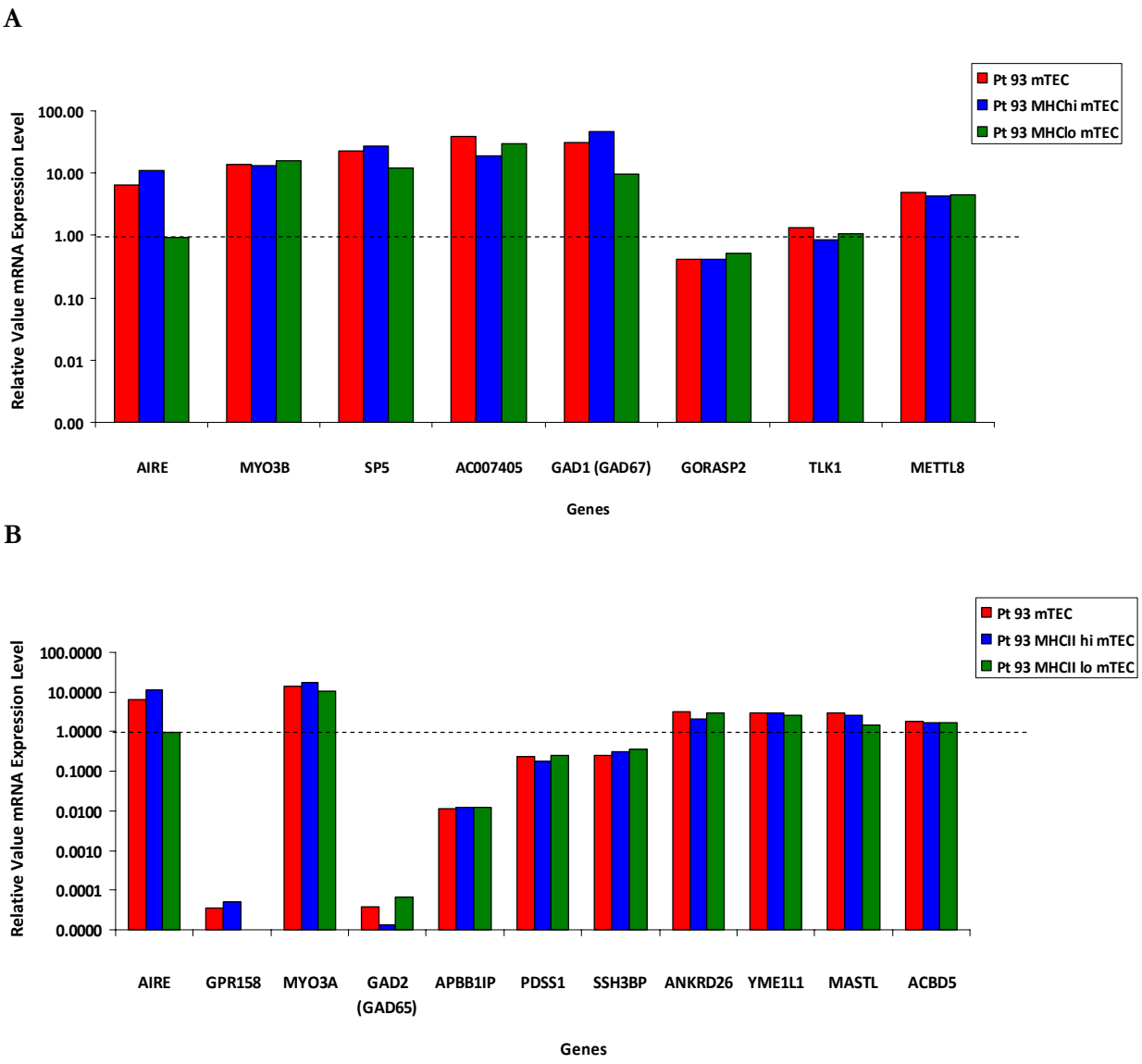

Figure 29

Gene expression profile in the GAD1/GAD2 clusters in human thymus

Purified mTECs, MHCII^{lo} and MHCII^{hi} mTECs from human thymus were used to perform real-time PCR analysis of GAD1 (A) and GAD2 (B) loci in human, spanning a region of ~1 Mb of the GAD1 locus and ~2 Mb of the GAD2 locus. The expression was normalized to GAPDH. Dotted line represents the level of Aire expression in MHCII^{lo} mTECs, which was considered as a minimal expression threshold. The GAD67 gene locus had a rather regular expression with genes 5' to GAD67 being more strongly expressed while the expression was more variable in the GAD65 locus, with low to almost absent levels of expression for GPR158 and GAD65 in the purified mTEC populations. Moreover, genes immediately downstream 3' to GAD65 showed a lower expression.

3.2.2. Regulation of the MYH6/MYH7 locus in human and murine thymus

The next target gene studied was the cardiac myosin heavy chain (MyHC), a primary contractile protein of the heart which is involved in the pathogenesis of myocarditis. Myocarditis is the most common cause of heart failure in young individuals (Towbin *et al.*, 2006). Individuals after open-heart surgery and myocardial infarction show auto-antibody responses against cardiac tissue-specific antigens, the most prominent of which is MyHC (Wolfgram *et al.*, 1985; Neu *et al.*, 1987). The heart expresses two highly homologous isoforms of MyHC, that differ by 6.5 % in their amino acid sequence: α-MyHC (MYH6), is expressed exclusively in cardiac muscle and β-MyHC (MYH7), is expressed in both cardiac and slow (type I) skeletal muscle (Weiss and Leinwand, 1996). In humans, β-MyHC is the major isoform expressed in heart, though autoimmune myocarditis is initiated by Th1 CD4 T-cell immune responses against α-MyHC. It was shown that IgG auto-antibodies are initially directed against unique epitopes of α-MyHC, but these responses rapidly broaden to epitopes of α-MyHC that are shared with β-MyHC, followed by recognition of other cardiac proteins. The basis of the immunogenicity unique to the α-MyHC isoform had been unclear. It was plausible that the same reasoning could apply as in the case of GAD65 where its absence in the thymus, i.e. lack of central tolerance, could explain the frequent occurrence of specific autoantibodies. Thus, the thymic expression of MYH6 and MYH7 in different mTEC subsets was analyzed.

The MYH6 and MYH7 gene loci are evolutionary highly conserved in human and mouse and present within a syntenic region on chromosome 14 (Figure 30). These two genes are adjacent to each other in both mouse and human (Figure 30B).

A

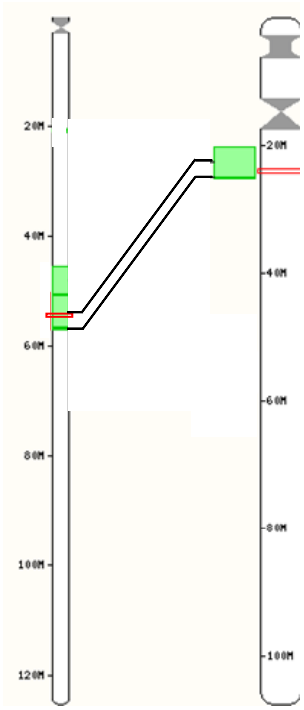

Mouse Chromosome 14 **Human Chromosome 14**

B

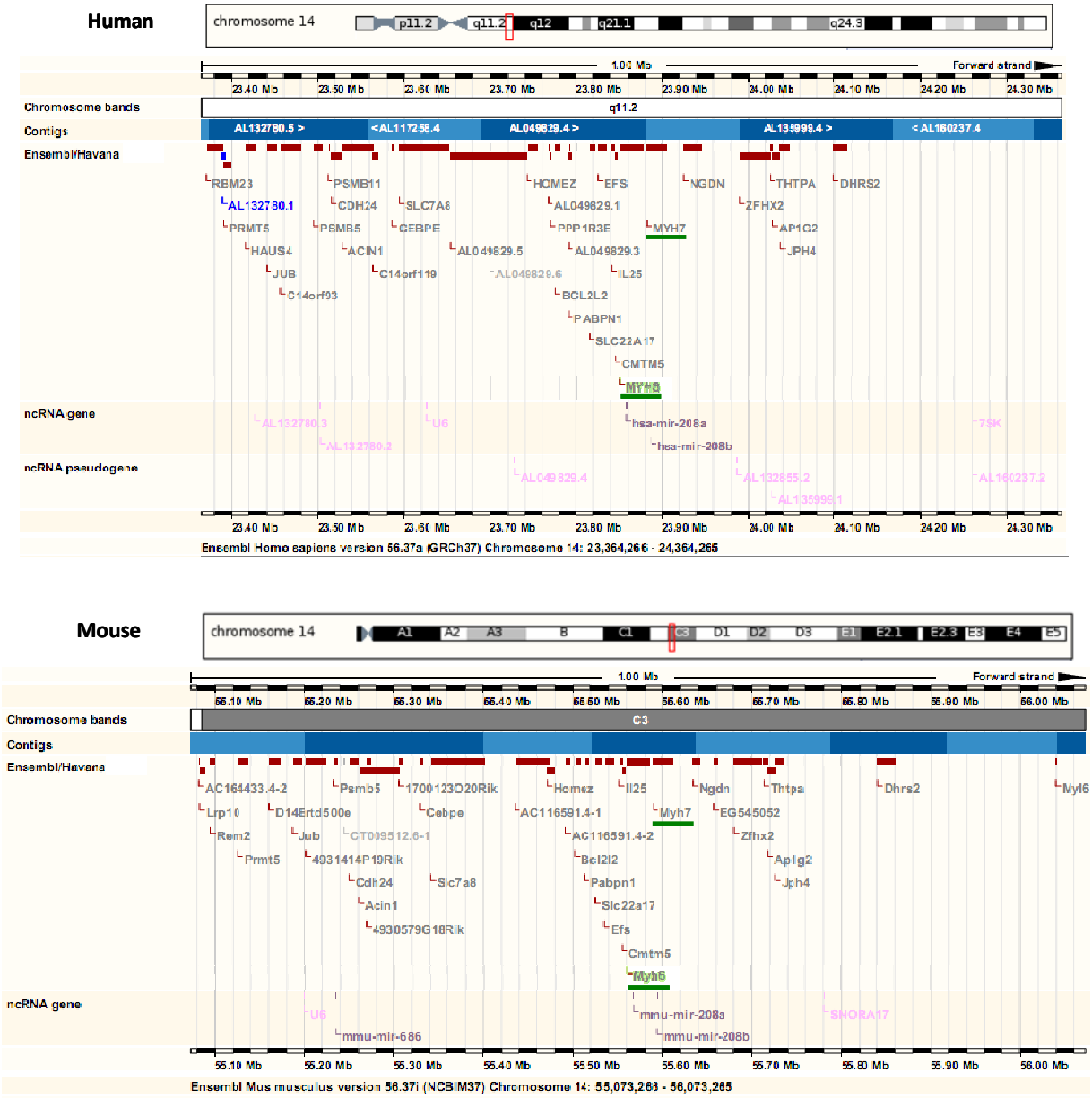

Figure 30

Comparison of genomic location of MYH6 and MYH7 in mouse and human

Red box depicts the location of MYH6 and MYH7 in each species.

(A) MYH6 and MYH7 are located on chromosome 14 in human and mouse.

(B) In depth view of the genomic location shows a high degree of conservation of the MYH gene cluster. Green lines indicate human/mouse MYH6 and MYH7 orthologs, for which PCR was performed. In both species the genes are immediately adjacent to each other, ~ 28-30 kb apart. They differ by 6.5 % in their amino acid sequence.

Real-time PCR of these two genes in mouse (Figure 31A) and human (Figure 31B) mTECs showed that the transcripts for α-MyHC (MYH6) were absent, while they were present for β-MyHC (MYH7). A similar situation was described above for GAD65 and GAD67. What is more striking is that MYH6 and MYH7 are not only present within the same gene cluster but are adjacent genes. Thus, the predominant autoimmune response to MYH6 in mouse and man is correlated with a lack of its expression in mTECs and thus is likely to be absent in the thymus.

A

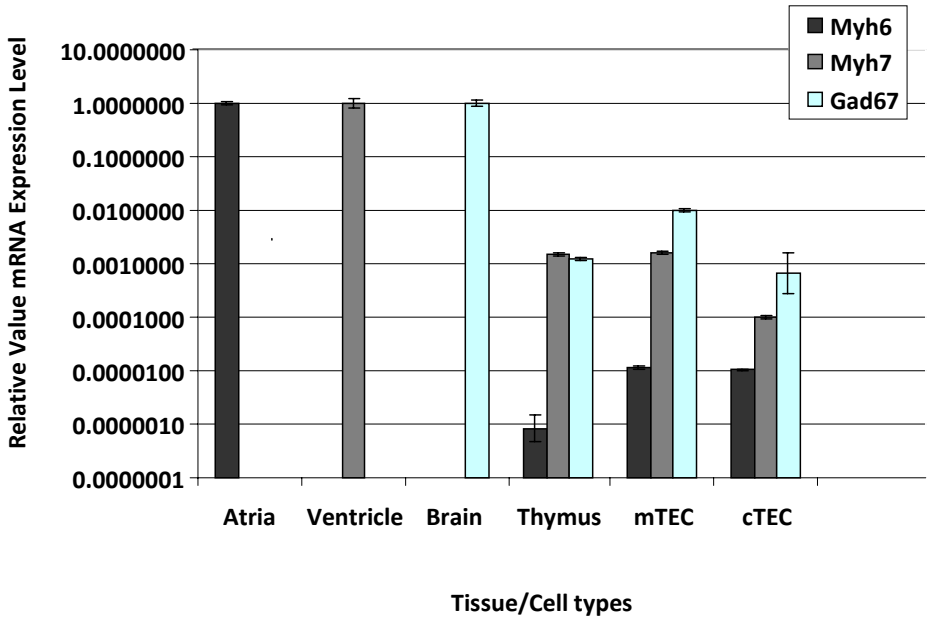

B

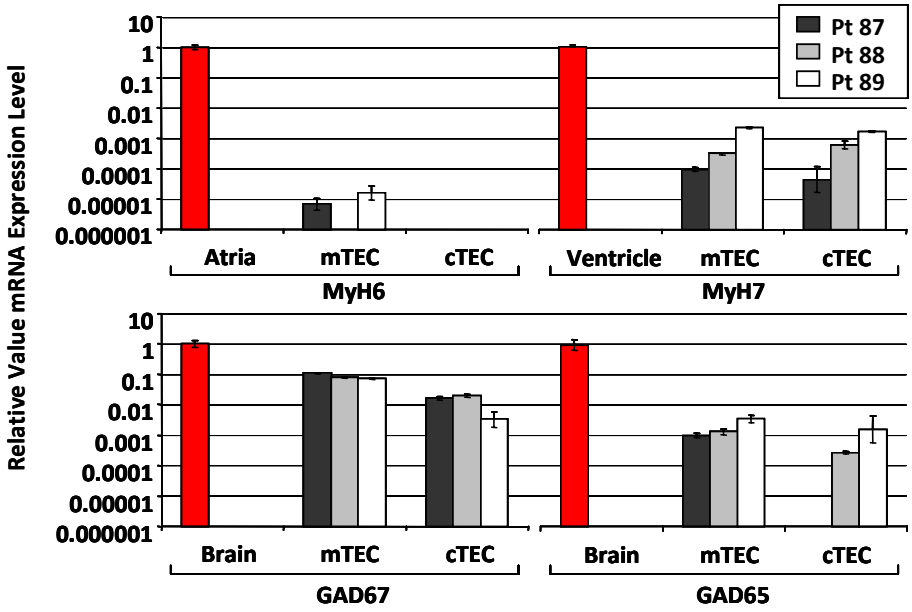

Figure 31

Expression patterns of MYH6 and MYH7 in mouse and human thymi

Purified mTECs and cTECs from mouse (A) and human (B) thymi were used to perform real-time PCR analysis of MYH6 and MYH7. The expression was normalized to beta-actin in mouse and GAPDH in human and relative to the respective positive organ (red bars), i.e. Atria for MYH6 expression, Ventricle for MYH7 expression and Brain for GAD67 or GAD65 expression. GAD67 was taken as the positive control, while GAD65 as the negative control for human mTECs. Real-time PCR in both mouse and human mTECs showed that the α-MyHC transcripts (MYH6) were absent, while present for β-MyHC (MYH7).

3.3. Study of pGE in mTEC subsets expressing a particular antigen

The population studies done prior in mouse and rat shows a fair representation of the genome in the thymic antigen repertoire. PGE was conserved between the studied species, however in the case of human the promiscuously expressed gene pool varied considerably. Previous studies showed that an individual gene is expressed in only few (~1-3 %) mTECs (Derbinski *et al.*, 2001; Cloosen *et al.*, 2007; Taubert *et al.*, 2007) and that genes within the casein locus were stochastically expressed in single cells (Derbinski *et al.*, 2008). What decides which given gene/group of genes is expressed in a single mTEC? Do individual mTECs have a free choice of selecting any combination of genes or do restrictions for co-expression exist? Conceivably the expression of a given gene would co-induce the expression of a certain set of linked genes. To address these intricate questions, mTECs that express a particular antigen were studied. The feasibility of this approach had been demonstrated by J. Arnold using antibodies to surface expressed antigens, mucin-1 (MUC1) and carcinoembryonic antigen (CEA) (Arnold, 2006).

3.3.1. Co-expression studies of MUC1 expressing mTECs at the population level

Previous studies at the population level indicated the existence of certain rules of co-expression; expression not does appear to be purely stochastic. Human $MUC1^+$ mTECs co-express CEACAM5 and MUC4 (Arnold, 2006). The frequency of co-expression was far above that expected on a stochastic basis; this implied a co-expression at the single cell level as well.

The same methodology of isolating MUC1 expressing mTEC as described by J. Arnold was used and extended in this study. $MUC1^+$ and $MUC1^-$ mTECs were sorted by flow cytometry (Sections 2.2.3.3.1, 2.2.3.3.4 and 2.2.3.3.5). From the sort profile (Figure 32) a clear population of $MUC1^+$ mTECs could be distinguished. These cells were primarily $MHCII^{hi}$, while the $MUC1^-$ mTECs covered the entire range of MHCII levels. The top 2 % $MUC1^+$ cells and the lower 4-5 % $MUC1^-$ cells were sorted (Arnold, 2006; Cloosen *et al.*, 2007), yielding rather low cell numbers in the range of 10,000-50,000 sorted cells per thymus sample. Hence we were limited in studying these cell populations.

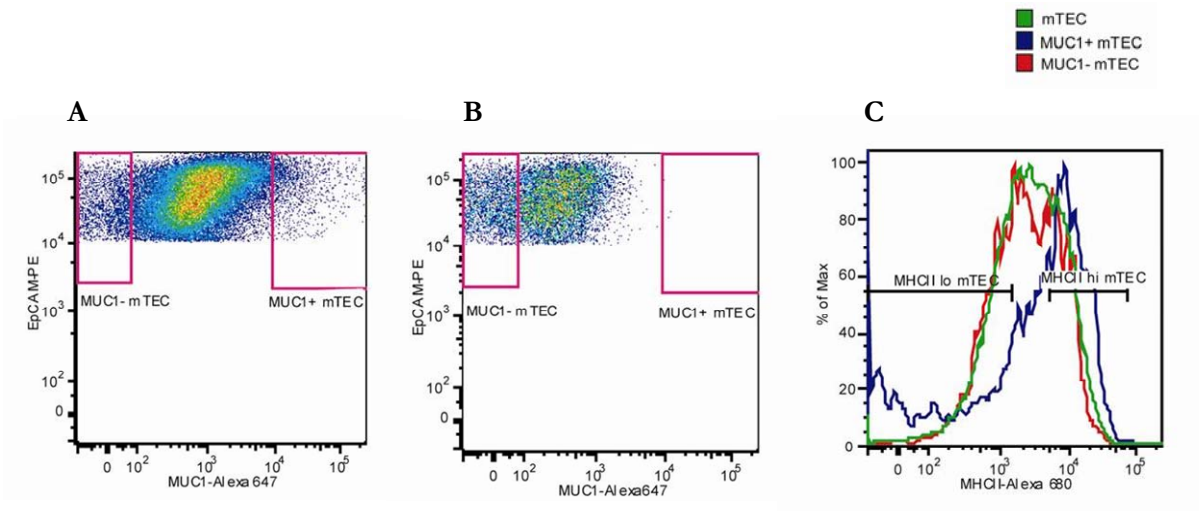

Figure 32

Isolation of MUC1 antigen expressing mTECs from human thymus

The human MUC1 expressing mTECs were stained and sorted for their (A) MUC1 expression versus non-expression negative control without MUC1 antibody (B). From the sort profile a clear population of $MUC1^+$ mTECs being primarily $MHCII^{hi}$ could be distinguished (C). The top 2 % $MUC1^+$ cells and the lower 4-5 % $MUC1^-$ cells were sorted.

Nonetheless, RNA was isolated, cDNA was prepared (Section 2.2.6) and qPCR was performed (Section 2.2.8). MUC1 mRNA was enriched in all samples in the $MUC1^+$ mTECs versus the $MUC1^-$ mTECs. Co-expression of MUC1 with MUC4 (a family member) and CEACAM5 at the population level was confirmed and further extended to other members of the CEA gene family. Interestingly the CEA family on chromosome 19 was only partially represented. MUC1 was also co-expressed with CEACAM6, though the expression of genes flanking CEACAM5 and CEACAM6, (CEACAM4, CEACAM7 and CEACAM3) were not up-regulated (low to absent) in $MUC1^+$ mTECs (Figures 33 and 34). Results were consistent for two individuals shown here as well as for an additional one (data not shown). Thus, inter-chromosomal co-expression patterns at the population level were confirmed as MUC1 is located on chromosome 1 while MUC4 is on chromosome 4 and CEACAM5 and CEACAM6 are on chromosome 19.

A

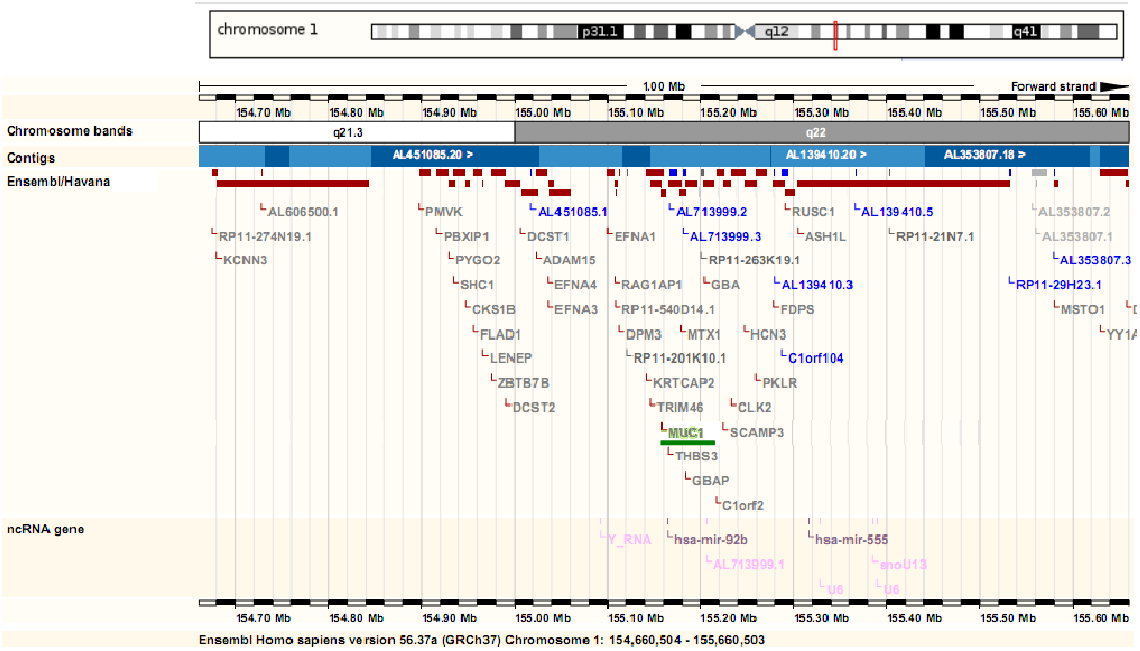
chromosome 1
p31.1
q12
q41
1.00 Mb
Forward strand
154.70 Mb
154.80 Mb
154.90 Mb
155.00 Mb
155.10 Mb
155.20 Mb
155.30 Mb
155.40 Mb
155.50 Mb
155.60 Mb
Chromosome bands
q21.3
q22
Contigs
AL451085.20 >
AL139410.20 >
AL353807.18 >
Ensembl/Havana
ALG6 500.1
PMVK
AL451085.1
AL713999.2
RUSC1
AL139410.5
AL353807.2
RP11-274N19.1
PBXIP1
DCST1
EFNA1
AL713999.3
ASH1L
RP11-21N7.1
AL353807.1
KCNN3
PYGO2
ADAM15
RP11-263K19.1
AL353807.3
SHC1
EFNA4
RAG1AP1
GBA
AL139410.3
RP11-29H23.1
CKS1B
EFNA3
RP11-540D14.1
FDPS
MSTO1
FLAD1
DPM3
MTX1
HCN3
LENEP
RP11-201K10.1
C1orf104
ZBTB7B
KRTCAP2
PKLR
DCST2
TRIM46
CLK2
MUC1
SCAMP3
THBS3
GBAP
C1orf2
ncRNA gene
Y_RNA
hsa-mir-92b
hsa-mir-555
AL713999.1
snoU13
U6
Ensembl Homo sapiens version 56.37a (GRCh37) Chromosome 1: 154,660,504 - 155,660,503

B

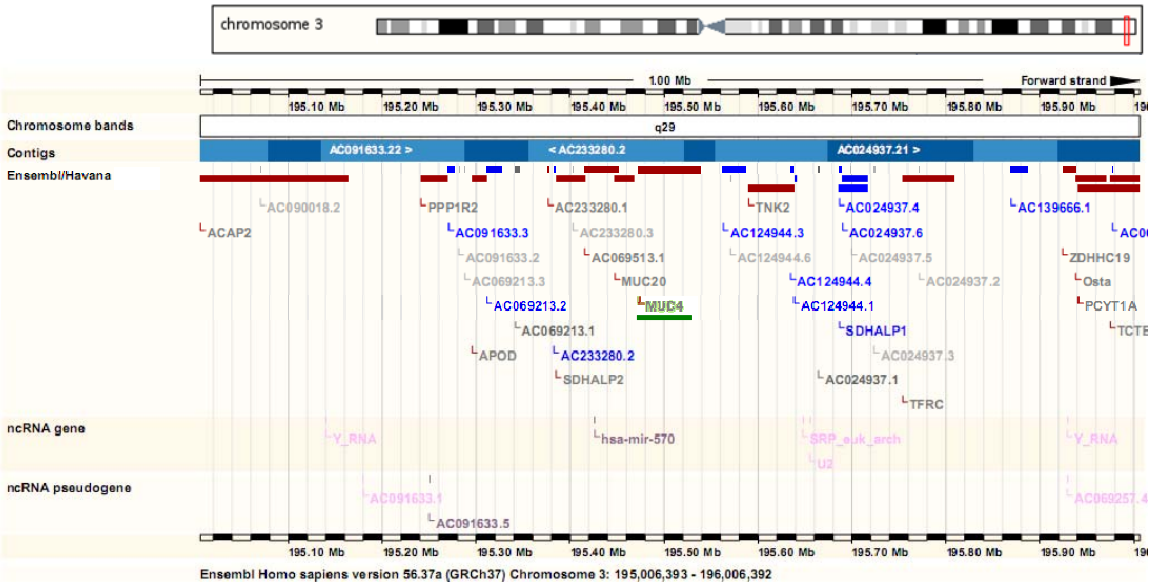
chromosome 3
1.00 Mb
Forward strand
195.10 Mb
195.20 Mb
195.30 Mb
195.40 Mb
195.50 Mb
195.60 Mb
195.70 Mb
195.80 Mb
195.90 Mb
Chromosome bands
q29
Contigs
AC091633.22 >
< AC233280.2
AC024937.21 >
Ensembl/Havana
AC090018.2
PPP1R2
AC233280.1
TNK2
AC024937.4
AC139666.1
ACAP2
AC091633.3
AC233280.3
AC124944.3
AC024937.6
AC091633.2
AC069513.1
AC124944.6
AC024937.5
ZDHHC19
AC069213.3
MUC20
AC124944.4
AC024937.2
Osta
AC069213.2
MUC4
AC124944.1
PCYT1A
AC069213.1
SDHALP1
APOD
AC233280.2
AC024937.3
SDHALP2
AC024937.1
TFRC
ncRNA gene
Y_RNA
hsa-mir-570
SRP_euk_arch
U2
ncRNA pseudogene
AC091633.1
AC091633.5
Ensembl Homo sapiens version 56.37a (GRCh37) Chromosome 3: 195,006,393 - 196,006,392

C

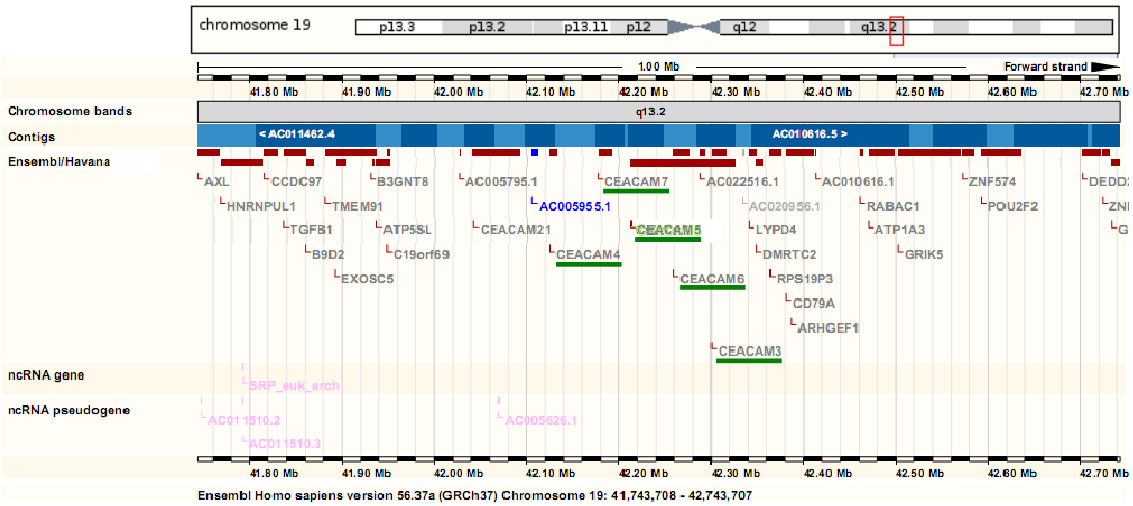

Figure 33

Genomic location of MUC1, MUC4 and CEA cluster in human

Location of MUC1 on chromosome 1 (A) MUC4 on chromosome 4 (B) and the CEA cluster on chromosome 19, consisting of CEACM4, CEACM7, CEACAM5, CEACAM6 and CEACM3 (C). All genes for inter-chromosomal co-expression in human MUC1^{+} mTECs studied by qPCR are underlined in green.

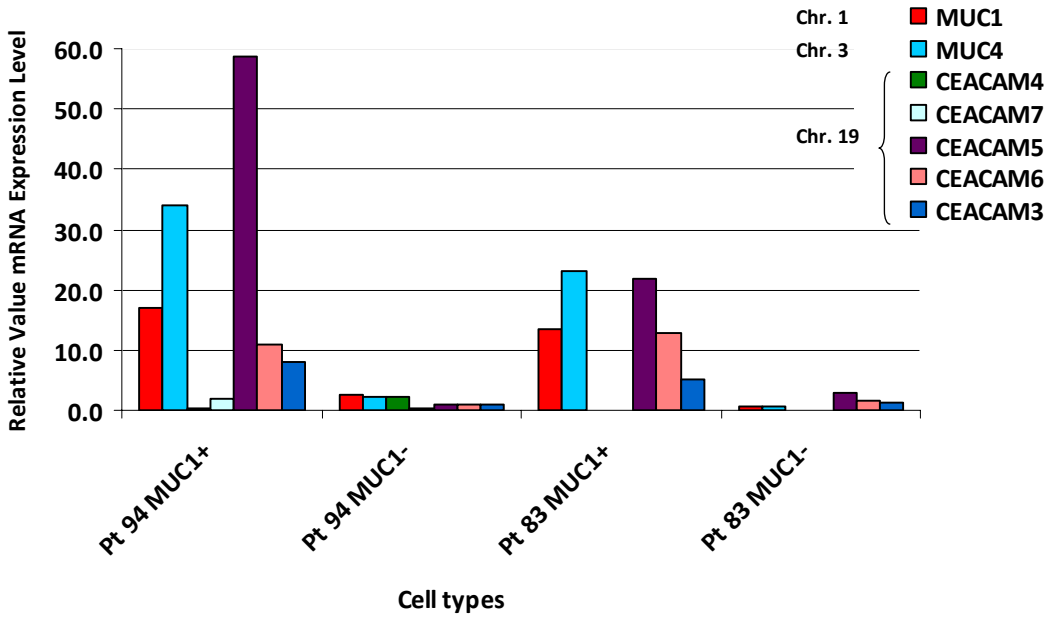

Figure 34

Co-expression patterns in human MUC1$^+$ and MUC1$^-$ mTECs

Purified MUC1$^+$ and MUC1$^-$ sorted mTECs were isolated from human thymus of two individuals (83 and 94). The expression was normalized to GAPDH. MUC1 was enriched 7-19 fold in MUC1$^+$ mTECs of both samples. Co-enrichment of MUC4 was observed in MUC1$^+$ mTECs, however within the CEA cluster only CEACAM5 and CEACM6 were co-expressed with MUC1 in MUC1$^+$ mTECs. CEACAM3 was modestly up-regulated and CEACAM4 and CEACAM7 were hardly different between both subsets. Though, CEACAM3 and CEACAM7 were barely detected in only one of the duplicates of both samples tested by PCR hence, it was considered low to absent.

To obtain a broader view of co-expression patterns, genome-wide microarrays were performed. Owing to the low cell number a modified protocol had to be established. We opted to use the µMACS™ SuperAmp™ Technology *(Miltenyi Biotech),* which can linearly amplify RNA of small/rare cell populations. We established this technology to hybridize the amplified labelled cDNA onto Illumina's expression profiling whole genome BeadArrays (Section 2.2.10) (Pinto *et al.*, 2009). For this method RNA from only 6000 cells was used.

Technical replicates of individual samples confirmed the reproducibility of the procedure of µMACS™ SuperAmp™ Technology for Illumina's expression profiling whole genome BeadArrays hybridization microarray analysis. The array results showed high degrees (~46-54 %) of overlap between the 3 individuals (Figure 35). This was a striking result as prior analysis of

immature versus mature mTECs using 11 individuals showed little to no overlap between any 2 individuals. Thus, the variability was reduced by precisely defining the mTEC population.

Since gene array results of the individuals were so similar, a combined analysis of individuals 94 (2 technical replicates), 96 and 97 was performed. A total of 633 probes were considered to be differentially expressed, fitting the criteria p value ≤ 0.01, out of which 412 were up-regulated and 221 were down-regulated in MUC1^{+} mTECs. In all samples MUC1 was enriched in the positive fraction. A comparison of fold change of qPCR and array results for individual 94 showed a good correlation (Table 3.6), except for CEACAM5. Differences in the fold change between microarrays and qPCR are a well known phenomenon, as the dynamic range of the microarray is limited to 4-5 logs whereas with qPCR typically 7 logs are achieved. Therefore, microarray data are more compressed, when compared to qPCR data.

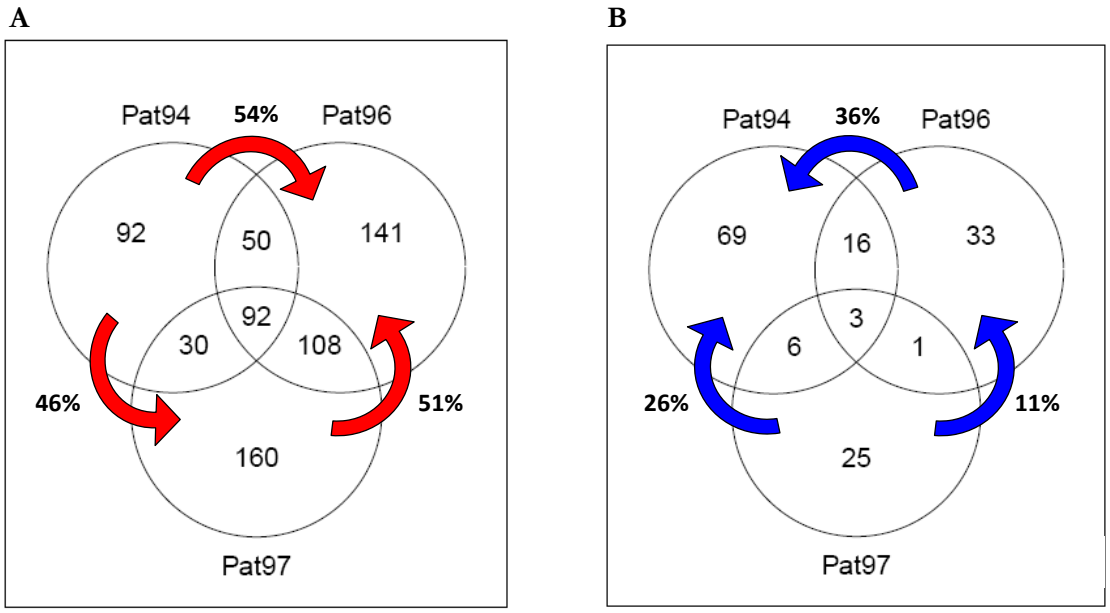

Figure 35

Overlap of differentially expressed genes between three human samples sorted for MUC1^{+} and MUC1^{-} mTECs

The µMACS™ SuperAmp™ Technology was used to amplify RNA from 6000 cells of each population (i.e. MUC1^{+} and MUC1^{-} mTECs) sorted from three individuals. The resulting labeled cDNA was then hybridized to Illumina's expression profiling whole genome BeadArrays. Log Fc ≥ or Log Fc ≤ 2 was the criteria used to identify the set of differentially expressed genes for each individual. The array results show a high degree of overlap of ~46-54 % between the individuals within the up-regulated genes (A) and a lesser degree of overlap (~11-36 %) in the down-regulated gene set (B). An example of how the percentage of overlap between the patients was calculated is as follows: Between individual 94 and 96; 54 %= [sum of gene overlap (50 + 92) x 100]/sum of genes of the individual having the smaller gene pool (individual 94; 92 + 50 + 92 + 30 = 264).

Genes	Fold change between MUC1$^+$ and MUC1$^-$ mTECs qPCR (Ind. 94)	Fold change between MUC1$^+$ and MUC1$^-$ mTECs Arrays (Ind. 94)	Fold change between MUC1$^+$ and MUC1$^-$ mTECs Arrays (Ind. 94 (2x), 96, 97)	Adjusted p value
MUC1	**6.84476**	2.59065	**2.173945676**	**0.005385109**
MUC4	**14.1723**	3.77751	**4.023302348**	**0.018842202**
CEACAM4	0.08021	0.31846	0.158109299	0.500033168
CEACAM7	*6.16884*	0.70515	0.477344922	0.09432146
CEACAM5	**66.7178**	2.40615	**2.999483104**	**0.026334518**
CEACAM6	**11.3924**	3.19566	**3.45087004**	**0.004138704**
CEACAM3	*8.11168*	1.64549	0.750290376	0.415159836

Table 3.6

Comparison of fold change between MUC1$^+$ and MUC1$^-$ mTECs using qPCR and microarray data

There was a good correlation of the fold change using qPCR and array data for the genes studied. Single array data for individual 94 only gave very similar results as the combined analysis of individuals 94 (2 technical replicates), 96 and 97. The qPCR results for CEACAM7 and CEACAM3 are in italics as they were barely detected and their expression was considered low to negative.

MUC1$^+$ mTECs were MHCII^{hi} and did not co-express AIRE at the protein level as shown by Arnold J. (Arnold, 2006). The corresponding mouse ortholog is also Aire-independent and up-regulated in mature MHCII^{hi} mTECs. This would classify MUC1 as an Aire-independent gene. Consistent with this, the top 50 up-regulated and down-regulated genes showed enrichment for TRAs, most of which fell into the same category of MUC1 as being "Aire-independent" (data not shown).

An enrichment test for entire chromosomes in the human genome showed that a large number of up-regulated genes tend to significantly localise to chromosome 19 (p= 0.0048 and Table 3.7). Thus, not only were CEACAM5 and CEACAM6 co-enriched but other genes of chromosome 19. The population studies were complemented by SC-PCR using the above defined set of genes.

Up-regulated genes		Down-regulated genes	
Chromosomes	**Fisher test score**	**Chromosomes**	**Fisher test score**
19	0.00489853936955524	3	0.088787764601465
1	0.0816691250640902	6	0.092421721283648
18	0.166085241762275	8	0.210147860171922
22	0.18291302286992	14	0.226571280995458
16	0.221558377398973	13	0.238474155017593
15	0.259295911021636	20	0.243507533923685
9	0.357044000184515	18	0.285992935578891
3	0.364399857096554	7	0.309906976056937
2	0.389452436158082	21	0.421170912248371
20	0.411148118189128	9	0.513070795808045
12	0.550615928953208	5	0.517757400342489
6	0.556374291646211	X	0.533390033624122
5	0.563332106438259	16	0.541432217163013
11	0.620224867831966	17	0.561330577229494
8	0.640779061541043	10	0.600634402512559
17	0.837596594112363	19	0.640308053093802
21	0.846710840867452	12	0.643663170054273
4	0.852563561987315	4	0.739819470812997
13	0.894241119691976	2	0.796389567788603
14	0.94185061722219	11	0.868535879269216
10	0.953747238622854	1	0.905083225255293
7	0.973911213370496	22	0.942657592338499
X	0.974752967184606	15	0.98771466552169
Y	1	Y	1

Table 3.7

Fisher test for the preferential localization of genes up- and down-regulated in MUC1^{+} mTECs on particular chromosomes

A number of up-regulated genes tend to significantly localise to chromosome 19 ($p = 0.0048$), where the CEA gene family is located. This chromosome was the only one with a significance value.

3.3.2. Co-expression studies of MUC1-expressing mTECs at the single cell level

Population studies on co-expression patterns were complemented by single cell analysis. Multiplex reverse-transcription PCR for EpCAM, MUC1, MUC4, CEACAM3, CEACAM5 and CEACAM6 was applied. The method was performed as described by Derbinski *et al.* ((Derbinski *et al.*, 2008) and Section 2.2.11).

Single-cell PCR analysis was performed on sorted $MUC1^+$ and $MUC1^-$ mTECs purified from two human thymus samples (156-158 single cells per individual analyzed). The $MUC1^+$ cells of both patients studied for SC-PCR gave highly consistent results. Surprisingly, EpCAM which was run as a marker gene for mTECs was barely present within either $MUC1^+$ or $MUC1^-$ mTECs (0 % in $MUC1^-$ mTECs and 6-30 % $MUC1^+$ mTECs). Approximately 90 % of all $MUC1^+$ mTECs analyzed were positive for MUC1, hence a good correlation between mRNA and protein was observed. Only 8-11 % $MUC1^-$ mTECs (6-9 single cells) expressed MUC1. All the other genes analyzed were absent in $MUC1^-$ mTECs. In contrast, in $MUC1^+$ mTECs, CECAM6 was expressed in a large number of cells, up to 67-68 % followed by MUC4 (55-67 %) and CEACAM5 (32-35 %). CEACAM3 was barely detectable in both individuals analyzed; hence it is present at low levels, which would fit the qPCR and array data (Figures 36 and 37). All together, the data shows that MUC1 is co-expressed with CEACAM6, MUC4 and CEACAM5 not only at a population level but also at the single cell level.

A correlation analysis of this dataset confirmed that co-expressed gene pairs MUC1- CEACAM6 and MUC1-MUC4 showed a high concordance index $\varkappa$ (Table 3.8). A weak concordance was observed for MUC1-CEACAM5, while MUC1-CEACAM3 showed no correlation at all.

In single mTECs analyzed from individual 105, the same was observed for EpCAM which was barely detected in ~10 % single cells. The basal expression frequency on random bases in single mTECs was in the range of 3-13 % (Figure 38). This was higher than comparable data published previously by Derbinski *et al.* in mice (Derbinski *et al.*, 2008).

From the single cell data, it appears that there is a highly regulated rather than stochastic co-expression pattern in $MUC1^+$ mTECs. The co-expression frequencies of the analyzed gene pool were much higher in $MUC1^+$ mTECs than expected on a random base in single mTECs (~ 1 %).

A

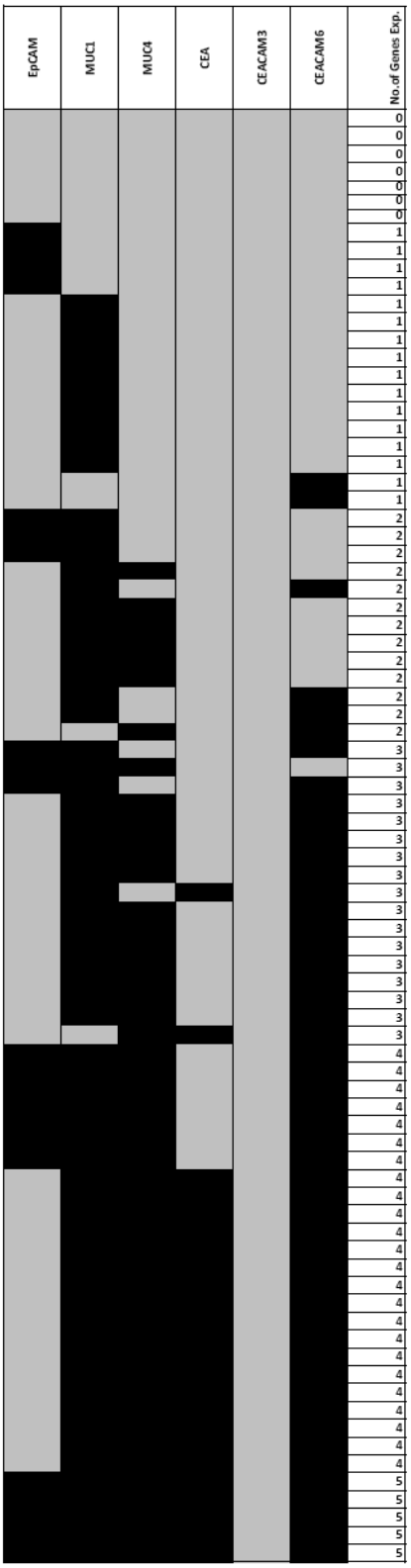
EpCAM
MUC1
MUC4
CEA
CEACAM3
CEACAM6
No.of Genes Exp.

B

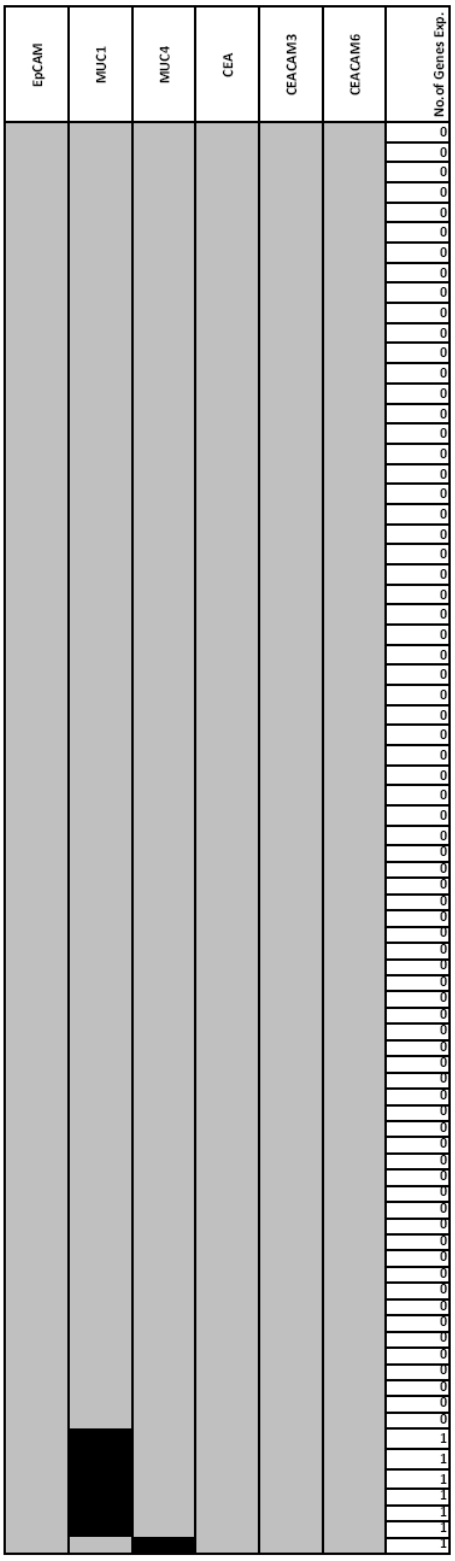
EpCAM
MUC1
MUC4
CEA
CEACAM3
CEACAM6
No.of Genes Exp.

C

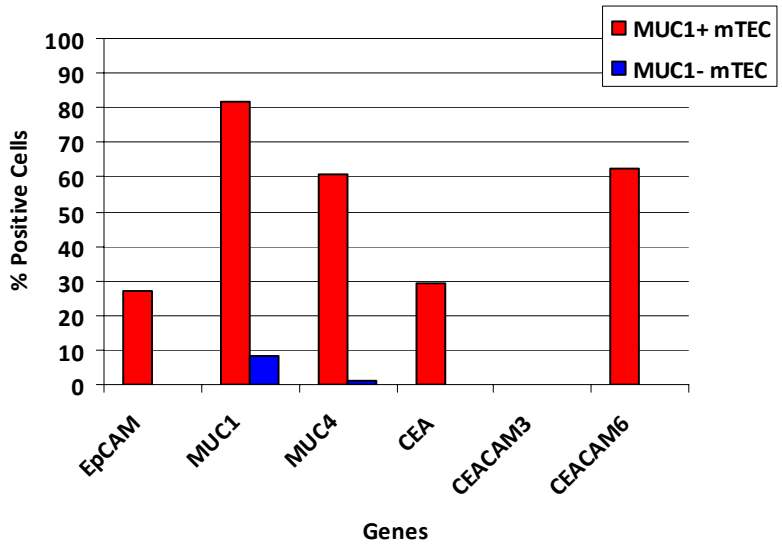

D

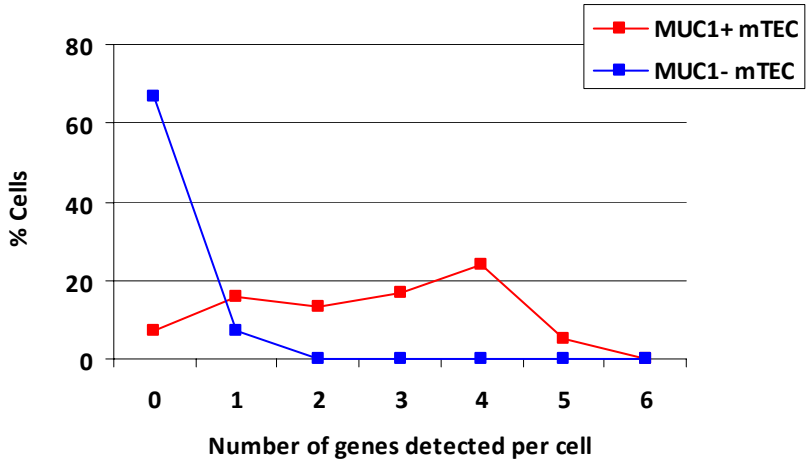

Figure 36

Co-expression patterns of single MUC1$^+$ and MUC1$^-$ mTECs from individual 103

(A) Each row represents a single MUC1$^+$ mTEC from individual 103 as analyzed for expression of the genes listed above the columns; the last column is the total number of genes expressed by each cell. Black stripes denote detected expression; gray stripes denote lack of expression. Expression patterns were arranged from top to bottom according to increasing numbers of genes expressed per cell.

(B) Represents the same as in A only in MUC1$^-$ mTECs from individual 103.

(C) Percentage of single cells expressing each of the tested genes in MUC1$^+$ and MUC1$^-$ mTECs from individual 103.

(D) The percentage of cells co-expressing 0-6 of the genes assessed was counted among MUC1$^+$ and MUC1$^-$ mTECs from individual 103.

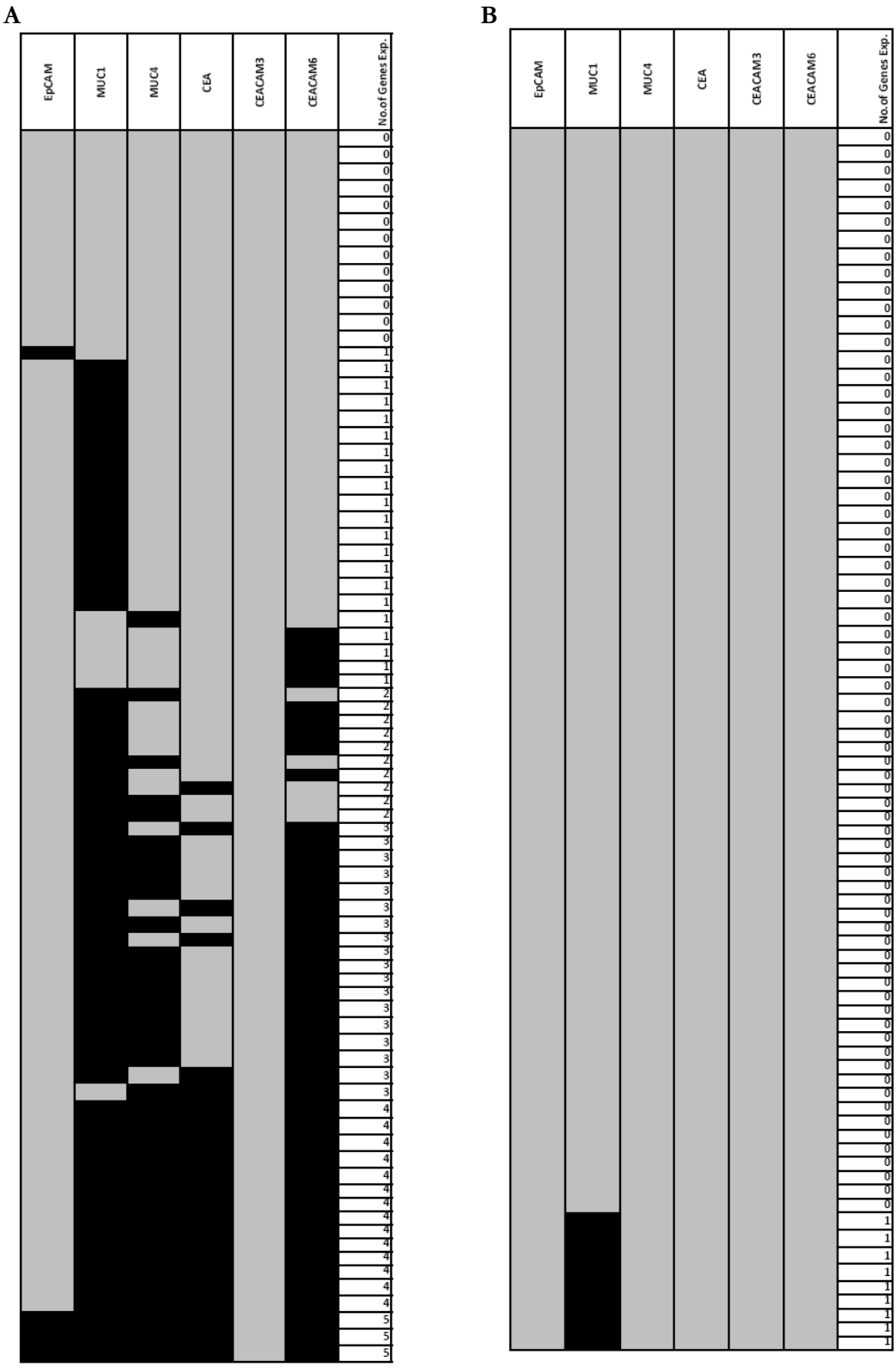
A
EpCAM
MUC1
MUC4
CEA
CEACAM3
CEACAM6
No.of Genes Exp.
B
EpCAM
MUC1
MUC4
CEA
CEACAM3
CEACAM6
No.of Genes Exp.

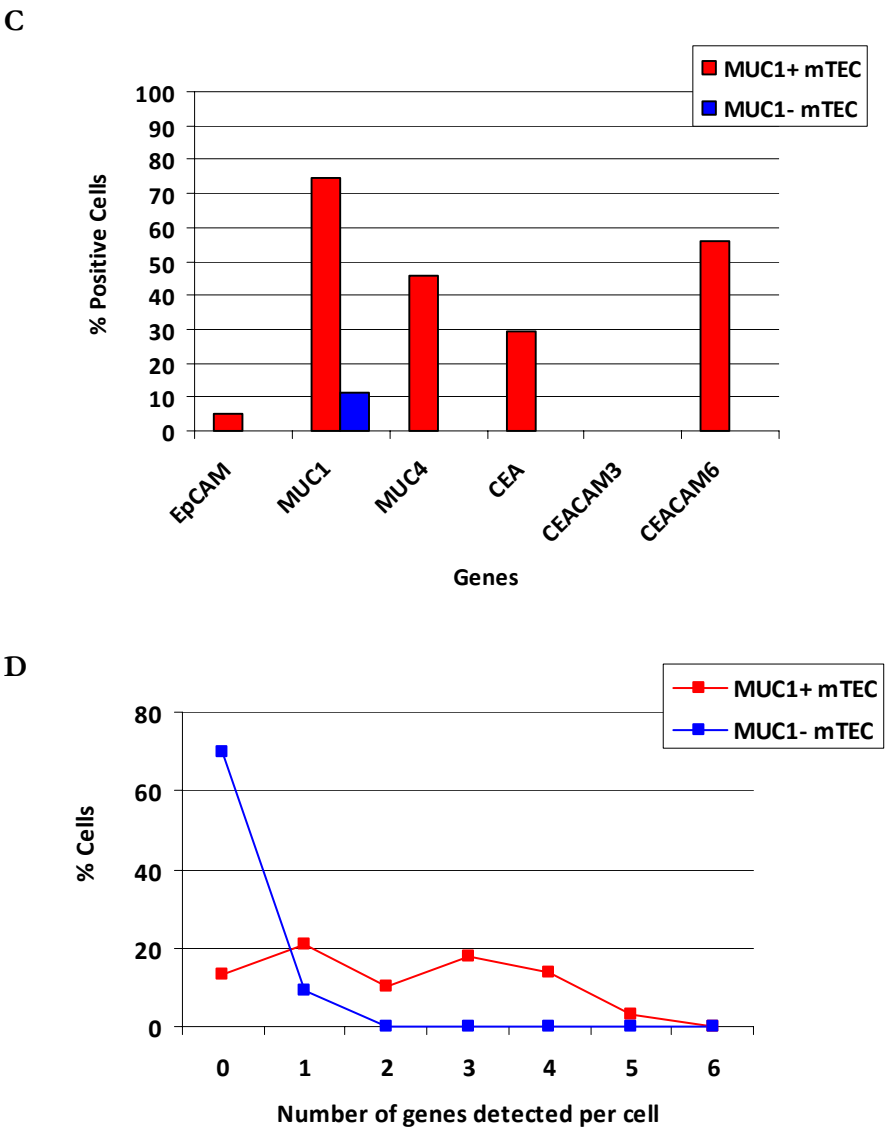

Figure 37

Co-expression patterns of single MUC1$^+$ and MUC1$^-$ mTECs from individual 105

(A) Each row represents a single MUC1$^+$ mTEC from individual 105 as analyzed for expression of the genes listed above the columns; the last column is the total number of genes expressed by each cell. Black stripes denote detected expression; gray stripes denote lack of expression. Expression patterns were arranged from top to bottom according to increasing numbers of genes expressed per cell.

(B) Represents the same as in A only in MUC1$^-$ mTECs from individual 105.

(C) Percentage of single cells expressing each of the tested genes in MUC1$^+$ and MUC1$^-$ mTECs from individual 105.

(D) The percentage of cells co-expressing 0-6 of the genes assessed was counted among MUC1$^+$ and MUC1$^-$ mTECs from individual 105.

A

Kappa Index	
Less than 0.1	No Concordance
0.10-0.40	Weak Concordance
0.41-0.60	Clear Concordance
0.61-0.80	Strong Concordance
0.81-1.00	Nearly complete Concordance

B

	Co-expression Analysis MUC 1^{+} & MUC1^{-} mTECs (Kappa Index)				
	CEACAM6	**CEACAM5**	**CEACAM3**	**MUC4**	**EPCAM**
MUC1 (Pt 103)	0.6067	0.3158	-	0.6239	0.2071
MUC1 (Pt 105)	0.5413	0.3399	-	0.5069	0.0373
MUC1 (Pt 103+105)	0.5753	0.3278	-	0.5730	0.1298

Table 3.8

Correlation analysis of gene expression in MUC1^{+} and MUC1^{-} mTECs from individuals 103 and 105 as detected by single-cell PCR

(A) Degree of concordance according to the kappa index.

(B) Kappa index of correlation, between MUC1 and the genes listed above each column.

A

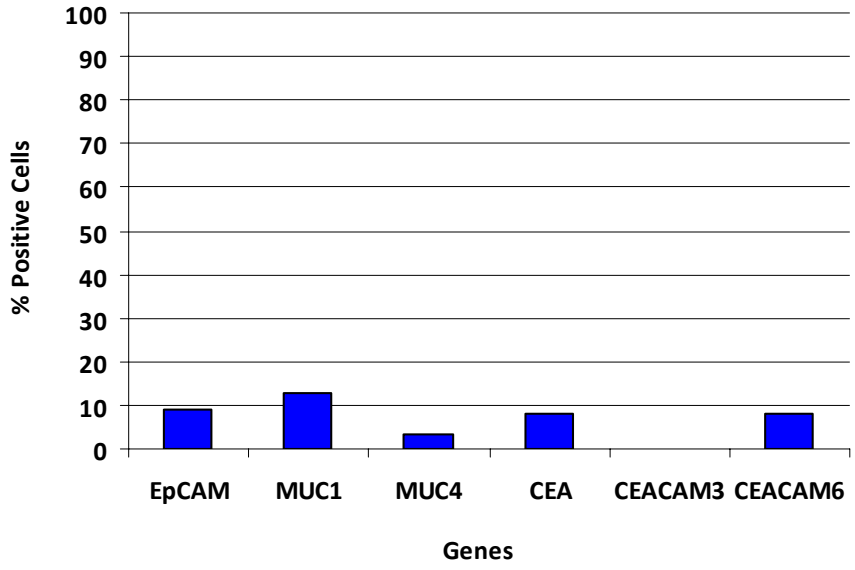

B

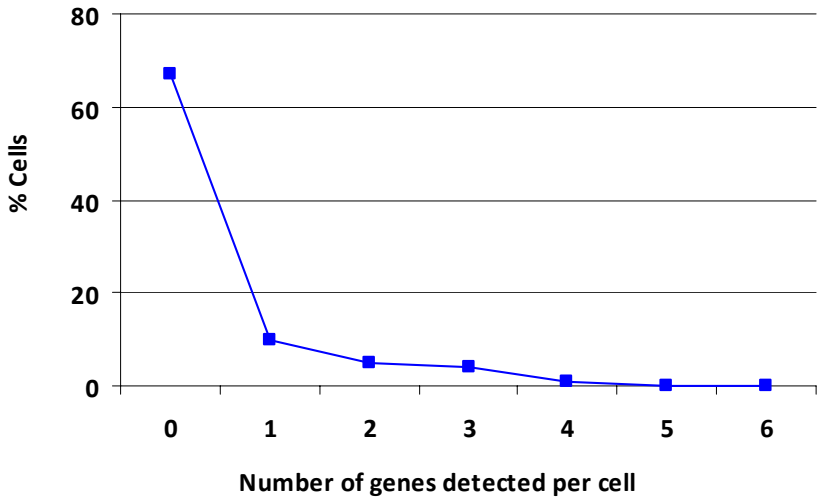

Figure 38

Co-expression patterns of single mTECs from individual 105

(A) Percentage of single cells expressing each of the tested genes in mTECs from individual 105.

(B) The percentage of cells co-expressing 0-6 of the genes assessed was counted among mTECs from individual 105.

3.3.3. Co-localization studies of chromosomes 1 and 19 in MUC1 expressing mTECs using FISH

Population and single cell studies of MUC1 expressing mTECs revealed the same co-expression pattern. Population studies showed that not only were CEACAM5 and CEACAM6 co-enriched with MUC1 but many more genes on chromosome 19. From the single cell data, it appears that there is a highly regulated rather than stochastic co-expression pattern in MUC1$^+$ mTECs. We wanted to investigate if genes present on these two different chromosomes i.e. chromosomes 1 and 19 could possibly be coordinately expressed through a mechanism that brings them together in a region of active transcription in the nucleus (transcription factories) as shown in earlier studies (Spilianakis and Flavell, 2006). Hence, fluorescent probes spanning regions on chromosomes 1 and 19 were used to perform FISH on MUC1$^+$ mTECs (Table 3.9).

BAC clone: RP11-343B1
4 genes on chromosome 19 are completely covered by this clone:
CEACAM3
CEACAM5
CEACAM6
LYPD4
2 genes partially covered by this clone
CEACAM7
DMRTC2

BAC clone: RP11-263K19
14 genes on chromosome 1 are completely covered by this clone:
C1orf2
CLK2
DPM3
EFNA1
GBA
HCN3
KRTCAP2
MTX1
MUC1
PKLR
RAG1AP1
SCAMP3
THBS3
TRIM46
There are no genes partially covered by this clone.

Table 3.9

Genes spanned by the labeled BAC clones (FISH probes)

The BAC clones were ~18 kb and completely spanned 4 genes on chromosome 19 including CEACAM3, CEACAM5, CEACAM6 and 14 genes on chromosome 1 including MUC1.

The method for hybridization, image analysis and co-localization was performed as described in Section 2.2.12. FISH studies for two human thymus samples (individuals 106 and 108) of $MUC1^+$ and $MUC1^-$ mTECs gave highly consistent results. There existed a population of $MUC1^+$ mTECs having distances ≤ 1.2 µm between either one or both allele pairs, which, as per our criteria are co-localized. This population was lacking or lower in $MUC1^-$ mTECs (Figure 39).

A

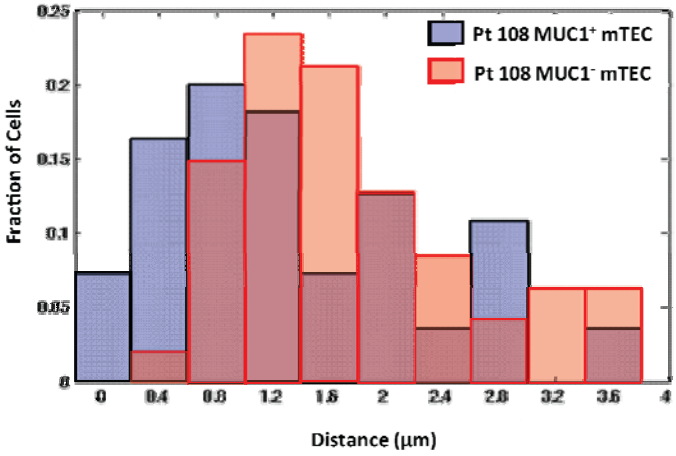

B

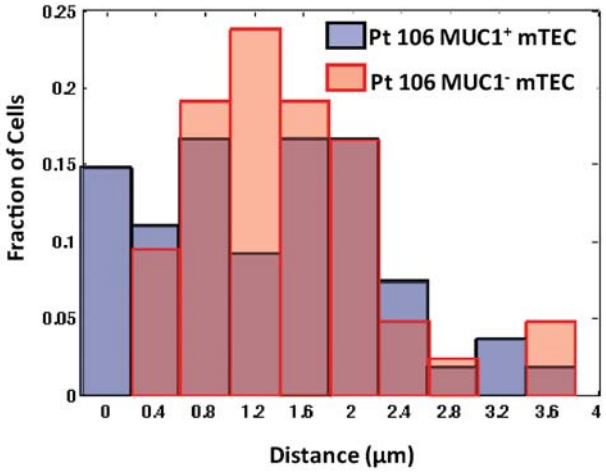

Figure 39

Distance measurements between alleles of chromosomes 1 and 19 in $MUC1^+$ and $MUC1^-$ mTECs of individuals 108 and 106

(A) Distance measurements (x-axis) versus fraction of cells (y-axis) of single $MUC1^+$ and $MUC1^-$ mTECs of individual 108.

(B) Represents the same in individual 106.

Three different scenarios exist for co-localization of two different chromosomes having each 2 alleles. Co-localization can be: mono-allelic- any one allele pair; bi-allelic- both allele pair; asymmetric mono- and bi-allelic- any one allele of one chromosome with both alleles the other chromosome (Figure 40).

As described earlier promiscuously expressed genes in mTECs could be mono- or bi-allelically transcribed (Villasenor *et al.*, 2008; Sinemus, 2009). In $MUC1^+$ mTECs of individual 108, 39 % showed mono-allelic and 3.5 % showed bi-allelic co-localization versus 16 % $MUC1^-$ mTECs showed mono-allelic co-localization (Figures 40 and 41). While for individual 106, $MUC1^+$ mTECs showed: 18.5 % mono-allelic co-localization, 13 % bi-allelic co-localization and 9.3 % had asymmetric mono- and bi-allelic co-localization. The bi-allelic and asymmetric mono- and bi-allelic co-localization was significant when compared with the $MUC1^-$ mTECs of this individual (Figures 40 and 42). Taken together, it appears that these two chromosomes i.e. chromosomes 1 and 19 tend to either show all three co-localization patterns in $MUC1^+$ mTECs to a significant extent when compared to the $MUC1^-$ mTECs. Most probably the alleles co-localize in a region of active transcription resulting in co-expression pattern seen at the population and single cell level.

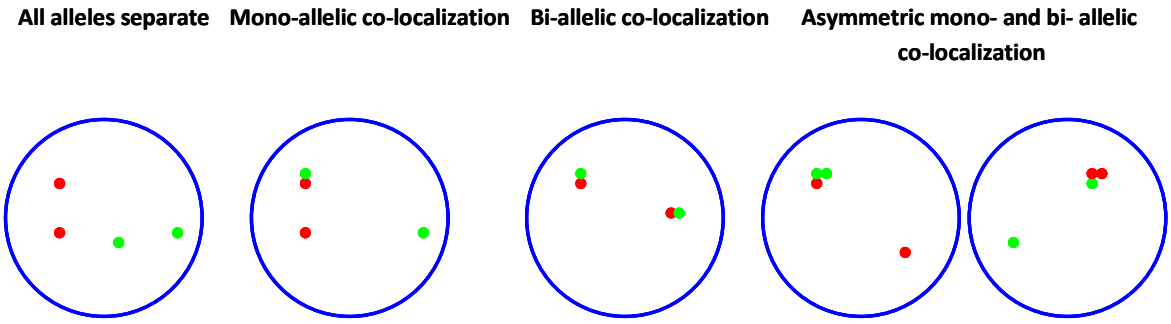

Pt 108	Number of cells	Mono-allelic co-localization	Bi-allelic co-localization	Asymmetric mono- and bi-allelic co-localization
MUC1^{+} mTEC	56	22 (39 %)	2 (3.5 %)	0
MUC1^{-} mTEC	49	8 (16.3 %)	0	0

Pt 106	Number of cells	Mono-allelic co-localization	Bi-allelic co-localization	Asymmetric mono- and bi-allelic co-localization
MUC1^{+} mTEC	54	10 (18.5 %)	7 (13 %)	5 (9.3%)
MUC1^{-} mTEC	42	10 (23.8 %)	0	1 (2.3 %)

Figure 40

Co-localization between alleles of chromosomes 1 and 19 in MUC1^{+} and MUC1^{-} mTECs of individuals 108 and 106

Co-localization studies of mono-allelic, bi-allelic and asymmetric mono- and bi-allelic co-localization in individual MUC1^{+} and MUC1^{-} mTECs of individuals 108 and 106. For both individual samples, MUC1^{+} mTECs either show a significant co-localization of chromosomes 1 and 19 for all three scenarios.

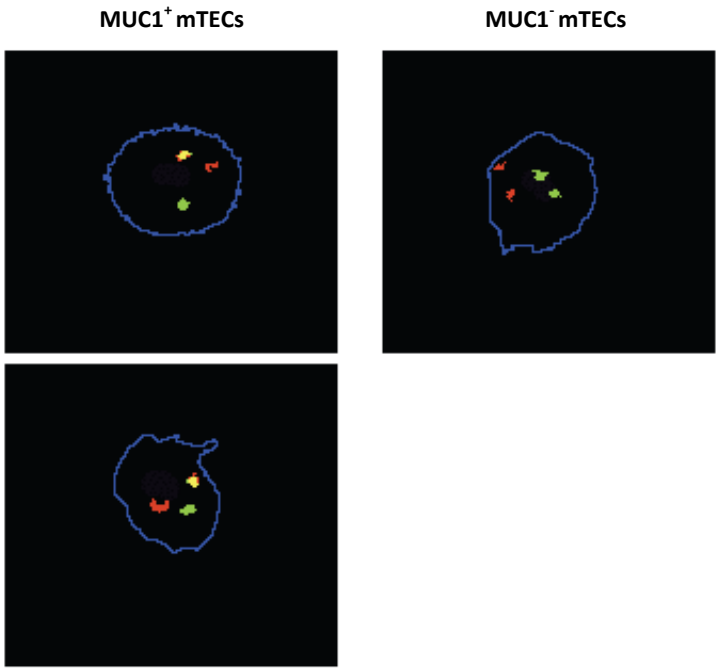

Figure 41

Co-localization studies of alleles of chromosomes 1 and 19 in MUC1$^+$ and MUC1$^-$ mTECs of individual 108

Mono-allelic co-localization observed in MUC1$^+$ mTECs. There was no co-localization (all alleles separated) in MUC1$^-$ mTECs of individual 108.

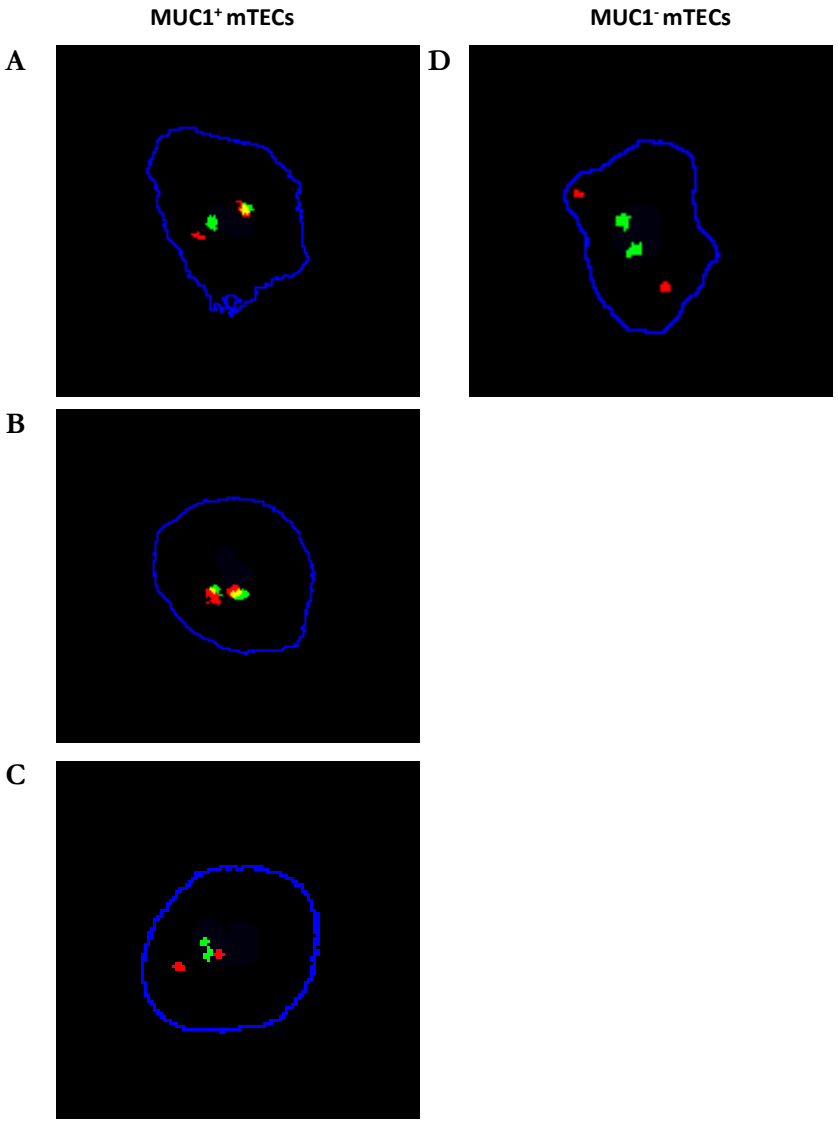

Figure 42

Co-localization studies of alleles of chromosomes 1 and 19 in MUC1$^+$ and MUC1$^-$ mTECs of individual 106

MUC1$^+$ mTECs of individual 106 showed mono-allelic co-localization (A), bi-allelic co-localization (B) and asymmetric mono- and bi-allelic co-localization (C), maximum projection across slices 9 to 11 was performed, as the other allele lies in a different confocal plane (C). There was no co-localization in MUC1$^-$ mTECs of individual 106 (D).

Note: Additional information on data bases of microarray analysis and gene cluster distribution is available on request.

4. Discussion

In view of the essential role of pGE by mTEC in central tolerance induction, we addressed the issues of defining the scope, regulation and evolutionary conservation of pGE. The precise genomic organization of the promiscuously expressed gene pool in mouse, rat and human was defined at the population level. Since, the complete representation at the population level is an additive result of the expression pattern in single mTECs, expression and co-regulation was also addressed at the single-cell level. Here we show that pGE is highly conserved between species, clustered in the genome at the population level and is governed by certain co-expression rules at the single cell level.

4.1. Evolutionary conservation of pGE

In order to define the scope and extent of pGE we focused on genes which are up-regulated upon maturation of mTECs. A comparative global gene expression was performed on the different differentiation stages of mTECs (immature, $MHCII^{lo}$ and mature, $MHCII^{hi}$ mTECs), thus restricting our study to one cell-lineage. We could have opted for the separation of complete mTECs from cTECs in order to gain an insight into the above queries. Since they represent two distinct lineages, it would have been however difficult to delineate the gene pools of promiscuously expressed from lineage-specific genes. Hence, we decided to study gene expression within the mTEC cell-lineage. Our analysis further extended to a species comparison between mouse, rat and human in order to assess evolutionary conservation of pGE. The mTEC population was separated on the basis of EpCAM and further distinguished into its lineage-specific differentiation stages on the basis of MHCII levels. Moreover, although the cTEC markers stained exclusively TECs in the cortex in histology, it is unclear whether they represent the same molecule in the studied species (i.e. His38 for rat (Kampinga *et al.*, 1987), CDR1 (Ly51) for mouse and CDR2 for human (Rouse *et al.*, 1988)).

Keeping in mind the importance of pGE in tolerizing T-cells towards self-antigens, one would expect the phenomenon of pGE to be evolutionary conserved and to date back to early vertebrates, though this prediction has yet to be tested. An ortholog of Aire, serving as a molecular tracer of pGE has been identified in zebrafish. It shows a remarkable resemblance to AIRE in man and its predominant intra-thymic expression suggests that pGE dates back to 400 million years (Saltis *et al.*, 2008). Here for the first time a side by side comparison of pGE between three species, mouse, rat and man was performed. A comparative analysis of gene expression at a global level between immature and mature mTECs in mouse, rat and human revealed a similar extent of pGE between the species, i.e., in terms of number of differentially expressed genes (Table 3.1). There is a methodological limitation to these results in that

microarray data under-estimate the true expression level due to low sensitivity. The use of a more sensitive semi-qualitative PCR on a particular gene locus (cluster 13 on mouse chromosome 13, Figure 23) gave a more sensitive insight into the extent of pGE, as more genes scored as positive. The PCR data was in concordance with those obtained by Derbinski *et al.* on the casein gene locus, which showed contiguous expression without a well defined boundary (Derbinski *et al.*, 2005). Extrapolating from this analysis, we estimate at least ~10 % of all known genes to be turned on in mTECs in addition to differentiation-dependent genes. The bulk of the promiscuously expressed genes is turned on only in the MHCII^{hi} mTECs, which strongly supports the "terminal differentiation model" and is in concordance with previous data in mice from our group (Derbinski *et al.*, 2005). This estimation of the scope of pGE needs to be reassessed by Deep Sequencing technology. Nonetheless, in spite of these limitations which apply for all the species we studied, the data demonstrate a high degree of conservation of pGE.

While studying pGE in rats for the first time we observed that a fairly large proportion (~65-75 %) of regulated genes followed the same regulation pattern in rats and mice (Table 3.4). A slightly lower TRA enrichment of ~40 % was observed in mature rat mTECs than in mouse (~50 %, Figures 22 and 25). This highlights the fact that the percentage of TRA content in mTECs is highly significant and far above the background of 10.8 % in the genome. Additionally a similar degree of TRA clustering (highly significant) was observed in all three species (Figure 19). These findings corroborate the notion of an evolutionary conservation of pGE. The comparison of pGE could not be further extended to man, as the inter-individual differences of the promiscuously expressed gene pool were too large and could not consolidate into a common signature (Table 3.5).

4.2. TRAs cluster genome-wide and project onto the thymus

The TRAs that we defined using robust computational methods tend to co-localize in clusters in the genome. A highly significant similar degree of clustering was observed in all three species (Figure 19). For the first time we directly link two features of pGE, i.e. enrichment for TRAs and clustering (Figure 15). Preferential chromosomal clustering has been reported for genes co-expressed in certain cell lineages and serving a common function i.e. muscle or red blood cell development (Wang *et al.*, 2001; Ramalho-Santos *et al.*, 2002; Hurst *et al.*, 2004). Clustering of co-regulated genes is frequent in eukaryotic genomes (Hurst *et al.*, 2004). In the simplest of cases, gene clusters are formed by gene duplication (Lercher *et al.*, 2003; Hurst *et al.*, 2004). In other cases, clusters of genes exist that participate in the same pathways or encoding organelle-related proteins or operons i.e. functionally related genes (Lefai *et al.*, 2000; Boutanaev *et al.*, 2002; Spellman and Rubin, 2002; Teichmann and Veitia, 2004). Here, we observed that TRAs are clustered irrespective of their structurally relatedness, tissue-specific expression patterns or

putative antigenic properties (Figure 21). Gene order in these clusters in mouse and man was mostly conserved and present in syntenic regions on the same or on different chromosomes (Figure 20). Previous reports show that clusters of both housekeeping genes and co-expressed genes are conserved in both mouse and human genomes by natural selection (Singer *et al.*, 2005; Sémon and Duret, 2006). This lends support to the hypothesis that these clusters have regulatory advantages: the same enhancers or locus control regions are shared and ensure coordinated expression in single cells. These types of genes play a fundamental role in the operation of every eukaryotic cell, and thus, if there is any benefit to arranging co-expressed genes together in the genome, housekeeping genes will likely be subject to the strongest selection to form such clusters. However, the reason for having an evolutionary conservation of clusters of structurally unrelated TRAs in the genome still poses the question of its selective benefit. Knowing that the arrangement of genes in the mammalian genome is non-random, a somewhat far-fetched speculation could be that gene-order has been influenced by pGE, in order to facilitate the preferential expression of TRAs in one cell-type of the thymus. This would reflect the co-evolution of TRA clustering and pGE.

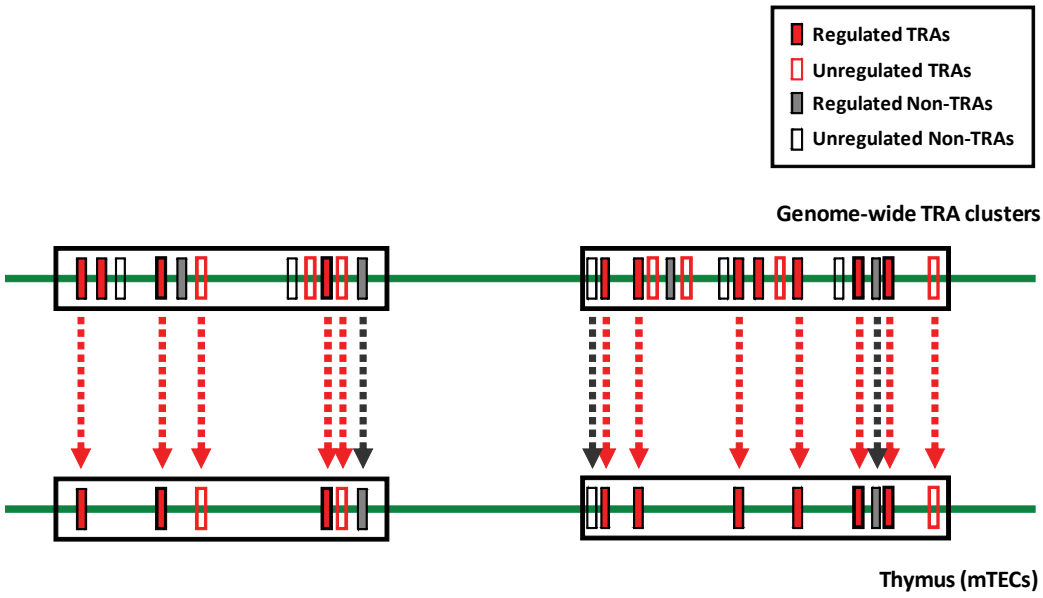

Figure 43

Projection of pGE in the thymus onto pre-existing genome-wide TRA clusters

TRAs are clustered in the genome. Within each cluster TRAs are intermingled with non-TRAs and it was rather rare that a cluster comprised purely TRAs.

In the thymus, the genomic TRA clusters are: 1) only partially represented (~10 %) in mTECs and enriched for TRAs in the projection onto the thymus

We propose the cluster to be the "operational genomic unit" of pGE in the thymus.

Taken together, our results show that TRAs *per se* are clustered in the genome in all three species irrespective of structural relatedness or apparent antigenic properties. In the thymus, promiscuously expressed genes are enriched in TRAs that are partitioned into clusters, again conserved between species. TRA and non-TRAs are harbored within individual clusters, with TRAs being preferentially regulated during mTEC differentiation. Moreover, genes within a particular gene cluster are subject to partial co-regulation (for e.g. human CEA gene family on chromosome 19). Based on these data, we propose these clusters to be the "operational genomic unit" of pGE in the thymus (Figure 43).

4.3. Aire's action: cluster-wide or gene-specific?

The transcriptional regulator Aire is known to regulate the expression of hundreds to thousands of promiscuously expressed genes, with a predilection for TRAs (Anderson *et al.*, 2002; Derbinski *et al.*, 2005; Johnnidis *et al.*, 2005). We show in mouse that $MHCII^{hi}$ mTECs express a large number of Aire-dependent and -independent genes, while in the $MHCII^{lo}$ mTECs the genes are Aire-independent. The $MHCII^{hi}$ are enriched for TRAs (53 % of Aire-dependent genes are TRAs; 48 % of Aire-independent genes are TRAs) and $MHCII^{lo}$ mTECs have a much lower absolute number of Aire-dependent genes (32 genes) though they have similar percentages of TRAs (50 % of Aire-dependent genes are TRAs; 39 % Aire-independent genes are TRAs) (Table 3.3 and Figure 22). From our data, it appears that the maturation stage i.e. $MHCII^{hi}$ mTECs and not Aire per se has an effect on both number and fraction of TRAs. The unabated expression of a sizable number of genes, especially TRAs (48 %) in the absence of Aire could explain the relatively mild autoimmune phenotype in $Aire^{-/-}$ mice. Within the clusters Aire-dependent and -independent genes were interspersed among each other and subjected to differential regulation. In several cases, such as the cluster 13 on chromosome 13 (Figure 23), an Aire-dependent TRA was directly adjacent to an Aire-independent TRA, as also observed in the casein cluster by others (Derbinski *et al.*, 2005; Johnnidis *et al.*, 2005). These results indicated that the impact of Aire was much more punctuate within the chromosomal stretches, often affecting only two or three genes while leaving neighboring and interspersed genes unaffected. Thus, it does not seem likely that this protein's influence can only be explained by locus-wide epigenetic alterations. Instead it has been recently shown that more complex mechanisms involving chromatin binding/structure, transcription and pre-mRNA processing come into play (Abramson *et al.*, 2010). By this model, Aire may still work in a gene-specific manner. The above data reflect the scenario at the population level. However, in single mTECs Derbinski *et al.* pointed out that although the expression of Aire-dependent genes was restricted to $Aire^{+}$ mTECs, majority of the Aire-dependent genes were not preferentially co-expressed in a single mTEC. Thus, suggesting that Aire is necessary but not sufficient for expression of a particular Aire-dependent gene (Derbinski *et al.*, 2008).

4.4. Highly variable promiscuously expressed gene pool in human thymus

The study of pGE between immature and mature mTECs from 11 human thymi showed substantial variation in the number of differentially expressed genes (~700-6000 genes) irrespective of the isolation method used. The extent of variability was so profound, that only 24 genes were common between all patients (Table 3.5).

This is the first time that such a striking inter-individual difference in pGE was found, though Taubert *et al.* also reported considerable quantitative variability in the expression of several target auto-antigen in mTECs (Taubert *et al.*, 2007). Possible parameters causing these variations could be: 1) (epi) genetic differences and non-genetic influences between the individuals; 2) short-term temporal fluctuations (e.g. circadian rhythms). Such variations in vivo at the single-cell level cannot be excluded. It is worth noting that clock genes steering circadian rhythms do not seem to be active in the thymus and testis (incidentally also displaying pGE) (Alvarez and Sehgal, 2005). All samples were collected around the same daily time, between 9 a.m.-11 a.m.; 3) one also cannot exclude that the particular anatomical region of the thymus removed during surgery could add to the variations. Gene expression and the proportion of $Aire^{+}$ cells could vary with the region of the thymus (for instance, outer versus deeper medulla) and disease status; 4) moreover, the pre-medication history of these individuals could be a further influence. The administration of immunosuppressants or high dosages of other drugs can induce immunosuppressive stress responses (Dhabhar *et al.*, 1994; Pruett *et al.*, 1999; Pruett *et al.*, 2000). Immunosuppressants have been shown in mice to cause extensive loss of tolerance-inducing $Aire^{+}$ mature mTECs (Fletcher *et al.*, 2009), which could also explain the high variability of mTEC subset composition observed in our human dataset.

The most likely reason for the highly variable promiscuous gene pool in human is the difference in mTEC subset composition. We used a four color sort to separate the lower and upper 30 % of $MHCII^{lo}$ and $MHCII^{hi}$ expressing mTEC stages and noticed a highly variable MHCII mTEC profile between individuals which was not the case in mouse and rat. Not only did it differ in the absolute fluorescence values, but also a shift in profile i.e. monophasic or biphasic was observed. These inter-individual profiles most likely relate to differences in the promiscuously expressed gene pool, which could not consolidate into a common set of differentially expressed genes (Table 3.5) in contrast to mouse and rat. Even though a standard criterion i.e. the upper and lower one-third MHCII was used to separate the immature and mature mTECs, it obviously did not result in a reproducible separation of comparable mTEC subsets in humans. AIRE is up-regulated along with mTEC differentiation and the ratio of AIRE in $MHCII^{hi}$ vs. $MHCII^{lo}$ mTECs can be considered as a measure for the degree of enrichment of the individual samples. Since AIRE is the driving force for about half of the promiscuously expressed genes in the mature mTEC population, the correlation between the number of differentially expressed genes

(between immature and mature mTECs) and fold change in AIRE expression was determined. We observed a correlation between the number of differentially expressed genes and fold change in AIRE expression (correlation coefficient, r = 0.5, Figure 26). Thus, AIRE could serve as a surrogate marker for the quality of cell separation. AIRE being a transcription factor requires fixing cells for intra-cellular staining after which it is not feasible to use these cells for down-stream applications. Hence, due to the lack of available markers, the distinction of immature and mature mTEC subsets in humans based on MHCII is the best that can be performed at present. Incidentally similar inter-individual differences were observed when genome-wide methylation patterns and miRNA level were assayed. Thus, immature and mature mTECs isolated from one patient were more closely related to each other than to the respective cell types isolated from a different patient. Thus, the signature in mTECs typifies the individual rather than the cell type (L. Tykocinski, unpublished). In contrast, thymocytes from the same individual were far less variable in the same assays. Thus, these variations appear to be a peculiarity of mTECs (L. Tykocinski, unpublished) and the differences observed when using different parameters to study various aspects of pGE in humans are biased by the heterogeneity of the samples. MTECs may be highly responsive to stress or other cytotoxic factors.

The observed variations in antigen expression are likely to influence T-cell repertoire selection and thus tolerance thresholds in human provided they reflect steady state values. Note that in genetic disorders like myasthenia gravis differences in the magnitude of 4-fold correlate with disease onset in the human population (Taubert *et al.*, 2007). According to the "threshold model of central tolerance" the degree of central tolerance towards a TRA is surprisingly sensitive to minor shifts in thymic antigen expression levels (Liston *et al.*, 2005; Taubert *et al.*, 2007). This could result in a shift in the threshold of self-tolerance to an extent that translates into significant alterations of disease susceptibility. In transgenic mice with defined copy numbers of intra-thymically expressed autoantigens, subtle differences in expression levels (two- to four- fold) can be sufficient to significantly modulate susceptibility or be the cause of autoimmunity (Chentoufi and Polychronakos, 2002; Miyamoto *et al.*, 2003). A similar threshold range seems to matter for self-antigens in humans as well.

No common signature was observed in human while separating immature and mature mTEC based on MHCII. However, when sorting for a defined mTEC population expressing a particular antigen i.e. MUC1, the inter-individual differences were greatly reduced. A high degree of over-lap ~46-54 % was observed (Figure 35). Narrowing down onto a more restricted mTEC subpopulation merges pGE signatures, thus emphasizing the heterogeneity of the human mTEC population (discussed in detail in later chapters).

4.5. Lack of antigen expression in the thymus subverts central tolerance

The mature mTEC subset shows a broad representation of pGE, though the upper threshold of this expression still remains ill defined. There exist examples in which missing expression of certain antigens in the thymus correlates with the existence of auto-antibodies and a break-down of central tolerance for these particular antigens (Chentoufi and Polychronakos, 2002; Gotter *et al.*, 2004). Some prominent examples are GAD65 and MYH6, both of which are involved in autoimmune diseases, i.e. insulin-dependent diabetes (IDD) (Tisch, 1996; Yoon *et al.*, 2000; Lernmark, 2002) and myocarditis, respectively (Wolfgram *et al.*, 1985; Neu *et al.*, 1987; Rose, 2000). Their expression is absent in the thymus and is predominant in the respective peripheral tissue. In both cases their homologous counter-parts i.e. GAD67 and MYH7 show the inverse expression pattern i.e. are well expressed in mTECs and at low levels in peripheral tissue (Figures 29 and 31). It was noted that the two GAD isoforms are located in the same chromosomal context in human and mouse (Figures 27 and 28), GAD67 is expressed in mTECs in both species while GAD65 is absent in human and expressed at basal levels in mouse (Derbinski, J, unpublished). The MYH6 and MYH7 isoforms are immediately adjacent to each other and present in syntenic regions in mouse and human (Figure 30). This lack of expression obviously represents one "pitfall" of pGE. It is possible that the non-expressed isoform is embedded in a silent chromosomal context i.e. "regions of closed chromatin". We started to investigate this supposition by studying the thymic expression of the flaking regions of the GAD gene loci. The lack of expression of GAD65 may indeed be related to the low overall transcriptional activity 3' of GAD65 (Figure 29). Similar studies have to be extended to the MYH gene locus.

Future work will probe into the plausible reasons for this differential expression of the different isoforms which could be: 1) structural constraints/restrictions exist that block pGE by affecting either the access or the DNA binding of transcription (co)factors? 2) the lack of expression in mTECs might safe-guard the mTECs, as expression of these antigens could be toxic? The two examples (GAD65 and MYH6) show that expression of the entire antigen can be lacking in the thymus. In the case of PLP this is only true for a particular exon. In the case of MBP, the fetal form of golli-MBP which is expressed in mTECs differs from the peripherally expressed adult classic-MBP in its transcriptional start site. Thus, non-censored T-cells specific for epitopes encoded only by the full-length form of PLP or classic MBP, respectively, can escape thymic selection, which again might predispose to autoimmunity (Klein *et al.*, 2000; Kyewski and Klein, 2006).

4.6. Co-regulated gene expression in single mTECs

Previous studies showed that a given individual gene is expressed in only few ~1-3 % mTECs (Derbinski *et al.*, 2001; Cloosen *et al.*, 2007; Taubert *et al.*, 2007). Moreover, an apparent stochastic gene expression pattern of the casein gene cluster as well as other genes was observed at the single cell level (Derbinski *et al.*, 2008; Villasenor *et al.*, 2008). Yet, initial hints for the existence of co-regulated rather than stochastic gene expression patterns came from population studies by J. Arnold (Arnold, 2006; Cloosen *et al.*, 2007), where two tumor-associated differentiation antigens, MUC1 and CEA were co-expressed far above the expected expression frequency based on each antigen alone in the same mTEC. Hence, we wanted to more precisely define these co-expression patterns and the underlying mechanisms.

The antigen pool expressed in mTECs, also includes tumor-associated antigens (i.e. cancer germ cell antigens) previously thought to be secluded from the immune system (Gotter *et al.*, 2004; Cloosen *et al.*, 2007). The feasibility of isolating mTECs expressing a particular antigen had been demonstrated by J. Arnold using antibodies to surface expressed antigens, mucin-1 (MUC1) (Arnold, 2006). We further extended this approach to our studies, isolating $MUC1^+$ and $MUC1^-$ mTECs from human thymus. The initial observations by J. Arnold were confirmed not only at the population level using real-time PCR and genome-wide microarrays, but also by single cell studies of $MUC1^+$ mTECs. The results obtained from all three methodological approaches were highly concordant revealing co-expression of MUC1 with MUC4, CEACAM5 and CEACAM6 (Figures 34, 36 and 37). MUC1 is located on Chromosome 1 while MUC4 is on Chromosome 4 and CEACAM5 and CEACAM6 are on Chromosome 19, thus co-expression groups in single cells not only defined intra-chromosomal but also inter-chromosomal gene co-regulation. The CEA family gene cluster however was not completely co-expressed (Figure 34 and Table 3.6). For the first time we show that neighboring genes within a particular gene cluster (i.e. CEACAM5 and CEACAM6) are consistently co-expressed in single mTECs which was not observed by Derbinski *et al.* when studying the casein gene cluster (Derbinski *et al.*, 2008).

We showed that pGE is highly conserved between the species, however in human the promiscuously expressed gene pool varied considerably. Yet, sorting for a restricted mTEC subpopulation i.e. $MUC1^+$ mTECs, a high degree of over-lap ~46-54 % was observed (Figure 35). Thus, narrowing down onto a restricted mTEC subpopulation merges the pGE signature again attesting to be the heterogeneity of the human mTEC population.

The single cell data reveal a deterministic component in the regulation of pGE. The co-expression frequencies of the analyzed gene pool were much higher in $MUC1^+$ mTECs (30-82 %) than expected on a random base in total mTECs (3-13 %) or $MUC1^-$ mTECs (0-11 %)

(Figures 36, 37 and 38), showing a high degree of concordance (Table 3.8). The observed co-expression patterns in $MUC1^+$ mTECs are not mimicked in other normal peripheral epithelial derived cells (Zotter *et al.*, 1998; Hammarstrom, 1999; Scholzel *et al.*, 2000). The co-expression patterns appear to be due to pGE rather than due to progressive differentiation of mTECs. Note that MUC1 and CEA are epithelial antigens. Being tumor antigens one would expect the MUC and CEA families to be expressed in malignant tissues, though this extended co-expression pattern as observed in mTECs has never been reported. Only selected expression pairs like MUC1-MUC4, CEACAM5-CEACAM6 and MUC1-CEACAM5 have been described to be expressed in malignant tissues either as unaltered or post-translational modified forms (Kinugasa *et al.*, 1998; Hammarstrom, 1999; Scholzel *et al.*, 2000; Rakha *et al.*, 2005). Hence, the co-expression pattern observed in mTECs does not appear to reflect that of peripheral counterpart tissues (Derbinski *et al.*, 2008; Villasenor *et al.*, 2008).

Gotter and co-workers showed that mTEC-over-expressed genes show no preference for any chromosome (Gotter *et al.*, 2004). When selecting for $MUC1^+$ mTECs, we found over-expressed genes to preferentially co-localize to chromosome 19 (Table 3.7). Strikingly, these co-expression patterns and chromosomal preferences correlated with *in situ* co-localization of the respective chromosomal domains (on chromosomes 1 and 19) upon mTEC maturation as analyzed by fluorescence *in situ* hybridization. For the first time, we document a direct interchromosomal interaction between two gene loci *ex vivo* in mTECs. The functional significance of the interchromosomal association is of great interest. $MUC1^+$ mTECs either show a significant mono-allelic, bi-allelic and asymmetric mono- and bi-allelic co-localization (Figures 40, 41 and 42). This fits with previous observations that pGE is neither strictly mono- nor bi-allelic and thus is distinct from known patterns of strict allele-specific gene expression as observed in peripheral tissues (Derbinski *et al.*, 2008; Villasenor *et al.*, 2008; Sinemus, 2009). The interchromosomal associations described here may be a more general phenomenon of pGE occurring at multiple genetic loci where coordinate regulation occurs.

Although the functional significance of association of co-regulated gene loci is still unclear, direct physical interactions between chromosomes are known to have regulatory functions as described in the case of T-cell differentiation. This has recently been established by the analysis of the Ifnγ and T_H2 cytokine loci in naive T cells (Spilianakis *et al.*, 2005). After antigen stimulation, the naive T_H cells develop into either T_H1 cells, which produce one set of effector molecules (i.e. interferon (IFN)-γ), or T_H2 cells, which produce a different set (i.e. interleukin (IL)-4, -5). In order to investigate what determines the fate of the naive T_H cells, the authors explored the organization of two genomic regions: the gene encoding IFN-γ (called *Ifng,* chromosome 10) and a multi-gene complex encoding IL-4 and IL-5 (*Il4* and *Il5,* chromosome 11). Using the chromosome conformation capture (3C) method and FISH, they found *Ifng* seems to be regulated by elements found near it on chromosome 10, whereas expression of *Il4* and *Il5* on chromosome 11 seems to

be regulated by a 'locus control region' (LCR) on the same chromosome. They observed inter-chromosomal interactions between the promoter region of the IFN- γ gene and the LCR of the T_H2 cytokine locus in naive bipotent T_H cells which are poised for transcription. Upon receiving an appropriate stimulus, one gene locus is activated (for example *Ifng* after a T_H1 stimulus), whereas the counterpart locus that is to remain silent (in this case the T_H2 genes) moves apart, presumably to a region of the nucleus, which is not transcriptionally active. So, at the time point of the association of the two loci, the T_H cells have the choice to select either signature. In contrast, in mTECs co-localization goes along with co-expression.

Similarly, in sensory neurons only a single olfactory receptor (OR) gene from a very large super-family (1300 genes in mouse), which is organized in multiple clusters, is selected for expression in individual olfactory neurons. Different choices are made in different neurons, such that the whole repertoire is deployed in the olfactory epithelium. It poses the question, how is the OR gene choice made? Lomvardas and colleagues showed that an odorant receptor gene on one chromosome is selected for expression by physical association of an odorant receptor- regulatory element (the H enhancer) on chromosome 14. Therefore, this work supports the hypothesis that a single element may drive the expression of all the OR genes in the genome by inter-chromosomal co-regulation (Lomvardas *et al.*, 2006).

Another remarkable finding was the initiation of X-chromosome inactivation (XCI) that involves 'counting' of the X chromosomes to ensure that only one X remains active per autosome set, and a random 'choice' as to which chromosome to inactivate. The molecular mechanisms underlying this remained one of the most challenging enigmas. Two studies, from Bacher *et al.* and Xu *et al.* showed that at the onset of XCI, and concomitant with the timing of counting and choice, the two X-chromosomes of female cells transiently come into close proximity with each other. The initial differential treatment of the two X chromosomes during X-chromosome inactivation is controlled by the X-inactivation centre (*Xic*). Critical control sequences in the *Xic* include the non-coding RNAs *Xist* and *Tsix*, and long-range chromatin elements (Bacher *et al.*, 2006; Xu *et al.*, 2006).

In each case the question still remains, what are the mechanisms that bring about the functional interactions between regulatory elements on the one hand and target genes on the other hand that are located on different chromosomes? Why do mTECs show co-regulation and co-localization of chromosomes? It is known that eukaryotic chromosomes occupy distinct territories in the cell nucleus. These territories intermingle little with each other. Contacts between different chromosomal loci, is called chromosome kissing. Chromosome kissing is not only restricted to vertebrate, but also found in Drosophila, plants and yeast, suggesting that this is a fundamental feature of nuclear organization that may contribute to either coordinate gene silencing or activation. Genes being actively expressed loop out from their condensed chromatin

territory and localize to a region of transcriptional activity, associated with "transcription factories" that are enriched in RNA polymerase II - in order to be efficiently transcribed. Owing to the limited number of factories, many genes share the same factory (Branco and Pombo, 2006; Branco and Pombo, 2007; Cavalli, 2007; Lanctôt *et al.*, 2007). The unentangled chromatin conformation along with nuclear actin and myosin provide molecular motors that drive gene mobility and direct movement towards a target region in the nucleus (Chuang *et al.*, 2006; Dundr *et al.*, 2007; Lieberman-Aiden *et al.*, 2009). From the initial results, we hypothesis that these two chromosomes i.e. chromosomes 1 and 19 tend to co-localize in MUC1$^+$ mTECs probably in a region of active transcription in the nucleus resulting in co-expression pattern seen at the population and single cell level (Figure 44). Obviously, many questions remain to be answered: Do other chromosome pairs also preferentially co-localize? What factors regulate these interactions? If we inversely sorted mTECs expressing an antigen on chromosome 19 would we select now for genes on chromosomes 1?

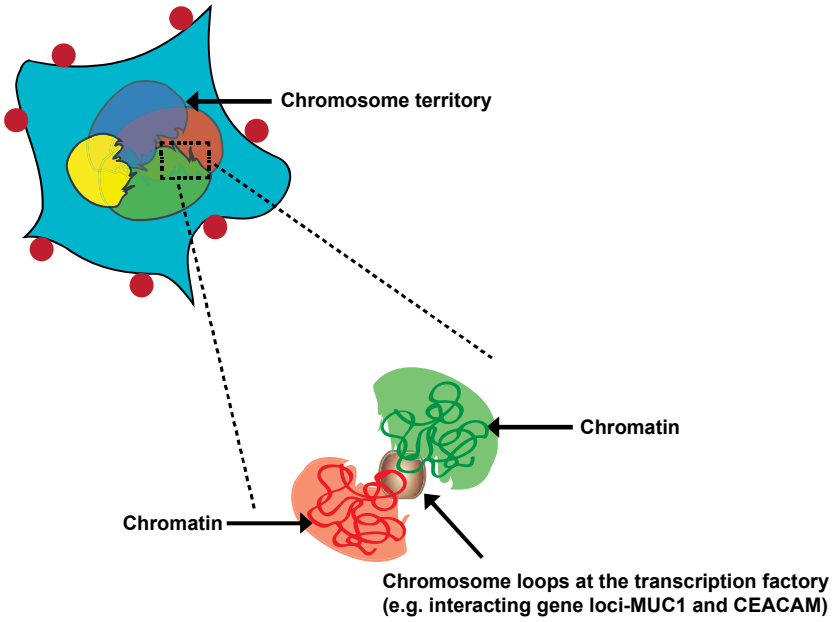

Figure 44

Schematic interpretation of FISH studies in MUC1$^+$ mTECs

FISH studies show an inter-chromosomal association possibly at transcription factories (Chromosome 1-MUC1 and Chromosome 19-CEACAM) leading to the co-regulation and co-expression patterns observed at the population and single cell level in MUC1$^+$ mTECs.

4.7. Analysis of mTECs reveal partially overlapping co-expression groups

From our population and single cell studies we observed co-expression of CEACAM5, CEACAM6 and MUC4 along with MUC1 in MUC1$^+$ mTECs (Figure 45A). J. Arnold, when selecting for CEACAM5$^+$ mTECs observed co-expression not only of MUC1, CEACAM5, and CEACAM6 but also of CEACAM3 (Figure 45B) (Arnold, 2006). Thus, mTECs isolated for two different but largely co-expressed antigens display overlapping but not identical co-expression groups. It appears that there exists a sliding pattern, that when sorting for MUC1$^+$ or CEACAM5$^+$ mTECs an over-lapping gene set but also a "new" set i.e. CEACAM3 in CEACAM5$^+$ mTECs is found. Selecting CEACAM3$^+$ mTECs might enrich for yet another partially overlapping gene pool. Conceivably as one slides along these group one may ultimately end up with a complete distinct expression pattern compared to the initial one (Figure 45C and 45D). Hence, it appears that selecting for a given gene also selects a distinct co-expression group. The genealogy of each of these co-expression groups is unknown. Does for instance MUC1 expression drive the subsequent expression of its co-expression partners, or are all genes concomitantly expressed? (Figure 46)

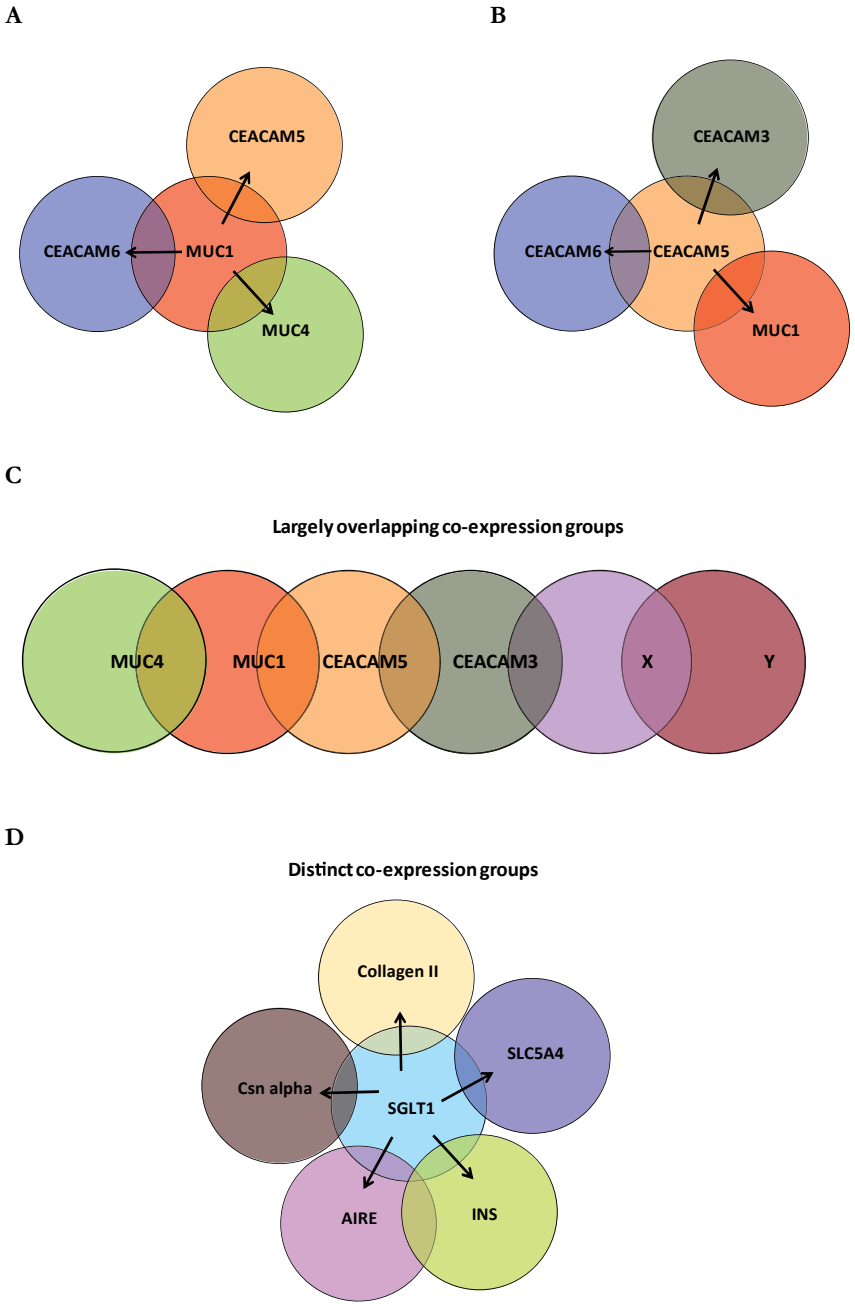

Figure 45

Schematic representation of co-expression groups in mTECs

(A) Co-expression group of sorted MUC1$^+$ mTECs.

(B) Co-expression group of sorted CEACAM5$^+$ mTECs as described by J. Arnold (Arnold, 2006). Both subsets reveal over-lapping and non-overlapping genes (e.g. CEACAM3)

(C) Model of sliding co-expression patterns in mTECs.

(D) An example of an unrelated co-expression group encomposing presumably Aire-dependent genes from J. Arnold (Arnold, 2006).

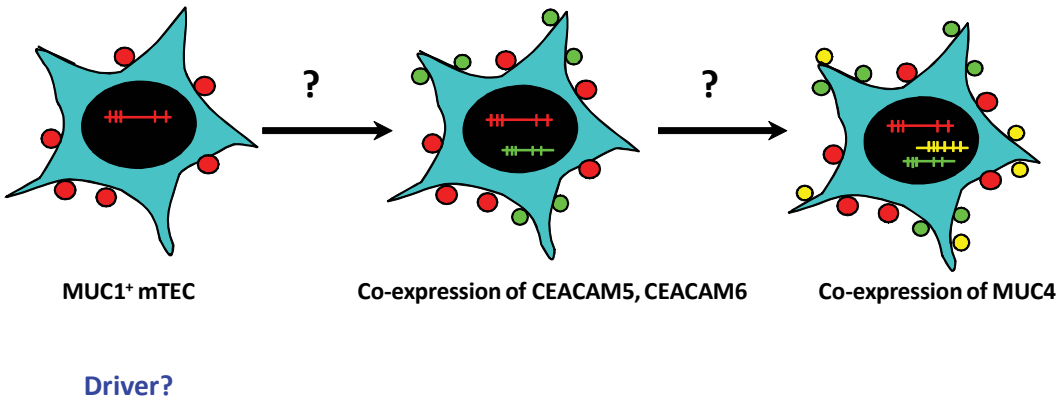

Figure 46

Possible genealogy of co-expression patterns

It is unknown what drives co-expression groups. Does initial MUC1 expression drive the subsequent expression of its co-expressed partners, or are all genes concomitantly expressed?

Previous work showed that an individual gene is expressed in only few ~1-3 % mTECs (Derbinski *et al.*, 2001; Cloosen *et al.*, 2007; Taubert *et al.*, 2007). Moreover an apparent stochastic gene expression was observed at the single cell level (Derbinski *et al.*, 2008; Villasenor *et al.*, 2008). For the first time our results highlight a new aspect of pGE that is a regulated, non-random component. What is the selective advantage of a single mTEC having such co-regulated co-expression patterns? At face value it is not apparent why a single mTEC should co-express genes from particular chromosomes (for example chromosomes 1 and 19). Co-expression patterns may be an economical way of preventing the same genes being redundantly expressed by other mTECs as would be expected, if pGE was entirely random. Having partially over-lapping co-expression patterns however makes the mechanism of pGE full-proof, thus safeguarding the completeness of the antigen repertoire. Thus, the sets of promiscuously expressed genes in single mTECs ultimately add up to a complete representation of the entire gene pool at the population level. Interestingly, despite dynamic mTEC renewal, the spectrum of expressed self-antigens in the mTEC population remains unchanged at the population level. Thus, at any time incoming thymocytes entering the medulla will encounter the full spectrum of promiscuously expressed genes, despite continuous *de novo* generation and possibly *in situ* redistribution of antigen display by mTECs.

4.8. Conclusions and future perspectives

The regulatory mechanisms governing pGE in mTECs still remain poorly understood. This study adds new perspectives to this issue.

1. The phenomenon of pGE is highly conserved between species and maps to gene clusters. We propose these clusters to be the "operational genomic unit" of pGE in the thymus.
2. PGE is characterized by certain intra- and inter-chromosomal co-expression patterns at the single cell level.

Future experiments need to:

1. More precisely delineate the complete extent of pGE in mouse, rat and human by new sequencing techniques.
2. Decipher the molecular explanation of "holes" in the thymic antigen repertoire.
3. Dissect the co-expression patterns, co-regulation rules and underlying mechanisms governing pGE and explore the functional implications of this phenomenon.

5. References

Abramson, J., Giraud, M., Benoist, C., and Mathis, D. (2010). Aire's partners in the molecular control of immunological tolerance. Cell *140*, 123-135.

Akiyama, T., Maeda, S., Yamane, S., Ogino, K., Kasai, M., Kajiura, F., Matsumoto, M., and Inoue, J. (2005). Dependence of self-tolerance on TRAF6-directed development of thymic stroma. Science *308*, 248-251.

Akiyama, T., Shimo, Y., Yanai, H., Qin, J., Ohshima, D., Maruyama, Y., Asaumi, Y., Kitazawa, J., Takayanagi, H., Penninger, J. M.*, et al.* (2008). The Tumor Necrosis Factor Family Receptors RANK and CD40 Cooperatively Establish the Thymic Medullary Microenvironment and Self-Tolerance. Immunity *29*, 423-437.

Alitheen, N. B., McClure, S., and McCullagh, P. (2010). B-cell development: one problem, multiple solutions. Immunology and Cell Biology 1-6.

Alvarez, J. D., and Sehgal, A. (2005). The thymus is similar to the testis in its pattern of circadian clock gene expression. J Biol Rhythms *20*, 111-121.

Anderson, G., and Jenkinson, E. (2001). Lymphostromal interactions in thymic development and function. Nat Rev Immunol *1*, 31–40.

Anderson, G., Lane, P. J., and Jenkinson, E. J. (2007). Generating intrathymic microenvironments to establish T-cell tolerance. Nat Rev Immunol *7*, 954-963.

Anderson, M. S., Venanzi, E. S., Klein, L., Chen, Z., Berzins, S. P., Turley, S. J., von Boehmer, H., Bronson, R., Dierich, A., Benoist, C., and Mathis, D. (2002). Projection of an immunological self shadow within the thymus by the aire protein. Science *298*, 1395-1401.

Arnold, J. (2006). Regulation ektopischer genexpression im thymus-mikroenvironment: vom medulla kompartiment zur einzelzellebene. Doctoral Thesis.

Asano, M., Toda, M., Sakaguchi, N., and Sakaguchi, S. (1996). Autoimmune disease as a consequence of developmental abnormality of a T cell subpopulation. J Exp Med *184*, 387-396.

Aschenbrenner, K., D'Cruz, L. M., Vollmann, E. H., Hinterberger, M., Emmerich, J., Swee, L. K., Rolink, A., and Klein, L. (2007). Selection of Foxp3+ regulatory T cells specific for self antigen expressed and presented by Aire+ medullary thymic epithelial cells. Nat Immunol *8*, 351-358.

Avichezer, D., Grajewski, R. S., Chan, C. C., Mattapallil, M. J., Silver, P. B., Raber, J. A., Liou, G. I., Wiggert, B., Lewis, G. M., Donoso, L. A., and Caspi, R. R. (2003). An immunologically privileged retinal antigen elicits tolerance: major role for central selection mechanisms. J Exp Med *198*, 1665-1676.

Bacher, C. P., Guggiari, M., Brors, B., Augui, S., Clerc, P., Avner, P., Eils, R., and Heard, E. (2006). Transient colocalization of X-inactivation centres accompanies the initiation of X inactivation. Nat Cell Biol *8*, 293-299.

Baldwin, T. A., Hogquist, K. A., and Jameson, S. C. (2004). The fourth way? Harnessing aggressive tendencies in the thymus. J Immunol *173*, 6515-6520.

Bennett, A. R., Farley, A., Blair, N. F., Gordon, J., Sharp, L., and Blackburn, C. C. (2002). Identification and characterization of thymic epithelial progenitor cells. Immunity *16*, 803-814.

Bensinger, S. J., Bandeira, A., Jordan, M. S., Caton, A. J., and Laufer, T. M. (2001). Major histocompatibility complex class II-positive cortical epithelium mediates the selection of CD4(+)25(+) immunoregulatory T cells. J Exp Med *194*, 427-438.

Benz, C., Heinzel, K., and Bleul, C. C. (2004). Homing of immature thymocytes to the subcapsular microenvironment within the thymus is not an absolute requirement for T cell development. Eur J Immunol *34*, 3652–3663.

Benz, C., Martins, V. C., Radtke, F., and Bleul, C. C. (2008). The stream of precursors that colonizes the thymus proceeds selectively through the early T lineage precursor stage of T cell development. J Exp Med *205*, 1187–1199.

Bleul, C. C., Corbeaux, T., Reuter, A., Fisch, P., Monting, J. S., and Boehm, T. (2006). Formation of a functional thymus initiated by a postnatal epithelial progenitor cell. Nature *441*, 992-996.

Boehm, T., Scheu, S., Pfeffer, K., and Bleul, C. C. (2003). Thymic medullary epithelial cell differentiation, thymocyte emigration, and the control of autoimmunity require lympho-epithelial cross talk via LTbetaR. J Exp Med *198*, 757-769.

Bouillet, P., Purton, J. F., Godfrey, D. I., Zhang, L. C., Coultas, L., Puthalakath, H., Pellegrini, M., Cory, S., Adams, J. M., and Strasser, A. (2002). BH3-only Bcl-2 family member Bim is required for apoptosis of autoreactive thymocytes. Nature *415*, 922-926.

Bousso, P., Bhakta, N. R., Lewis, R. S., and Robey, E. (2002). Dynamics of thymocyte-stromal cell interactions visualized by two-photon microscopy. Science *296*, 1876-1880.

Boutanaev, A. M., Kalmykova, A. I., Shevelyov, Y. Y., and Nurminsky, D. I. (2002). Large clusters of co-expressed genes in the Drosophila genome. Nature *420*, 666-669.

Boyd, R. L., Tucek, C. L., Godfrey, D. I., Izon, D. J., Wilson, T. J., Davidson, N. J., Bean, A. G., Ladyman, H. M., Ritter, M. A., and Hugo, P. (1993). The thymic microenvironment. Immunol Today *14*, 445-459.

Branco, M. R., and Pombo, A. (2006). Intermingling of chromosome territories in interphase suggests role in translocations and transcription-dependent associations. PLoS Biol *4*, e138

Branco, M. R., and Pombo, A. (2007). Chromosome organization: new facts, new models. Trends Cell Biol *17*, 127-134.

Bruno, R., Sabater, L., Sospedra, M., Ferrer-Francesch, X., Escudero, D., Martinez-Caceres, E., and Pujol-Borrell, R. (2002). Multiple sclerosis candidate autoantigens except myelin oligodendrocyte glycoprotein are transcribed in human thymus. Eur J Immunol *32*, 2737-2747.

Burkly, L., Hession, C., Ogata, L., Reilly, C., Marconi, L. A., Olson, D., Tizard, R., Cate, R., and Lo, D. (1995). Expression of relB is required for the development of thymic medulla and dendritic cells. Nature *373*, 531-536.

Cannon, J. P., Haire, R. N., Rast, J. P., and Litman, G. W. (2004). The phylogenetic origins of the antigen binding receptors and somatic diversification mechanisms. Immunol Rev *200*, 12-22.

Cavalli, G. (2007). Chromosome kissing. Curr Opin Genet Dev *17*, 443-450.

Chen, Z., Benoist, C., and Mathis, D. (2005). How defects in central tolerance impinge on a deficiency in regulatory T cells. PNAS *102*, 14735-14740.

Chentoufi, A. A., Palumbo, M., and Polychronakos, C. (2004). Proinsulin expression by Hassall's corpuscles in the mouse thymus. Diabetes *53*, 354-359.

Chentoufi, A. A., and Polychronakos, C. (2002). Insulin expression levels in the thymus modulate insulin-specific autoreactive T-cell tolerance: the mechanism by which the IDDM2 locus may predispose to diabetes. Diabetes *51*, 1383-1390.

Chin, R. K., Lo, J. C., Kim, O., Blink, S. E., Christiansen, P. A., Peterson, P., Wang, Y., Ware, C., and Fu, Y. X. (2003). Lymphotoxin pathway directs thymic Aire expression. Nat Immunol *4*, 1121-1127.

Chuang, C. H., Carpenter, A. E., Fuchsova, B., Johnson, T., de Lanerolle, P., and Belmont, A. S. (2006). Long-range directional movement of an interphase chromosome site. Curr Biol *16*, 825-831.

Cloosen, S., Arnold, J., Thio, M., Bos, G. M., Kyewski, B., and Germeraad, W. T. (2007). Expression of tumor-associated differentiation antigens, MUC1 glycoforms and CEA, in human thymic epithelial cells: implications for self-tolerance and tumor therapy. Cancer Res *67*, 3919-3926.

Cooper, M. D., and Alder, M. N. (2006). The evolution of adaptive immune systems. Cell *124*, 815-822.

Cooper, M. D., Peterson, R. D., and Good, R. A. (1965). Delineation of the thymic and bursal lymphoid systems in the chicken. Nature *205*, 143-146.

Daniels, M. A., Teixeiro, E., Gill, J., Hausmann, B., Roubaty, D., Holmberg, K., Werlen, G., Hollander, G. A., Gascoigne, N. R., and Palmer, E. (2006). Thymic selection threshold defined by compartmentalization of Ras/MAPK signalling. Nature *444*, 724-729.

Derbinski, J., Gabler, J., Brors, B., Tierling, S., Jonnakuty, S., Hergenhahn, M., Peltonen, L., Walter, J., and Kyewski, B. (2005). Promiscuous gene expression in thymic epithelial cells is regulated at multiple levels. J Exp Med *202*, 33-45.

Derbinski, J., and Kyewski, B. (2005). Linking signalling pathways, thymic stroma integrity and autoimmunity. Trends Immunol *26*, 503-506.

Derbinski, J., Pinto, S., Rösch, S., Hexel, K., and Kyewski, B. (2008). Promiscuous gene expression patterns in single medullary thymic epithelial cells argue for a stochastic mechanism. Proc Natl Acad Sci U S A *105*, 657-662

Derbinski, J., Schulte, A., Kyewski, B., and Klein, L. (2001). Promiscuous gene expression in medullary thymic epithelial cells mirrors the peripheral self. Nat Immunol *2*, 1032-1039.

DeVoss, J., Hou, Y., Johannes, K., Lu, W., Liou, G. I., Rinn, J., Chang, H., Caspi, R. R., Fong, L., and Anderson, M. S. (2006). Spontaneous autoimmunity prevented by thymic expression of a single self-antigen. J Exp Med *203*, 2727-2735.

Dhabhar, F. S., Miller, A. H., Stein, M., McEwen, B. S., and Spencer, R. L. (1994). Diurnal and acute stress-induced changes in distribution of peripheral blood leukocyte subpopulations. Brain Behav Immun *8*, 66-79.

Diez, J., Park, Y., Zeller, M., Brown, D., Garza, D., Ricordi, C., Hutton, J., Eisenbarth, G. S., and Pugliese, A. (2001). Differential splicing of the IA-2 mRNA in pancreas and lymphoid organs as a permissive genetic mechanism for autoimmunity against the IA-2 type 1 diabetes autoantigen. Diabetes *50*, 895-900.

Dooley, J., Erickson, M., and Farr, A. G. (2008). Alterations of the medullary epithelial compartment in the Aire-deficient thymus: implications for programs of thymic epithelial differentiation. J Immunol *181*, 5225-5232.

Du Pasquier, L. (1993). Evolution of the immune system. In Fundamental Immunology, ed W Paul, 221-226.

Dundr, M., Ospina, J. K., Sung, M.-H., John, S., Upender, M., Ried, T., Hager, G. L., and Matera, A. G. (2007). Actin-dependent intranuclear repositioning of an active gene locus in vivo. J Cell Biol *179*, 1095-1103.

Egerton, M., Scollay, R., and Shortman, K. (1990). Kinetics of mature T-cell development in the thymus. Proc Natl Acad Sci USA *87*, 2579–2582.

Egwuagu, C. E., Charukamnoetkanok, P., and Gery, I. (1997). Thymic expression of autoantigens correlates with resistance to autoimmune disease. J Immunol *159*, 3109-3112.

Ehrlich, L. I., Oh, D. Y., Weissman, I. L., and Lewis, R. S. (2009). Differential Contribution of Chemotaxis and Substrate Restriction to Segregation of Immature and Mature Thymocytes. Immunity *31*, 986-998.

Fan, Y., Rudert, W. A., Grupillo, M., He, J., Sisino, G., and Trucco, M. (2009). Thymus-specific deletion of insulin induces autoimmune diabetes. EMBO J *28*, 2812-2824.

Farr, A., Nelson, A., Truex, J., and Hosier, S. (1991). Epithelial heterogeneity in the murine thymus: a cell surface glycoprotein expressed by subcapsular and medullary epithelium. J Histochem Cytochem *39*, 645-653.

Ferguson, B. J., Cooke, A., Peterson, P., and Rich, T. (2008). Death in the AIRE. Trends Immunol *29*, 306-312.

Flajnik, M. F., and Du Pasquier, L. (2004). Evolution of innate and adaptive immunity: Can we draw a line? Trends Immunol *25*, 640–644.

Fletcher, A. L., Lowen, T. E., Sakkal, S., Reiseger, J. J., Hammett, M. V., Seach, N., Scott, H. S., Boyd, R. L., and Chidgey, A. P. (2009). Ablation and regeneration of tolerance-inducing medullary thymic epithelial cells after cyclosporine, cyclophosphamide, and dexamethasone treatment. J Immunol *183*, 823-831.

Fontenot, J. D., Rasmussen, J. P., Williams, L. M., Dooley, J. L., Farr, A. G., and Rudensky, A. Y. (2005). Regulatory T cell lineage specification by the forkhead transcription factor foxp3. Immunity *22*, 329-341.

Fossa, D. L., Donskoya, E., and Goldschneider, I. (2001). The importation of hematogenous precursors by the thymus is a gated phenomenon in normal adult mice. J Exp Med *193*, 365–374.

Gabler, J., Arnold, J., and Kyewski, B. (2007). Promiscuous gene expression and the developmental dynamics of medullary thymic epithelial cells. Eur J Immunol *37*, 3363-3372.

Gallegos, A. M., and Bevan, M. J. (2004). Central tolerance to tissue-specific antigens mediated by direct and indirect antigen presentation. J Exp Med *200*, 1039-1049.

Gardner, J. M., Devoss, J. J., Friedman, R. S., Wong, D. J., Tan, Y. X., Zhou, X., Johannes, K. P., Su, M. A., Chang, H. Y., Krummel, M. F., and Anderson, M. S. (2008). Deletional tolerance mediated by extrathymic Aire-expressing cells. Science *321*, 843-847.

Gavanescu, I., Kessler, B., Ploegh, H., Benoist, C., and Mathis, D. (2007). Loss of Aire-dependent thymic expression of a peripheral tissue antigen renders it a target of autoimmunity. Proceedings of the National Academy of Sciences *104*, 4583-4587.

Gavin, M. A., Rasmussen, J. P., Fontenot, J. D., Vasta, V., Manganiello, V. C., Beavo, J. A., and Rudensky, A. Y. (2007). Foxp3-dependent programme of regulatory T-cell differentiation. Nature *445*, 771-775.

Gershon, R. K., and Kondo, K. (1970). Cell interactions in the induction of tolerance: the role of thymic lymphocytes. Immunology *18*, 723-737.

Gillard, G. O., and Farr, A. G. (2005). Contrasting models of promiscuous gene expression by thymic epithelium. J Exp Med *202*, 15-19.

Goldrath, A. W., and Bevan, M. J. (1999). Selecting and maintaining a diverse T-cell repertoire. Nature *402*, 255–262.

Gommeaux, J., Grégoire, C., Nguessan, P., Richelme, M., Malissen, M., Guerder, S., Malissen, B., and Carrier, A. (2009). Thymus-specific serine protease regulates positive selection of a subset of CD4+ thymocytes. European Journal of Immunology *39*, 956-964.

Gotter, J., Brors, B., Hergenhahn, M., and Kyewski, B. (2004). Medullary epithelial cells of the human thymus express a highly diverse selection of tissue-specific genes colocalized in chromosomal clusters. J Exp Med *199*, 155-166.

Gray, D., Abramson, J., Benoist, C., and Mathis, D. (2007). Proliferative arrest and rapid turnover of thymic epithelial cells expressing Aire. J Exp Med *204*, 2521-2528.

Guo, P., Hirano, M., Herrin, B. R., Li, J., Yu, C., Sadlonova, A., and Cooper, M. D. (2009). Dual nature of the adaptive immune system in lampreys. Nature *460*, 784-786.

Hammarstrom, S. (1999). The carcinoembryonic antigen (CEA) family:structures, suggested functions and expression in normal and malignant tissues. Cancer Biology *9*, 67-81.

Hanahan, D. (1998). Peripheral-antigen-expressing cells in thymic medulla: factors in self-tolerance and autoimmunity. Curr Opin Immunol *10*, 656-662.

Hansen, J. D., and Zapata, A. G. (1998). Lymphocyte development in fish and amphibians. Immunol Rev *166*, 199-220.

Havran, W. L., and Allison, J. P. (1988). Developmentally ordered appearance of thymocytes expressing different T-cell antigen receptors. Nature *335*, 443–445.

Heath, V. L., Moore, N. C., Parnell, S. M., and Mason, D. W. (1998). Intrathymic expression of genes involved in organ specific autoimmune disease. J Autoimmun *11*, 309-318.

Hikosaka, Y., Nitta, T., Ohigashi, I., Yano, K., Ishimaru, N., Hayashi, Y., Matsumoto, M., Matsuo, K., Penninger, J. M., Takayanagi, H.*, et al.* (2008). The Cytokine RANKL Produced by Positively Selected Thymocytes Fosters Medullary Thymic Epithelial Cells that Express Autoimmune Regulator. Immunity *29*, 438-450.

Hinterberger, M. (2009). Direct antigen presentation by medullary thymic epithelial cells is essential for CD4 T cell tolerance. Doctoral Thesis.

Hogquist, K. A., Baldwin, T. A., and Jameson, S. C. (2005). Central tolerance: learning self-control in the thymus. Nat Rev Immunol *5*, 772-782.

Hogquist, K. A., Jameson, S. C., Heath, W. R., Howard, J. L., Bevan, M. J., and Carbone, F. R. (1994). T cell receptor antagonist peptides induce positive selection. Cell *76*, 17-27.

Hogquist, K. A., and Moran, A. E. (2009). Treg cells meet their limit. Nat Immunol *10*, 565-566.

Hurst, L. D., Pal, C., and Lercher, M. J. (2004). The evolutionary dynamics of eukaryotic gene order. Nat Rev Genet *5*, 299-310.

Irla, M., Hugues, S., Gill, J., Nitta, T., Hikosaka, Y., Williams, I. R., Hubert, F.-X., Scott, H. S., Takahama, Y., Holländer, G. A., and Reith, W. (2008). Autoantigen-Specific Interactions with CD4+ Thymocytes Control Mature Medullary Thymic Epithelial Cell Cellularity. Immunity *29*, 451-463.

Jameson, S. C., Hogquist, K. A., and Bevan, M. J. (1995). Positive selection of thymocytes. Annu Rev Immunol *13*, 93–126.

Jenkinson, W. E., Jenkinson, E. J., and Anderson, G. (2003). Differential requirement for mesenchyme in the proliferation and maturation of thymic epithelial progenitors. J Exp Med *198*, 325-332.

Jenkinson, W. E., Rossi, S. W., Jenkinson, E. J., and Anderson, G. (2005). Development of functional thymic epithelial cells occurs independently of lymphostromal interactions Mechanisms of Development *122*, 1294-1299

Johnnidis, J. B., Venanzi, E. S., Taxman, D. J., Ting, J. P., Benoist, C. O., and Mathis, D. J. (2005). Chromosomal clustering of genes controlled by the aire transcription factor. Proc Natl Acad Sci U S A *102*, 7233-7238.

Jolicoeur, C., Hanahan, D., and Smith, K. M. (1994). T-cell tolerance toward a transgenic beta-cell antigen and transcription of endogenous pancreatic genes in thymus. Proc Natl Acad Sci U S A *91*, 6707-6711.

Kajiura, F., Sun, S., Nomura, T., Izumi, K., Ueno, T., Bando, Y., Kuroda, N., Han, H., Li, Y., Matsushima, A.*, et al.* (2004). NF-kappa B-inducing kinase establishes self-tolerance in a thymic stroma-dependent manner. J Immunol *172*, 2067-2075.

Kampinga, J., Kroese, F. G. M., Duijvestijn, A. M., Murawska, M. B., Pol, G. H., and Nieuwenhuis, P. (1987). The rat thymus microenvironment: subsets of thymic epithelial cells defined by monoclonal antibodies. Transplant Proc *19*, 3171-3174.

Kappler, J. W., Roehm, N., and Marrack, P. (1987). T cell tolerance by clonal elimination in the thymus. Cell *49*, 273-280.

Kinugasa, T., Kuroki, M., Takeo, H., Matsuo, Y., Ohshima, K., Yamashita, Y., Shirakusa, T., and Matsuoka, Y. (1998). Expression of four cea family antigens (CEA, NCA, BGP and CGM2) In normal and cancerous gastric epithelial cells: Up-regulation of BGP and CGM2 in carcinomas. Int J Cancer *76*, 148–153.

Kishimoto, H., and Sprent, J. (1999). Several different cell surface molecules control negative selection of medullary thymocytes. J Exp Med *190*, 65-73.

Klein, L., Hinterberger, M., Wirnsberger, G., and Kyewski, B. (2009). Antigen presentation in the thymus for positive selection and central tolerance induction. Nat Rev Immunol *9*, 833-844.

Klein, L., Klein, T., Ruther, U., and Kyewski, B. (1998). CD4 T Cell Tolerance to Human C-reactive Protein, an Inducible Serum Protein, Is Mediated by Medullary Thymic Epithelium. J Exp Med *188*, 5-16.

Klein, L., Klugmann, M., Nave, K. A., Tuohy, V. K., and Kyewski, B. (2000). Shaping of the autoreactive T-cell repertoire by a splice variant of self protein expressed in thymic epithelial cells. Nat Med *6*, 56-61.

Klein, L., and Kyewski, B. (2000a). "Promiscuous" expression of tissue antigens in the thymus: a key to T-cell tolerance and autoimmunity? Journal of Molecular Medicine *78*, 483-494.

Klein, L., and Kyewski, B. (2000b). Self-antigen presentation by thymic stromal cells: a subtle division of labor. Curr Opin Immunol *12*, 179-186.

Klein, L., Roettinger, B., and Kyewski, B. (2001). Sampling of complementing self-antigen pools by thymic stromal cells maximizes the scope of central T cell tolerance. Eur J Immunol *31*, 2476-2486.

Klug, D. B., Carter, C., Gimenez-Conti, I. B., and Richie, E. R. (2002). Cutting edge: thymocyte-independent and thymocyte-dependent phases of epithelial patterning in the fetal thymus. J Immunol *169*, 2842-2845.

Koble, C., and Kyewski, B. (2009). The thymic medulla: a unique microenvironment for intercellular self-antigen transfer. J Exp Med *206*, 1505-1513.

Kojima, K., Reindl, M., Lassmann, H., Wekerle, H., and Linington, C. (1997). The thymus and self-tolerance: co-existence of encephalitogenic S100 beta-specific T cells and their nominal autoantigen in the normal adult rat thymus. Int Immunol *9*, 897-904.

Kuroda, N., Mitani, T., Takeda, N., Ishimaru, N., Arakaki, R., Hayashi, Y., Bando, Y., Izumi, K., Takahashi, T., Nomura, T*., et al.* (2005). Development of autoimmunity against transcriptionally unrepressed target antigen in the thymus of Aire-deficient mice. J Immunol *174*, 1862-1870.

Kyewski, B., and Derbinski, J. (2004). Self-representation in the thymus: an extended view. Nat Rev Immunol *4*, 688-698.

Kyewski, B., and Klein, L. (2006). A central role for central tolerance. Annu Rev Immunol *24*, 571-606.

Kyewski, B., and Peterson, P. (2010). Aire, master of many trades. Cell *140*, 24-26.

Kyewski, B. A., Fathman, C. G., and Kaplan, H. S. (1984). Intrathymic presentation of circulating non-major histocompatibility complex antigens. Nature *308*, 196-199.

Lanctôt, C., Cheutin, T., Cremer, M., Cavalli, G., and Cremer, T. (2007). Dynamic genome architecture in the nuclear space: regulation of gene expression in three dimensions. Nature Reviews Genetics *8*, 104-115.

Le Douarin, N., Corbel, C., Bandeira, A., Thomas-Vaslin, V., Modigliani, Y., Coutinho, A., and Salaun, J. (1996). Evidence for a thymus-dependent form of tolerance that is not based on elimination or anergy of reactive T cells. Immunol Rev *149*, 35-53.

Le Douarin, N. M., and Jotereau, F. V. (1975). Tracing of cells of the avian thymus through embryonic life in interspecific chimeras. J Exp Med *142*, 17-40.

Lee, J.-W., Epardaud, M., Sun, J., Becker, J. E., Cheng, A. C., Yonekura, A.-r., Heath, J. K., and Turley, S. J. (2007). Peripheral antigen display by lymph node stroma promotes T cell tolerance to intestinal self. Nat Immunol *8*, 181-190.

Lefai, E., Fernandez-Moreno, M. A., Kaguni, L. S., and Garesse, R. (2000). The highly compact structure of the mitochondrial DNA polymerase genomic region of Drosophila melanogaster: functional and evolutionary implications. Insect Mol Biol *9*, 315-322.

Lercher, M. J., Blumenthal, T., and Hurst, L. D. (2003). Coexpression of neighboring genes in Caenorhabditis elegans is mostly due to operons and duplicate genes. Genome Res *13*, 238-243.

Lernmark, A. (2002). Controlling the controls: GAD65 autoreactive T cells in type 1 diabetes. J Clin Invest *109*, 869-870.

Lieberman-Aiden, E., van Berkum, N. L., Williams, L., Imakaev, M., Ragoczy, T., Telling, A., Amit, I., Lajoie, B. R., Sabo, P. J., Dorschner, M. O.*, et al.* (2009). Comprehensive mapping of long-range interactions reveals folding principles of the human genome. Science *326*, 289-293.

Lind, E. F., Prockop, S. E., Porritt, H. E., and Petrie, H. T. (2001). Mapping precursor movement through the postnatal thymus reveals specific microenvironments supporting defined stages of early lymphoid development. J Exp Med *194*, 127–134.

Linsk, R., Gottesman, M., and Pernis, B. (1989). Are tissues a patch quilt of ectopic gene expression? Science *246*, 261.

Liston, A., Lesage, S., Gray, D. H., Boyd, R. L., and Goodnow, C. C. (2005). Genetic lesions in T-cell tolerance and thresholds for autoimmunity. Immunol Rev *204*, 87-101.

Lo, D., and Sprent, J. (1986). Identity of cells that imprint H-2-restricted T-cell specificity in the thymus. Nature *319*, 672-675.

Lomvardas, S., Barnea, G., Pisapia, D. J., Mendelsohn, M., Kirkland, J., and Axel, R. (2006). Interchromosomal interactions and olfactory receptor choice. Cell *126*, 403-413.

Mallet, V., Blaschitz, A., Crisa, L., Schmitt, C., Fournel, S., King, A., Loke, Y. W., Dohr, G., and Le Bouteiller, P. (1999). HLA-G in the human thymus: a subpopulation of medullary epithelial but not CD83(+) dendritic cells expresses HLA-G as a membrane-bound and soluble protein. Int Immunol *11*, 889-898.

Maloy, K. J., and Powrie, F. (2001). Regulatory T cells in the control of immune pathology. Nat Immunol *2*, 816-822.

Marrack, P., Lo, D., Brinster, R., Palmiter, R., Burkly, L., Flavell, R. H., and Kappler, J. (1988). The effect of thymus environment on T cell development and tolerance. Cell *53*, 627-634.

Martins, V. C., Boehm, T., and Bleul, C. C. (2008). Ltbetar signaling does not regulate Aire-dependent transcripts in medullary thymic epithelial cells. J Immunol *181*, 400-407.

Mathis, D., and Benoist, C. (2009). Aire. Annu Rev Immunol *27*, 287-312.

Mathis, D., and Benoist, C. (2010). Levees of immunological tolerance. Nat Immunol *11*, 3-6.

Matzinger, P., and Guerder, S. (1989). Does T-cell tolerance require a dedicated antigen-presenting cell? Nature *338*, 74-76.

McCaughtry, T. M., Wilken, M. S., and Hogquist, K. A. (2007). Thymic emigration revisited. J Exp Med *204*, 2513-2520.

Miller, J. F. (1961). Immunological function of the thymus. Lancet *2*, 748-749.

Misslitz, A., Pabst, O., Hintzen, G., Ohl, L., Kremmer, E., Petrie, H. T., and Förster, R. (2004). Thymic T cell development and progenitor localization depend on CCR7. J Exp Med *200*, 481–491.

Miyamoto, K., Miyake, S., Schachner, M., and Yamamura, T. (2003). Heterozygous null mutation of myelin P0 protein enhances susceptibility to autoimmune neuritis targeting P0 peptide. Eur J Immunol *33*, 656-665.

Mueller, D. L. (2010). Mechanisms maintaining peripheral tolerance. Nat Immunol *11*, 21-27.

Murata, S., Sasaki, K., Kishimoto, T., Niwa, S.-i., Hayashi, H., Takahama, Y., and Tanaka, K. (2007). Regulation of CD8+ T Cell Development by Thymus-Specific Proteasomes. Science *316*, 1349-1353.

Nakagawa, T., Roth, W., Wong, P., Nelson, A., Farr, A., Deussing, J., Villadangos, J. A., Ploegh, H., Peters, C., and Rudensky, A. Y. (1998). Cathepsin L: critical role in Ii degradation and CD4 T cell selection in the thymus. Science *280*, 450-453.

Nedjic, J., Aichinger, M., Emmerich, J., Mizushima, N., and Klein, L. (2008). Autophagy in thymic epithelium shapes the T-cell repertoire and is essential for tolerance. Nature *455*, 396-400.

Nehls, M., Kyewski, B., Messerle, M., Waldschutz, R., Schuddekopf, K., Smith, A. J., and Boehm, T. (1996). Two genetically separable steps in the differentiation of thymic epithelium. Science *272*, 886-889.

Nelson, A. J., Hosier, S., Brady, W., Linsley, P. S., and Farr, A. G. (1993). Medullary thymic epithelium expresses a ligand for CTLA4 in situ and in vitro. J Immunol *151*, 2453-2461.

Neu, N., Beisel, K. W., Traystman, M. D., Rose, N. R., and Craig, S. W. (1987). Autoantibodies specific for the cardiac myosin isoform are found in mice susceptible to Coxsackievirus B3-induced myocarditis. J Immunol *138*, 2488-2492.

Nitta, T., Murata, S., Sasaki, K., Fujii, H., Ripen, A. M., Ishimaru, N., Koyasu, S., Tanaka, K., and Takahama, Y. (2010). Thymoproteasome Shapes Immunocompetent Repertoire of CD8(+) T Cells. Immunity *32*, 29-40.

Ohki, H., Martin, C., Corbel, C., Coltey, M., and Le Douarin, N. M. (1987). Tolerance induced by thymic epithelial grafts in birds. Science *237*, 1032-1035.

Pacholczyk, R., Ignatowicz, H., Kraj, P., and Ignatowicz, L. (2006). Origin and T cell receptor diversity of Foxp3+CD4+CD25+ T cells. Immunity *25*, 249-259.

Pacholczyk, R., Kern, J., Singh, N., Iwashima, M., Kraj, P., and Ignatowicz, L. (2007). Nonself-antigens are the cognate specificities of Foxp3+ regulatory T cells. Immunity *27*, 493-504.

Pearse, M., Wu, L., Egerton, M., Wilson, Shortman, K., and Scollay, R. (1989). A murine early thymocyte developmental sequence is marked by transient expression of the interleukin 2 receptor. Proc Natl Acad Sci *86*, 1614–1618.

Peixoto, A., Monteiro, M., Rocha, B., and Veiga-Fernandes, H. (2004). Quantification of multiple gene expression in individual cells. Genome Res *14*, 1938-1947.

Peterson, P., Org, T., and Rebane, A. (2008). Transcriptional regulation by AIRE: molecular mechanisms of central tolerance. Nat Rev Immunol *8*, 948-957.

Petrie, H. T. (2003). Cell migration and the control of post-natal T-cell lymphopoiesis in the thymus. Nat Rev Immunol *3*, 859-866.

Petrie, H. T., and Zuniga-Pflucker, J. C. (2007). Zoned out: functional mapping of stromal signaling microenvironments in the thymus. Annu Rev Immunol *25*, 649-679.

Pinto, S., Wiencek, Y., Wild, S., Henze, S., Korn, B., Schmitt, S., and Kyewski, B. (2009). Increase sensitivity of Illumina® BeadArray™ with µMACS™ SuperAmp™ Technology. TechNote.

Pitkanen, J., and Peterson, P. (2003). Autoimmune regulator: from loss of function to autoimmunity. Genes Immun *4*, 12-21.

Plotkin, J., Prockop, S. E., Lepique, A., and Petrie, H. T. (2003). Critical role for CXCR4 signaling in progenitor localization and T cell differentiation in the postnatal thymus. J Immunol *171*, 4521–4527.

Porritt, H. E., Gordon, K., and Petrie, H. T. (2003). Kinetics of steady-state differentiation and mapping of intrathymic-signaling environments by stem cell transplantation in nonirradiated mice. J Exp Med *198*, 957-962.

Pribyl, T. M., Campagnoni, C., Kampf, K., Handley, V. W., and Campagnoni, A. T. (1996). The major myelin protein genes are expressed in the human thymus. J Neurosci Res *45*, 812-819.

Prockop, S. E., Palencia, S., Ryan, C. M., Gordon, K., Gray, D., and Petrie, H. T. (2002). Stromal cells provide the matrix for migration of early lymphoid progenitors through the thymic cortex. J Immunol *169*, 4354–4361.

Pruett, S. B., Collier, S., Wu, W. J., and Fan, R. (1999). Quantitative relationships between the suppression of selected immunological parameters and the area under the corticosterone concentration vs. time curve in B6C3F1 mice subjected to exogenous corticosterone or to restraint stress. Toxicol Sci *49*, 272-280.

Pruett, S. B., Fan, R., Myers, L. P., Wu, W.-J., and Collier, S. D. (2000). Quantitative analysis of the neuroendocrine-immune axis: Linear modeling of the effects of exogenous corticosterone and restraint stress on lymphocyte subpopulations in the spleen and thymus in female B6C3F1 mice. Brain Behav Immun *14*, 270-287.

Pugliese, A., Zeller, M., Fernandez, A., Jr., Zalcberg, L. J., Bartlett, R. J., Ricordi, C., Pietropaolo, M., Eisenbarth, G. S., Bennett, S. T., and Patel, D. D. (1997). The insulin gene is transcribed in the human thymus and transcription levels correlated with allelic variation at the INS VNTR-IDDM2 susceptibility locus for type 1 diabetes. Nat Genet *15*, 293-297.

Punt, J. A., Osborne, B. A., Takahama, Y., Sharrow, S. O., and Singer, A. (1994). Negative selection of CD4+CD8+ thymocytes by T cell receptor-induced apoptosis requires a costimulatory signal that can be provided by CD28. J Exp Med *179*, 709-713.

Rakha, E. A., Boyce, R. W. G., El-Rehim, D. A., Kurien, T., Green, A. R., Paish, E. C., Robertson, J. F. R., and Ellis, I. O. (2005). Expression of mucins (MUC1, MUC2, MUC3,MUC4, MUC5AC and MUC6) and their prognostic significance in human breast cancer. Modern Pathology *18*, 1295–1304.

Ramalho-Santos, M., Yoon, S., Matsuzaki, Y., Mulligan, R. C., and Melton, D. A. (2002). "Stemness": transcriptional profiling of embryonic and adult stem cells. Science *298*, 597-600.

Ramsdell, F., Lantz, T., and Fowlkes, B. J. (1989). A nondeletional mechanism of thymic self tolerance. Science *246*, 1038-1041.

Ramsey, C., Winqvist, O., Puhakka, L., Halonen, M., Moro, A., Kampe, O., Eskelin, P., Pelto-Huikko, M., and Peltonen, L. (2002). Aire deficient mice develop multiple features of APECED phenotype and show altered immune response. Hum Mol Genet *11*, 397-409.

Rathmell, J. C., Lindsten, T., Zong, W. X., Cinalli, R. M., and Thompson, C. B. (2002). Deficiency in Bak and Bax perturbs thymic selection and lymphoid homeostasis. Nat Immunol *3*, 932-939.

Rodewald, H. R. (2008). Thymus organogenesis. Annu Rev Immunol *26*, 355-388.

Rose, N. R. (2000). Viral damage or 'molecular mimicry'-placing the blame in myocarditis. Nat Med *6*, 631-632.

Rossi, F. M., Corbel, S. Y., Merzaban, J. S., Carlow, D. A., Gossens, K., Duenas, J., So, L., Yi, L., and Ziltener, H. J. (2005). Recruitment of adult thymic progenitors is regulated by P-selectin and its ligand PSGL-1. Nat Immunol *6*, 626-634.

Rossi, S. W., Jenkinson, W. E., Anderson, G., and Jenkinson, E. J. (2006). Clonal analysis reveals a common progenitor for thymic cortical and medullary epithelium. Nature *441*, 988–991.

Rossi, S. W., Kim, M. Y., Leibbrandt, A., Parnell, S. M., Jenkinson, W. E., Glanville, S. H., McConnell, F. M., Scott, H. S., Penninger, J. M., Jenkinson, E. J.*, et al.* (2007). RANK signals from CD4(+)3(-) inducer cells regulate development of Aire-expressing epithelial cells in the thymic medulla. J Exp Med *204*, 1267-1272.

Rouse, R. V., Bolin, L. M., Bender, J. R., and Kyewski, B. A. (1988). Monoclonal antibodies reactive with subsets of mouse and human thymic epithelial cells. J Histochem Cytochem *36*, 1511-1517.

Sakaguchi, S. (2005). Naturally arising Foxp3-expressing CD25+CD4+ regulatory T cells in immunological tolerance to self and non-self. Nat Immunol *6*, 345-352.

Sakaguchi, S., Wing, K., and Miyara, M. (2007). Regulatory T cells – a brief history and perspective. Eur J Immunol *37*, S116–S123.

Salaun, J., Bandeira, A., Khazaal, I., Calman, F., Coltey, M., Coutinho, A., and Le Douarin, N. M. (1990). Thymic epithelium tolerizes for histocompatibility antigens. Science *247*, 1471-1474.

Salaun, J., Corbel, C., and Le-Douarin, N. M. (2005). Regulatory T cells in the establishment and maintenance of self-tolerance: role of the thymic epithelium. Int J Dev Biol *49*, 137-142.

Saltis, M., Criscitiello, M. F., Ohta, Y., Keefe, M., Trede, N. S., Goitsuka, R., and Flajnik, M. F. (2008). Evolutionarily conserved and divergent regions of the autoimmune regulator (Aire) gene: a comparative analysis. Immunogenetics *60*, 105-114.

Scholzel, S., Zimmermann, W., Schwarzkopf, G., Grunert, F., Rogaczewski, B., and Thompson, J. (2000). Carcinoembryonic antigen family members CEACAM6 and CEACAM7 are differentially expressed in normal tissues and oppositely deregulated in hyperplastic colorectal polyps and early adenomas. Am J Pathol *156*, 595–605.

Scollay, R., Wilson, A., D'Amico, A., Kelly, K., Egerton, M., Pearse, M., Wu, L., and Shortman, K. (1988). Developmental status and reconstitution potential of subpopulations of murine thymocytes. Immunol Rev *104*, 81–120.

Seach, N., Ueno, T., Fletcher, A. L., Lowen, T., Mattesich, M., Engwerda, C. R., Scott, H. S., Ware, C. F., Chidgey, A. P., Gray, D. H., and Boyd, R. L. (2008). The lymphotoxin pathway regulates Aire-independent expression of ectopic genes and chemokines in thymic stromal cells. J Immunol *180*, 5384-5392.

Sebzda, E., Wallace, V. A., Mayer, J., Yeung, R. S., Mak, T. W., and Ohashi, P. S. (1994). Positive and negative thymocyte selection induced by different concentrations of a single peptide. Science *263*, 1615-1618.

Sémon, M., and Duret, L. (2006). Evolutionary origin and maintenance of coexpressed gene clusters in mammals. Mol Biol Evol *23*, 1715-1723.

Shinkai, Y., Rathbun, G., Lam, K. P., Oltz, E. M., Stewart, V., Mendelsohn, M., Charron, J., Datta, M., Young, F., Stall, A. M., and Alt, F. W. (1992). RAG-2-deficient mice lack mature lymphocytes owing to inability to initiate V(D)J rearrangement. Cell *68*, 855-867.

Sinemus, A. (2009). Promiscuous gene expression in the thymic medulla - on regulation at the epigenetic and single cell level. Doctoral Thesis.

Singer, A., Adoro, S., and Park, J. H. (2008). Lineage fate and intense debate: myths, models and mechanisms of CD4- versus CD8-lineage choice. Nat Rev Immunol *8*, 788-801.

Singer, G. A., Lloyd, A. T., Huminiecki, L. B., and Wolfe, K. H. (2005). Clusters of co-expressed genes in mammalian genomes are conserved by natural selection. Mol Biol Evol *22*, 767-775.

Smith, K. M., Olson, D. C., Hirose, R., and Hanahan, D. (1997). Pancreatic gene expression in rare cells of thymic medulla: evidence for functional contribution to T cell tolerance. Int Immunol *9*, 1355-1365.

Sospedra, M., Ferrer-Francesch, X., Dominguez, O., Juan, M., Foz-Sala, M., and Pujol-Borrell, R. (1998). Transcription of a broad range of self-antigens in human thymus suggests a role for central mechanisms in tolerance toward peripheral antigens. J Immunol *161*, 5918-5929.

Spellman, P. T., and Rubin, G. M. (2002). Evidence for large domains of similarly expressed genes in the Drosophila genome. J Biol *1*, 1-5.

Spilianakis, C. G., and Flavell, R. A. (2006). Molecular biology. Managing associations between different chromosomes. Science *312*, 207-208.

Spilianakis, C. G., Lalioti, M. D., Town, T., Lee, G. R., and Flavell, R. A. (2005). Interchromosomal associations between alternatively expressed loci. Nature *435*, 637-645.

Sprent, J. (2005). Proving negative selection in the thymus. J Immunol *174*, 3841-3842.

Starr, T. K., Jameson, S. C., and Hogquist, K. A. (2003). Positive and negative selection of T cells. Annu Rev Immunol *21*, 139-176.

Su, A. I., Wiltshire, T., Batalov, S., Lapp, H., Ching, K. A., Block, D., Zhang, J., Soden, R., Hayakawa, M., Kreiman, G.*, et al.* (2004). A gene atlas of the mouse and human protein-encoding transcriptomes. Proc Natl Acad Sci USA *101*, 6062-6067.

Takahama, Y. (2006). Journey through the thymus: stromal guides for T-cell development and selection. Nat Rev Immunol *6*, 127-135.

Taubert, R., Schwendemann, J., and Kyewski, B. (2007). Highly variable expression of tissue-restricted self-antigens in human thymus: Implications for self-tolerance and autoimmunity. Eur J Immunol *37*, 838-848.

Teichmann, S. A., and Veitia, R. A. (2004). Genes encoding subunits of stable complexes are clustered on the yeast chromosomes: an interpretation from a dosage balance perspective. Genetics *167*, 2121-2125.

Tisch, R. a. M., H. (1996). Insulin-dependent diabetes mellitus. Cell *85*, 291–297.

Tonegawa, S. (1983). Somatic generation of antibody diversity. Nature *302*, 575-581.

Towbin, J. A., Lowe, A. M., Colan, S. D., Sleeper, L. A., Orav, E. J., Clunie, S., Messere, J., Cox, G. F., Lurie, P. R., Hsu, D.*, et al.* (2006). Incidence, causes, and outcomes of dilated cardiomyopathy in children. JAMA *296*, 1867-1876.

Tykocinski, L. O., Sinemus, A., and Kyewski, B. (2008). The thymus medulla slowly yields its secrets. Ann N Y Acad Sci *1143*, 105-122.

Ueno, T., Saito, F., Gray, D. H., Kuse, S., Hieshima, K., Nakano, H., Kakiuchi, T., Lipp, M., Boyd, R. L., and Takahama, Y. (2004). CCR7 signals are essential for cortex-to-medulla migration of developing thymocytes. J Exp Med *200*, 493–505.

van Ewijk, W., Hollander, G., Terhorst, C., and Wang, B. (2000). Stepwise development of thymic microenvironments in vivo is regulated by thymocyte subsets. Development *127*, 1583-1591.

van Ewijk, W., Shores, E. W., and Singer, A. (1995). Crosstalk in the mouse thymus. Immunol Today *15*, 214-217.

Villasenor, J., Benoist, C., and Mathis, D. (2005). AIRE and APECED: molecular insights into an autoimmune disease. Immunol Rev *204*, 156-164.

Villasenor, J., Besse, W., Benoist, C., and Mathis, D. (2008). Ectopic expression of peripheral-tissue antigens in the thymic epithelium: probabilistic, monoallelic, misinitiated. Proc Natl Acad Sci U S A *105*, 15854-15859.

Vogel, A., Strassburg, C. P., Obermayer-Straub, P., Brabant, G., and Manns, M. P. (2002). The genetic background of autoimmune polyendocrinopathy-candidiasis-ectodermal dystrophy and its autoimmune disease components. J Mol Med *80*, 201-211.

von Boehmer, H., and Fehling, H. J. (1997). Structure and function of the pre-T cell receptor. Annu Rev Immunol *15*, 433–452.

Wakkach, A., Guyon, T., Bruand, C., Tzartos, S., Cohen-Kaminsky, S., and Berrih-Aknin, S. (1996). Expression of acetylcholine receptor genes in human thymic epithelial cells: implications for myasthenia gravis. J Immunol *157*, 3752-3760.

Wang, P. J., McCarrey, J. R., Yang, F., and Page, D. C. (2001). An abundance of X-linked genes expressed in spermatogonia. Nat Genet *27*, 422-426.

Watanabe, N., Wang, Y. H., Lee, H. K., Ito, T., Wang, Y. H., Cao, W., and Liu, Y. J. (2005). Hassall's corpuscles instruct dendritic cells to induce CD4+CD25+ regulatory T cells in human thymus. Nature *436*, 1181-1185.

Weiss, A., and Leinwand, L. A. (1996). The mammalian myosin heavy chain gene family. Annu Rev Cell Dev Biol *12*, 417-439.

White, A. J., Withers, D. R., Parnell, S. M., Scott, H. S., Finke, D., Lane, P. J., Jenkinson, E. J., and Anderson, G. (2008). Sequential phases in the development of Aire-expressing medullary thymic epithelial cells involve distinct cellular input. Eur J Immunol *38*, 942-947.

Williams, J. A., Sharrow, S. O., Adams, A. J., and Hodes, R. J. (2002). CD40 ligand functions non-cell autonomously to promote deletion of self-reactive thymocytes. J Immunol *168*, 2759-2765.

Wirnsberger, G., Mair, F., and Klein, L. (2009). Regulatory T cell differentiation of thymocytes does not require a dedicated antigen-presenting cell but is under T cell-intrinsic developmental control. Proc Natl Acad Sci U S A *106*, 10278-10283.

Witt, C. M., Raychaudhuri, S., Schaefer, B., Chakraborty, A. K., and Robey, E. A. (2005). Directed migration of positively selected thymocytes visualized in real time. PLoS Biol *3*, e160.

Wolfgram, L. J., Beisel, K. W., and Rose, N. R. (1985). Heart-specific autoantibodies following murine coxsackievirus B3 myocarditis. J Exp Med *161*, 1112-1121.

Xu, N., Tsai, C. L., and Lee, J. T. (2006). Transient homologous chromosome pairing marks the onset of X inactivation. Science *311*, 1149-1152.

Yanagi, Y., Yoshikai, Y., Leggett, K., Clark, S. P., Aleksander, I., and Mak, T. W. (1984). A human T cell-specific cDNA clone encodes a protein having extensive homology to immunoglobulin chains. Nature *308*, 145-149.

Yoon, J. W., Sherwin, R. S., Kwon, H., and Jun, H. S. (2000). Has GAD a central role in type 1 diabetes? J Autoimmun *15*, 273–278.

Zotter, S., Hageman, P. C., Lossnitzer, A., Mooi, W. J., and Hilgers, J. (1998). Tissue and tumor distribution of human polymorphic epithelial mucin. Cancer Rev *11-12*, 55–101.

Zuniga-Pflucker, J. C. (2004). T-cell development made simple. Nature Rev Immunol *4*, 67–72.

Acknowledgements

I would like to express my sincere gratitude to the following persons for their role during my study, research work and stay in Germany, culminating in this thesis:-

Prof. Dr. Bruno Kyewski for giving me the opportunity to work on this fascinating topic and for his supervision, fruitful discussions and tremendous help during my thesis.

Prof. Dr. Günter Hämmerling for willingly accepting to be the first referee for this thesis.

Prof. Buselmaier and Dr. Ralf Bischoff for willingly accepting to be my examiners.

Dr. Benedikt Brors and Maria Dinkelacker (Computational Oncology Department) for the Bioinformatic analysis.

Dr. Steffen Schmitt and Klaus Hexel (Core Facility Flow Cytometery) for FACS sorting of thymic epithelial cells and their valuable guidance for staining schemes.

Dr. Bernhard Korn, Sabine Henze and Oliver Heil (Genomics and Proteomics Core Facility) for the Microarray studies.

Dr. Felix Bestvater (Microscopy Core Facility) for help and guidance into Confocal Microscopy.

Dr. Hannah Schmidt-Glenewinkel (Quantitative Modeling and Simulation) for FISH image analysis.

Stefanie Egle and Esmail Rezavandy for their excellent technical help and support.

The entire Developmental Immunology group (D090), the Schwartz-Albiez' Lab and the lab of Prof. Petra Boukamp at the DKFZ for all their support and friendly working atmosphere.

Anil Demirata (Dr. m.s. Adobe) for helping me with the figures and final formatting of my thesis.

Dias family for making me feel at home and being like my family.

Chloé, Dorothee, Marissa, Martina, Monica, Sandra, Steffi, Willy and all my friends for all your support, encouragement, cheerful and stressful moments and bearing with me during the thesis and rest of the time!

This note of thanks will not be complete without a special mention of the unstinting support and encouragement from my family and parents in particular who have sacrificed much to help my dreams, like this thesis, turn to reality.